LBL-596
c.1

Progress Report in Space Radiobiology

For Reference

Not to be taken from this room

Donner Laboratory and
Lawrence Berkeley Laboratory
University of California
Berkeley, California

LBL-596
c.1

DISCLAIMER

This document was prepared as an account of work sponsored by the United States Government. While this document is believed to contain correct information, neither the United States Government nor any agency thereof, nor the Regents of the University of California, nor any of their employees, makes any warranty, express or implied, or assumes any legal responsibility for the accuracy, completeness, or usefulness of any information, apparatus, product, or process disclosed, or represents that its use would not infringe privately owned rights. Reference herein to any specific commercial product, process, or service by its trade name, trademark, manufacturer, or otherwise, does not necessarily constitute or imply its endorsement, recommendation, or favoring by the United States Government or any agency thereof, or the Regents of the University of California. The views and opinions of authors expressed herein do not necessarily state or reflect those of the United States Government or any agency thereof or the Regents of the University of California.

0 0 0 0 3 7 0 2 3 0 8

LBL-596

PROGRESS REPORT IN SPACE RADIOBIOLOGY

prepared for

Committee of Space Biology and Medicine

and

Radiobiological Advisory Panel of the
Space Science Board of the
National Academy of Sciences

January 1972

Donner Laboratory and
Lawrence Berkeley Laboratory
University of California
Berkeley, California 94720

Work done under the auspices of the
National Aeronautics and Space Administration
and the U.S. Atomic Energy Commission

0 0 0 0 3 7 0 3 3 0 9

PROGRESS REPORT IN SPACE RADIOBIOLOGY

CONTENTS

Introduction v

GRAVITY COMPENSATION AND RADIATION 1

The Dynamics of a Discrete Geotropic Sensor Subject to Rotation-induced Gravity Compensation
I. L. Silver 3

The Combined Effect of Radiation and Compensated Gravity on the Wing Development in Tribolium confusum
C-h Yang, Beverly D. Heinze, I. L. Silver, and C. A. Tobias 15

Studies on Geotropism and Radiation in Phycomyces blakesleeanus
John Risius, Chui-hsu Yang, Jean Luci, and C. A. Tobias 23

Preliminary Results of a Selection Experiment to Decrease Radiosensitivity of the Flour Beetle, Tribolium confusum
W. J. Heinze, Laurie Craise, and C. A. Tobias 43

RADIOBIOLOGY OF NEURONS IN CULTURE 71

Radiobiological Studies with Explanted Cerebellar Tissue
A. Mamoon, W. Schlapfer, B. Gahwiler, C. Tobias, J. Miquel, and W. Haymaker 73

Temperature-Controlled Micro-Chamber for Electrical Recording from Nerve Tissue Cultures
B. H. Gahwiler, A.-M. Mamoon, and C. A. Tobias . . . 101

Effects of Temperature on Spontaneous Bioelectric Activity of Cultured Nerve Cells
B. H. Gahwiler, A.-M. Mamoon, W. Schlapfer, and C. A. Tobias 111

Neuronal Reaggregation -- A Model System for Investigation of Radiation Effects on Nondividing Cells
J. Leith and W. Schilling 127

LONG-TERM EFFECTS OF ACCELERATED IONS 139

Aging in Laboratory Mice After Whole-Skin Irradiation with Accelerated Helium Ions
J. Leith, G. Welch, W. Schilling, R. McGregor, and C. A. Tobias 141

0 0 0 0 3 7 0 3 3 1 0

INTRODUCTION

This report contains brief articles by members of the Donner Laboratory Group working on radiobiological aspects of space biology.

The report is divided into three sections. The first section deals with the interactions between radiation and the effects of gravitational forces. Some years ago, at the recommendation of the Committee on Space Biology of the National Academy of Sciences, NASA undertook support of the construction of a clinostat with accompanying radiation source in order to find out whether or not we can learn about the effects of weightlessness faster without the necessity of resorting to space flights, by substituting gravity compensation for weightlessness and rerunning some of the radiobiological experiments on Biosatellite II. The second model of the "Clino-irradiator" is now complete, combined with a cesium gamma-ray source, and the possibility for control of temperature, light, humidity, and composition of the atmosphere.

We are indebted to Solon Gordon of the Argonne National Laboratory for supplying plans for some of the clinostats he built and for consultations. Ira Silver was in charge of the construction; (LBL Report #511). The device will be available for use by qualified scientists from various laboratories.

Ira Silver has recently demonstrated that gravity compensation is not fully equivalent to weightless condition, even if conditions relating clinostat rotation vs presentation time are fulfilled. The first experiments were performed by I. Yang with the clinostat on the flour beetle, *Tribolium confusum*. It was shown that, as in the 48-hour spaceflight under near weightless conditions, radiation-induced wing abnormalities

were more severe than without rotation at a 1-g force. It is possible that enzymatic repair of molecular lesions produced by radiation is less efficient under weightlessness or gravity compensation than at 1 g.

Two years ago the group proposed an improved space flight experiment using flour beetles, that could be performed in Skylab or in space shuttle flights. A population of these organisms would be kept in a weightless environment for more than one life cycle. Modifying factors would include radiation from radioisotopes on board and an "artificial," 1-g environment in a centrifuge. Tribolium is suitable for such long-term experiments because its life support system is exceedingly simple (it needs only dry flour and an appropriate gaseous atmosphere). Accelerated heavy ions (and presumably primary cosmic rays) produce known classes of developmental abnormalities. William Heinze has initiated some experiments in population genetics in order to provide strains most suitable for such work.

Work was initiated on another organism, Phycomyces, because of its suitability to approach the problems of geotropism and of radiation injury at the molecular level. Professor Max Delbrück of the California Institute of Technology, who has actively studied the mechanism of phototropism, kindly sent us some of his mutant strains: one of these, Car 10, responds to geotropic forces about 10 times faster than the wild type. In our laboratory it was found that light is necessary to induce and maintain the geotropic response. Organisms grown in complete darkness do not have it. These experiments are described by J. Resius and I. Yang.

0 0 0 0 3 7 0 0 3 1 1

The second section deals with work on the biophysics of neural networks grown in culture, and the radiobiology of neurons. The basis of this work is to be found in the Ph. D. theses by A. M. Mamoon (UCRL-19481, 1969) and W. Schlapfer (UCRL-19393, 1969). Culture techniques appear to be essential for studying the effects of heavy accelerated particles as these relate to primary cosmic rays. Four articles comprise this section.

The final section is an account of the effect of cyclotron-accelerated helium particles on the whole skin of mice; life-span shortening and carcinogenesis are covered by John Leith, et. al. Heavy ions may be even more carcinogenic than helium ions; as heavy ion beams become available it appears essential that the space program undertake a study of their long-term effects.

January 1972 Cornelius A. Tobias

D 0 0 0 3 7 0 3 3 1 2

GRAVITY COMPENSATION AND RADIATION

0 0 0 0 3 7 0 3 1 3

THE DYNAMICS OF A DISCRETE GEOTROPIC SENSOR SUBJECT TO ROTATION-INDUCED GRAVITY COMPENSATION

Ira Lee Silver

Donner Laboratory and Lawrence Berkeley Laboratory
University of California
Berkeley, California 94720

ABSTRACT

A clinostat achieves gravity compensation by providing circular rotation with uniform speed, about a horizontal axis. The dynamics of an assumed, discrete and free-moving subcellular gravity receptor, subject to clinostat rotation, is analyzed. The results imply that there is an optimum rotation rate; higher speeds result in circular motions with diameters more comparable to thermal noise fluctuations, but with greater linear velocities due to increasing centrifugal forces. An optimizing function is proposed. The nucleolus and mitochondria are possible gravity receptors; the characteristics of their clinostat-induced motions are incorporated with experimental results on *Avena* plant shoots in an illustrative example.

Rotation-Induced Gravity Compensation

Introduction

Investigations into the physiology of inactivity and weightlessness have utilized various methods for simulating these conditions, (McCalley, ed., 1968). The most practical way of achieving gravity compensation in the laboratory is by means of a " clinostat ". In its simplest form (1π), a clinostat provides circular rotation with uniform speed about a horizontal axis, thereby causing the time averaged gravitational force to be zero.

Numerous geotropic investigations have employed clinostats, (e.g., Briegleb, 1968, Shen-Miller, Hinchman and Gordon, 1968). Under a joint program of the NASA Biosciences Division and the AEC, two 1π clinostats have been designed at the Donner Laboratory (Silver, 1971), to investigate possible synergistic or antagonistic relations of gravity compensation to radiation. More sophisticated 2π devices are possible whereby variable simultaneous rotation about a vertical axis will induce any desired fractional " gravitational" force. A three-dimensional (4π) clinostat has been pioneered by Solon Gordon (1963). Here, a series of gimbal mounts are computer-driven, enabling a point specimen to trace over the surface of a sphere so that the time averaged position, angular velocity, and angular acceleration are zero. In this manner, it is hoped to negate the possible effects of all external tropic stimuli on biological development.

The clinostat cannot provide a true weightless, or free-fall environment, since it precludes neither mechanical stresses, nor subcellular and macromolecular tumbling in biological regions off the axis of rotation. Coupled to this is the fact that the nature of the " gravity receptor "

is unknown; e.g., is it a discrete subcellular particle or not, and what is the potential range of movement? Thus, it is desirable to develop appropriate theoretical guidelines for clinostat investigations.

Theory

For this analysis, it will be assumed that the geotropic receptor is a discrete subcellular component. In particular, it is required to quantify the dynamics of its motion, and how the motion is affected by varying the rate of rotation. Consider a 1π clinostat rotating at a constant angular velocity of $\omega = 2\pi n$ radians/unit time where n is the rate of revolution. The dynamics of 2π and 4π clinostats, while involving an added dimension, will be basically of a similar nature. The assumed receptor, immersed in the cytoplasmic fluid, will then be subjected to the following resultant forces:

$$\begin{aligned} |\bar{G}| &\equiv \text{magnitude of the gravitational force} \sim (1 - m_f/m_r)\, g \equiv K_1 \\ |\bar{C}| &\equiv \text{magnitude of the centrifugal force} \sim (1 - m_f/m_r) R\, \omega^2 \equiv K_2 \\ \bar{V} &\equiv \text{viscous force} \sim -\bar{v} \end{aligned} \qquad (1)$$

where: m_r is the mass of the geotropic receptor

m_f is the mass of the displaced cellular fluid

g is the acceleration of gravity

R is the clinostat radius of rotation

$\bar{v}$ is the instantaneous velocity

and $|\ |$ represents the magnitude of the vector force.

The $(1 - m_f/m_r)$ accounts for the Archimedean loss due to buoyancy. Let the fluid movement about the receptor be approximated by the Stokes Law:

$$\bar{V} = -6\pi\eta r_r \bar{v} \equiv -K_3 m_r \bar{v} \qquad (2)$$

where η is the fluid viscosity

and r_r the effective radius of the sensor.

The free-body force diagrams of Figure 1 delineate the forces on the receptor, during a 360° rotation of the clinostat. Note that the coordinate system is fixed to the rotating cellular compartment. V_x and V_y represent the components of the viscous damping force, acting in a direction opposite to the receptor's assumed motion.

The consequent differential equation for Newton's law of motion is thus:

$$\ddot{y} = K_1 \sin(\omega t) + K_2 - K_3 \dot{y}$$
$$\ddot{x} = K_1 \cos(\omega t) - K_3 \dot{x} \,. \tag{3}$$

Based on the initial conditions that

$$x = \dot{x} = 0, \; y = (K_2/K_3^2) - (K_1/\omega K_3) \text{ and } \dot{y} = 0$$

at $t = 0$, (4)

and assuming an isothermal and homogeneous cytoplasm, result in:

$$y(t) = \left[\left(\frac{K_2(\omega^2 + K_3^2)}{K_1 K_3^2} - \frac{\omega}{K_3}\right) \exp(-K_3 t) - \frac{K_3}{\omega} \cos(\omega t) - \sin(\omega t)\right] \frac{K_1}{(\omega^2 + K_3^2)} + \frac{K_2}{K_3} t \tag{5}$$

$$x(t) = \left[\exp(-K_3 t) - \cos(\omega t) + \frac{K_3}{\omega} \sin(\omega t)\right] \frac{K_1}{(\omega^2 + K_3^2)}$$

The seemingly arbitrary datum point for $y(0)$ has simplified the general expression for $y(t)$. The characteristics of the steady state motion are observed to be harmonic, being approximately circular with a period equaling $2\pi/\omega$. This motion, however, is constantly being displaced in

the direction of the centrifugal force.

The special case where $K_3/\omega \sim \eta r_r/m_r n >> 1$ is specifically applicable to cellular components. The harmonic contribution to the particular solution of y(t) will be denoted by the subscript p. Then,

$$\dot{y}_p(t_m) = 0 \rightarrow K_3 \sin(\omega t_m) = \omega \cos(\omega t_m)$$

and so the eigenvalues $t_m = \frac{1}{\omega}\left[\tan^{-1}(\frac{\omega}{K_3}) + m\pi\right]$, $m = 0, 1, 2, \cdots$

Since $\omega/K_3 \ll 1$, $t_m \simeq \frac{1}{K_3} + \frac{m\pi}{\omega}$, $m = 0, 1, 2, \cdots$

so that:
$$y_p(t_m) \simeq \frac{K_1}{K_3^2}\left[\frac{-K_3}{\omega}\cos(\frac{\omega}{K_3} + m\pi) - \sin(\frac{\omega}{K_3} + m\pi)\right]$$
$$\simeq \frac{K_1}{K_3\omega}. \qquad (6)$$

Therefore, the maximum amplitude of the harmonic motion is proportional to $1/\omega$. Taking the difference in y(t), at successive periods; e.g., $y(t_{m+2}) - y(t_m)$, results in:

$$y(t_{m+2}) - y(t_m) \equiv \Delta y = \frac{K_2}{K_3}(t_{m+2} - t_m)$$
$$\simeq \frac{K_2}{K_3}\left(\frac{(m+2)\pi}{\omega} - \frac{m\pi}{\omega}\right) = \frac{2\pi K'_2}{K_3}\omega \qquad (7)$$

where $K'_2 \equiv (1 - m_f/m_r)R$, and where the transient damping, which has a relaxation time of $1/K_3$, has rapidly become negligible. Therefore, the centrifugal force displacement per period is proportional to ω.

Application

Let us apply this theory to possible discrete geotropic receptors. Pollard (1965) has shown that in cells of an order of 1μ (10^{-4} cm) height; e.g., bacterial cells, the statistical distribution of cellular material due to Brownian motion is approximately independent of

gravity. In larger cells; e.g., mammalian cells of 10μ diameter, the most interesting organelles are: mitrochrondira with volume = 10^{-12}cc and density = 1.1g/cc, and the nucleolus with volume = 10^{-12} cc and density = 1.5 g/cc. The density of the cytoplasm is assumed to be 1 g/cc with a concomittant viscosity of 0.10 poise.

The subsequent clinostat motion of these organelles is summarized in Table 1, for ω = 0.209 and 13.4 radians/sec.

These speeds correspond to 2 rpm and 128 rpm respectively, at a rotational radius of 0.5 mm. These revolution rates are typical of clinostat experiments. The 1/2 mm radius is currently being employed by the author and his coinvestigator, Dr. T. C. Yang, in their investigations on the Tribolium confusum (flour beetle) eggs.

Any force-oriented motion must necessarily compete with the random disorder of Brownian motion. The resulting statistical distribution is:

$$N_i/N_o \equiv P_i = \exp\left[-\frac{(E_i - E_o)}{kT}\right] \tag{8}$$

where: N_o is the number density of particles at energy E_o and N_i, the number density at E_i,

P_i is the probability of a particle having the energy increment $(E_i - E_o)$.

k is Boltzman's constant,

T is the absolute temperature,

and $kT = 4.14 \times 10^{-14}$ ergs at 27°, is the average thermal energy.

Let $(E_i - E_o)$ be the potential energy of a particle in a buoyant fluid that traverses a distance equivalent to the diameter of the harmonic

motion. It can then be ascertained whether the dimension of the induced harmonicity is comparable with that of thermal fluctuations, (when N_i/N_o is exactly one). Therefore, utilizing Equation (6):

$$P_i = \exp\left[\frac{-(m_r - m_f)\, g\, (2y_p(t_m))}{kT}\right]. \qquad (9)$$

It is evident that gravity compensation is more significant at higher speeds. Utilizing the data of Table 1: for the nucleolus, $P_i = .613$ and .992 at 2 rpm and 128 rpm respectively; and for the mitochondria, $P_i = .980$ and $> .999$ for the same respective speeds.

The rate of displacement due to the centrifugal force, however, increases with increasing rotation rate. One means of evaluating this effect is to compare the induced linear velocity to that due to a unidirectional gravitational field. This ratio reduces to

$$\frac{\dot{y}_{centrifuge}}{\dot{y}_{gravity}} = R\omega^2/g \quad . \qquad (10)$$

Thus, at 2 rpm the ratio equals 2.2×10^{-6}; at 128 rpm, it equals 9.2×10^{-3}. As before, R equals 1/2 mm.

Conclusion

The dynamics of a discrete and free-moving geotropic receptor subject to clinostat rotation, results in two opposing tendencies. Circular motion, i.e., a short range effect, is induced with an amplitude $\sim 1/\omega$ and with a consequent deviation from thermal motion $\sim \exp(A/\omega)$. Concurrently, there is also induced a unidirectional motion, i.e., long range effect, $\sim \omega^2$.

In the absence of mechanical stresses (which can be exceedingly difficult to reduce), the efficacy & of the attempted gravity compensation

is a function of these two factors. Let us assume that the function has the form:

$$\mathcal{E} \sim \left[\exp(A/\omega) \right]^a (\omega^2)^b \tag{11}$$

where: $A = (m_r - m_f)\, g\, (2K_1/K_3)/kT$

a and b are "weighting factors," > 0 .

Most likely, these weighting factors will vary with the system being investigated. For a given system, the "best" rotation rate will be when $\mathcal{E}$ is extremized. Therefore,

$$\frac{\partial \mathcal{E}}{\partial \omega} = 0 \rightarrow \omega = \left(\frac{A}{2}\right)\left(\frac{a}{b}\right) \tag{12}$$

A second differentiation, evaluated at condition (12), shows that the extremum is indeed a minimum.

It has been found that for certain organisms, the product of exposure, or "presentation" time, and force gives rise to a constant geotropic curvature. For example, Rutten-Peckelharing (1910) exposed vertically oriented Avena plant shoots to various transverse centrifugal forces and determined that a produce of roughly 300 gave a constant minimal curvature. The reciprocity held over three orders of magnitude (down to 0.04G). The result implies that, at least for this particular case, a minimum "critical" distance has to be traversed by the sensor; i.e., geotropism is regulated by the long range factor.

Let us consider the mitochondria as a possible geotropic receptor for this example, and let us assume that the reciprocity can be extrapolated to lower G forces.

To establish the critical distance: At 2 rpm and 1/2 mm, the centrifugal force is 2.2×10^{-6} of normal gravity. Therefore, the presentation time is

$(3. \times 10^2)/(2.2 \times 10^{-6}) = 1.4 \times 10^8$ sec. From Table 1, the centrifugal force displacement of mitochondria at this rpm is 5.9×10^{-11} cm/period, thus resulting in a lineal speed of 2.0×10^{-12} cm/sec. The critical distance is then $(1.4 \times 10^8)(2.0 \times 10^{-12}) = 2.8 \times 10^{-4}$ cm.

To obtain the optimum speed: Since the amplitude $\sim 1/\omega$, from Table 1 we see that $2(2 \times 4.14 \times 10^{-6})/(2.8 \times 10^{-4}) = 0.059$ is the rpm's such that the diameter of the induced harmonic motion be equal to the critical distance.

The corresponding period is $(3.0)(2.0/0.059) = 1020$ sec; the displacement period is $(5.9 \times 10^{-11})(0.059/2.) = 1.7 \times 10^{-12}$ cm. Therefore, the time required for the centrifugal force to move the sensor over the critical distance is $(2.8 \times 10^{-4})(1.02 \times 10^3)/(1.7 \times 10^{-12}) = 1.7 \times 10^{11}$ sec.

The optimum speed for gravity compensation at 1/2 mm radius is equivalent to 0.059 rpm. Any lower rpm's will result in harmonic motions covering the critical distance in $\mathcal{O}(10^3$ sec); any larger rpm's will induce centrifugal force displacements traversing the critical distance in less than 10^{11} sec. Referring to Equation (12), at the optimum speed, $a/b \simeq 3$.

Acknowledgment

This research was sponsored by a joint program of the Bioscience Division of NASA, and the Atomic Energy Commission. Support came under NASA Contract W12-792, Task 6 with the Donner Laboratory, Lawrence Berkeley Laboratory, University of California, Berkeley.

Literature Cited

1. Briegleb, W., (1968), "Simulated Weightlessness for the Ontogenesis of the Otolith Organ, "Naturwissenschaften 55, pg 397.

2. Gordon, S. A., (1963), "Gravity and Plant Development: Bases for Experiment," in Space Biology, Proceedings of the 24th Annual Biology Colloquium, Oregon University Press, pp. 75-105.

3. McCalley, M., (ed.)(1968), "Hypodynamics and Hypogravics," Academic Press, Inc., N.Y. and London.

4. Pollard, E. C., (1965), " Theoretical Studies on Living Systems in the Absence of Mechanical Stress," J. Theoret. Biol. 8, pp 113-123.

5. Rutten-Peckelharing, C. J., (1910), "Research on the Perception of the Geotropic Stimulus," Rec. Trav. Bot. Neerl. 7, pp 241-348.

6. Shen-Miller, J., Hinchman, R., Gordon, S., (1968), " Thresholds for Georesponse to Acceleration in Gravity Compensated Avena Seedlings," Plant Physiol 43, pp. 338-344.

7. Silver, I. L., (1971), " The Modified and Completed 1π Clinostat-Irradiation System," Lawrence Berkeley Laboratory Report LBL-511.

Table 1

Geotropic receptor motion due to 1π clinostat rotation

Organelle	ω, (n)	Period(sec)	Max. Amplitude (cm), cf. Eq. (6)	Displacement/period (cm), cf. Eq. (7)
Mitochondria	0.209, (2)	30.	4.14×10^{-6}	5.90×10^{-11}
	13.4, (128)	0.47	6.46×10^{-8}	3.77×10^{-9}
Nucleolus	0.209, (2)	30.	2.07×10^{-5}	2.90×10^{-10}
	13.4, (128)	0.47	3.23×10^{-7}	1.88×10^{-8}

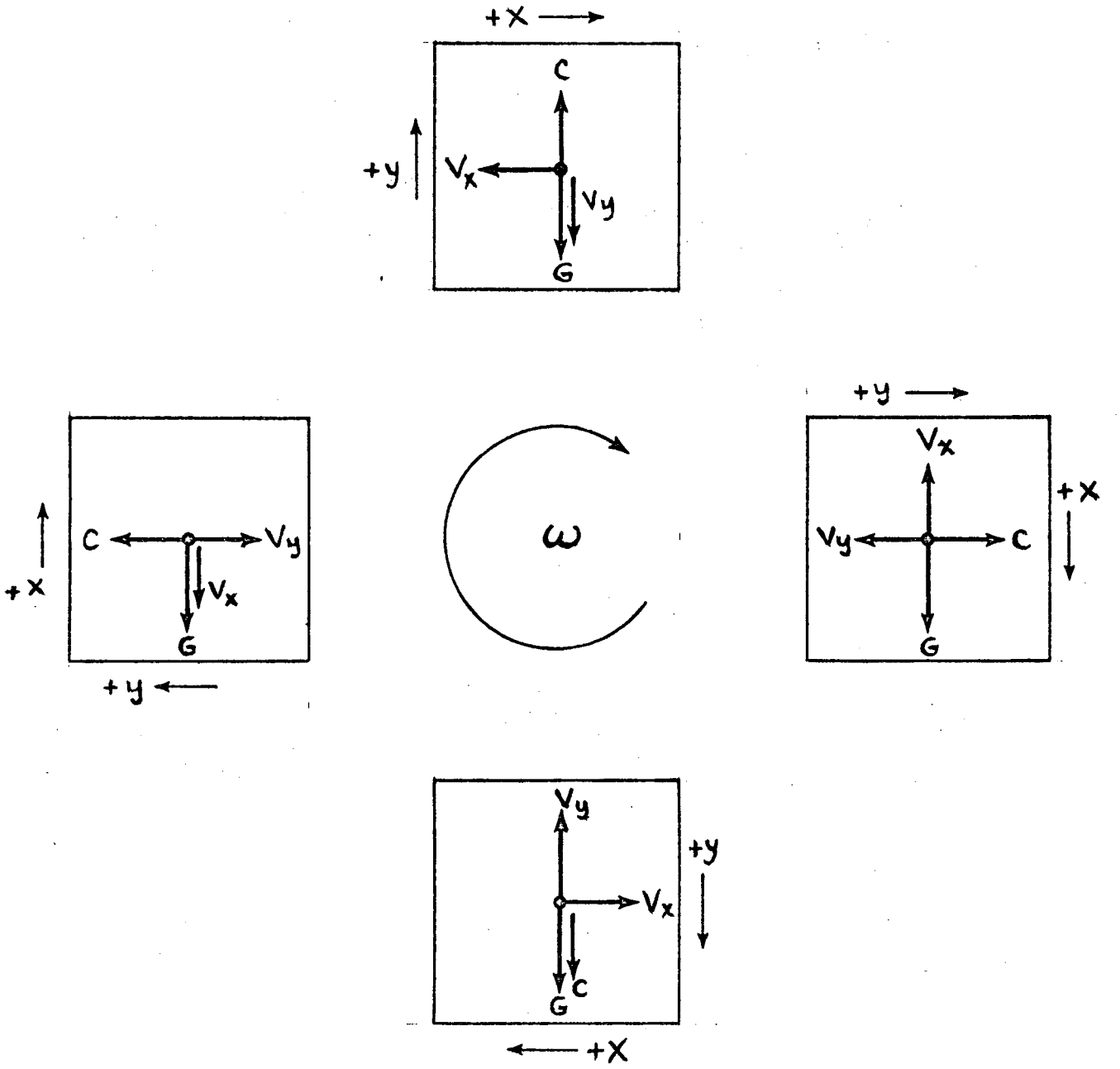

Fig. 1: The free-body force diagrams on a discrete geotropic receptor during a 360° rotation of the clinostat. The receptor, indicates as ·, is immersed in a cellular compartment.

THE COMBINED EFFECT OF RADIATION AND COMPENSATED GRAVITY ON THE WING DEVELOPMENT IN *TRIBOLIUM CONFUSUM*

By

Chui-hsu Yang, Beverly D. Heinze, Ira L. Silver, and C. A. Tobias

Lawrence Berkeley Laboratory, Donner Laboratory, University of California, Berkeley, California 94720

INTRODUCTION

On the space probe, Biosatellite II, groups of pupae of the flour beetle, *Tribolium confusum*, were included in order to determine whether developmental abnormalities would result either from weightlessness alone or from weightlessness combined with radiation. From the pupae exposed on that flight, we observed that those which received a portion of their radiation exposure in flight, while nearly weightless, exhibited more wing abnormalities when they reached full development during the post-flight period than controls kept at ground level, or controls exposed to radiation at ground level and flown in space subsequently.

The significance of this result remained in doubt since we were unable to repeat the observations of actual weightlessness, on another orbital flight. However, assuming that the effect observed in Biosatellite II was real, it may have a relatively simple explanation: that post-irradiation repair processes are less efficient under a condition of weightlessness than at ground level. A connotation of this assumption

is the possibility that the kinetics of motion of repair enzymes, and perhaps the rate of their action, may be dependent upon gravitational conditions. Ducoff (1) has clearly demonstrated the existence of a repair system in Tribolium, and his observations were confirmed and extended in our laboratory (2).

In order to learn more about the effects of radiation and weightlessness, we built a clinostat combined with a cesium gamma-ray source recently described by Silver (3). With this device we began the exploration of the question: Are radiation-induced wing abnormalities modified by gravity compensation? If this should be found true, it would reinforce the validity of the findings in Biosatellite II. This would also augur for further exploration of the possible mechanism of the synergistic effects.

Several preliminary experiments were performed. In the course of these we realized that gravity compensation is not exactly equivalent to weightlessness. The effect might be similar to that of weightlessness if the critical time period for action in the organism ("presentation time") is much longer than the period of rotation (4). Even in this case there may be differences due to sedimentation flow in clinostats (5). The preliminary experiments also demonstrated that exceedingly careful control of temperature and humidity is essential to obtaining reproducible results, and much time was spent by the group improving the apparatus. Organisms must be placed near the axis of the clinostat, and the capacity of this machine is small. The work presented here is the result of about seven different experiments that establish,

as shown below, that gravity compensation or weightlessness produce similar effects.

MATERIALS AND METHODS

Tribolium confusum pupae, between 22 and 27 hours old (30° C), were collected from stock cultures and used for all experiments. Culture medium was standard whole wheat flour, with 4% yeast additive.

The detail about the "1π" clinostat-irradiation system has been reported elsewhere (3).

For this study, pupae were carefully placed into small holes of clean plastic discs that were used as adapters for specimen holders. The specimen holder was then attached to a selected spindle of the clinostat. For each experiment one group of pupae was rotated horizontally at a speed of 4 rpm, and another group was maintained in a horizontal stationary position. The rotating speed, 4 rpm, was chosen for all experiments because at this speed a centrifugal force less than 10^{-4} g can be generated and, thus, only very minimum mechanical damage will be incurred by the pupae. The temperature in the "environmental chamber", in which the clinostat is housed, was maintained at 38 ± 1° C by an Aminco air conditioner and a resistance heater. Pupae, after being kept in the clinostat system for three days, were taken from pupae adapters and transferred back to a 30° C incubator. The number of wing abnormalities in Tribolium adults was checked about three days after their eclosion.

Pupae were irradiated at a nominal strength of 1000 curie cesium-137 source and at a dose rate of 10 R/min.

RESULTS AND DISCUSSION

The combined effect of radiation and compensated gravity on the wing development in Tribolium confusum is shown in Fig. 1. Each point in the figure represents an average of about 200 pupae. The combined results of seven experiments showed that pupae rotated horizontally had a higher percentage of wing abnormalities, about 4% to 9% in the dose range of 2000 to 3000 R, indicating an enhancement effect. It is interesting to note that there is no difference in the number of wing deformities between horizontally rotated and nonrotated groups in the plateau region. The observed enhancement effect, thus, seems to be dose dependent. A statistical analysis of the obtained data gives support to this idea. The significance of difference between two groups increase from near significant ($P \simeq 0.05$) at a dose of 2200 R to highly significant ($P \simeq 0.01$) at a dose of 3000 R.

Comparing our results with those obtained from Biosatellite II experiment (6), we find that the magnitude of enhanced effect in wing abnormalities observed in our study is about 30% less. This difference is not totally unexpected, and might be due to the following reasons: (a) the clinostat provided a state of gravity compensation, not a true "weightlessness" condition; (b) irradiation time in this study was quite short, only about five hours. In any case statistical variations in both experiments also contribute to the possibility of finding different values.

In spite of the fact that the present results are preliminary, the small synergistic effect observed is significant and should be further investigated. We believe, therefore, that the newly constructed

0 0 0 0 3 7 0 0 8 2 0

clinostat-irradiation system can be very useful in getting valuable information about the responses of animals as well as plants in the space environment.

Much further work needs to be done on this phenomenon. In the near future we plan to explore the effect at different temperatures and with different radiation dosages and rotation rates. Experiments are in progress where the rotation axis is vertical. Evidence is accumulating that the effect is due to a different rate of the repair process. Additional biological endpoints are also being used by studying eclosion as well as fertilized egg and larval stages.

For organisms generally, many of the effects of radiation are due to damage to DNA, and when low LET radiation is delivered at a low dose rate, many of the lesions are repaired. If the repair process should be impaired or inhibited in space flight, this factor should be seriously considered in relation to the safety of astronaut in long term space flight.

REFERENCES

1. Ducoff, H. S., Vaughan, A. P., and Crossland, J. L., "Dose-fractionation Studies on Adult Flour Beetles." Radiation Res. 39:472 (1969).

2. Yang, T. C., Silver, I. V., and Heinze, B., "Kinetics of Recovery in X-irradiated Tribolium confusum Pupae." Tribolium Information Bulletin, 13:93-94 (1970).

3. Silver, Ira L., "The Modified and Completed 1π Clinostat-irradiation System." LBL-511, (1971).

4. Gordon, S. A., and Shen-Miller, J., "Simulated Weightlessness Studies by Compensation." Gravity and the Organism (S. A. Gordon and M. J. Cohen, ed.), pp. 415-426. The University of Chicago Press, Chicago, Ill., (1971).

5. Silver, Ira L., this volume.

6. Slater, John V., Buckhold, Brenda, and Tobias, C. A., "Effect on a Flour Beetle of Irradiation During Space Flight." Bioscience 18:595-597 (1968).

0 0 0 0 3 7 0 0 3 2 1

FIGURE CAPTION

Fig. 1. Synergistic effect of radiation and compensated gravity on the wing development in *Tribolium confusum*.

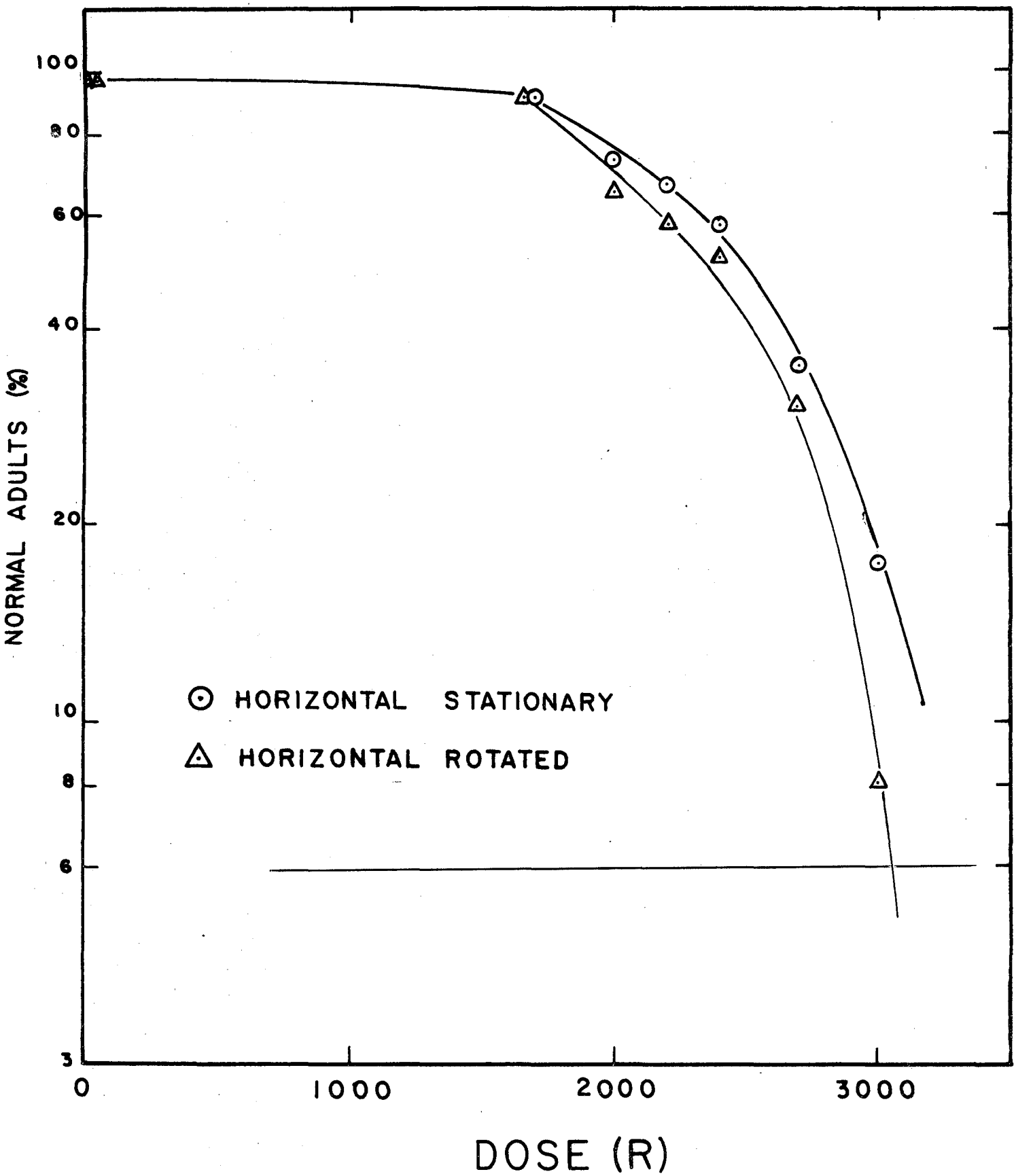
100
80
60
40
20
10
8
6
3
NORMAL ADULTS (%)
HORIZONTAL STATIONARY
HORIZONTAL ROTATED
0
1000
2000
3000
DOSE (R)

Fig. 1

0 0 0 0 3 7 0 0 3 2 2

STUDIES ON GEOTROPISM AND RADIATION IN PHYCOMYCES BLAKESLEEANUS

John Risius, Chui-Hsu Yang, Jean Luci, and C. A. Tobias

ABSTRACT

Phycomyces is a unicellular plant that responds to a variety of physical stimuli by changing its growth rate (growth response) or its direction of growth (tropic response). These stimuli include gravitational fields, light, and objects or fluids placed on or near the growing zone. The growth response to ionizing radiation is measurable for doses as low as 10 millirads, making this one of the most radiosensitive biological end points.

This report demonstrates that the development of geotropism requires previous exposure to light and that in darkness the absence of geotropism leads to branching of the sporangiophore. Growth and trophic responses to x-irradiation and to liquid droplets placed on the sporangium are also discussed.

INTRODUCTION

The sporangiophore of Phycomyces blakeslianus has an intriguingly wide potential as a system for the study of growth regulation and sensory physiology at the cellular level. This fungus is a single, multinucleate eucaryotic cell that grows in a mesh of branched tubular hyphae along the surface of a suitable medium. The sporangiophore, a specialized form of hypha, grows from the medium into the air and following a series of morphological changes, it grows at a constant rate for many hours by elongation within its tapered cylindrical growing zone (Fig. 1). When exposed to diffuse light the sporangiophore grows straight upward antiparallel to the gravitational force.

Several environmental factors affect the rate of growth and the direction of growth and responses to these are termed growth responses and tropic responses, respectively. The sporangiophore exhibits strong positive phototropism and weaker negative geotropism, that is it bends in a direction opposite the Earth's gravitational field. In addition, the organism responds to ultraviolet and x-irradiation, air currents, and solid and liquid objects placed on or near the growing zone.

Phototropism has been studied in detail by Max Delbrück and group (1) who have kindly sent us the initial strains for geotrophic studies in our laboratory. Geotropism has recently been reviewed by Dennison (2).

The responses, which generally begin within a few minutes, can be accurately measured from a series of photographs. At room temperature (23°C) and high relative humidity (> 60%), the linear growth

rate (2-4mm/hour) and the predictable size and location of the growing zone (approximately 3mm long x 0.17mm in diameter, beginning 0.4mm beneath the sporangium) make it possible to microscopically observe changes in the angle or position of the sporangiophore with time. Despite the ease of observation and the large number of stimuli which produce responses--and there are many published observations--the physiological sensors and the affector mechanisms are unknown. A major block in the path of understanding the sensor-affector system is the fact that the mechanism of cell wall elongation, the interaction of turgor-produced stress, and the wall synthetic chemistry are not understood in Phycomyces or in any other plant. This paper will present some observations on the influence of liquid droplets on tropic responses, on light requirements for geotropism and on responses to x-irradiation.

MATERIALS AND METHODS

Phycomyces and growth conditions: Standard stocks of Phycomyces spores are maintained frozen in distilled water. These source stocks consist of a series of dilutions of the original preparation, and one of these dilutions provides the plating stocks that are used for the routine plating. The following Phycomyces are maintained in the source stocks:

Phycomyces blakesleeanus

Wild type (-), car-10 (highly geotropic albino mutant)	Obtained from the Delbrück group, CIT, 1970

Wild type ( )	Obtained from UC Fungus Collection, 1971. Origin: McGill Univ., 1938.

Phycomyces nitens:

Wild type (?)	Obtained from a wild growth in No. Calif., 1971. J. Luce and J. Lyman.

The spores are plated in glass vials (1.2 cm. dia. x 4.5 cm. length) on the surface of 4 cm. deep potato dextrose agar. The medium is fortified with ammonium acetate to increase the germination efficiency. When 5 spores per vial are plated, more than 90 percent of the vials grow mycellium. The plated vials are cultured at 23°C in a ventilated clear plastic growth chamber (relative humidity ~75%). The fluorescent ceiling lights produce an approximate light intensity of 150 foot-candles ($\log_2 I/250 \approx -1$) in the growth chamber.

Life Cycle

Fig. 1 illustrates aspects of the vegetative development of Phycomyces and the nomenclature of the growth stages. The growth stages of the sporangiophore refer to states of differentiation; stage 1 is the period of early growth before sporulation, stage 2 is the period when sporulation occurs and the sporangium developes, stage 3 is a stationary period following the full expansion of the sporangium, and stage 4 is the period of maturity characterized by a steady cellular elongation. Stage 4 is divided into an early period, 4a, when the sporangium rotation is counterclockwise, and the later period, 4b, when the rotation is clockwise. Most of our experiments use the stage 4b sporangiophore.

Observational apparatus: An apparatus was developed that provides reasonably high accuracy in measurements of the growth and tropic responses and, in addition, is readily portable and flexible enough to be used for the observation of specimens in the clinostat. The apparatus can measure displacements with a resolution of about 1 micron.

Gas applications: Various gases can be applied to the entire sporangiophore or to specific regions. The regions of the cell are isolated by compartmentalizing the growth chamber with wax paper and sealing around the sporangiophore with vaseline. Pure O_2 and N_2, and combinations of these gases with air, have been applied.

Manipulation of drops: Drops of various solutions can be applied to the sporangiophore by using a 10 λ microsyringe fitted with a glass capillary tube drawn to a fine tip (10μ - 100μ). The positioning of the syringe relative to the sporangiophore is done using a micromanipulator. Generally, the drop is first placed at the upper boundary of the growing zone; then, using the micromanipulator, the drop is run down the near side to the growing zones lower edge and returned so it is centered about 0.7mm below the sporangium.

Radiation exposure: The radiation source is a 250 KVP Phillips x-ray machine operated at 200 KVP or 50 KVP depending on the desired exposure rates. The observational apparatus with Phycomyces in a small glass growth chamber (R.H. 95%) is positioned in front of the x-ray window. After the growth rate has stabilized, the growth rate is measured for ten minutes before and 20 minutes after the x-ray exposure. For a comparison of dose, dose rate, or synergistic effects, the specimen is used and a one-hour interval is allowed between exposures.

RESULTS AND DISCUSSION

I. Experiments on Geotropism

We have carried out some measurements to compare the growth rate, latency time, and the geotropic response of the mutant car-10 against the wild-type Phycomyces. The measured values are indicated in Table 1 for stage 4b growth in nonphototropic red light (wave length > 5200 Å).

Table 1.

	Rate of elongation	Latency*	Initial rate of bending
car-10 mutant	2.4 mm/hr	~ 3 min	~ 1.0°/min
wild type	3.6 mm/hr	~ 25 min	~ 0.3°/min

Temperature 23 C°

Ambient red light ($\lambda > 5200$Å)

Relative humidity ~ 90%

*Latency: time interval between the horizontal placement of the sporangiophore and the first observed upward growth.

These organisms were previously exposed to white light. Figure 2 indicates the normal rate of growth of the car-10 strain in a direction opposing the gravitational field. The pictures were taken 15 minutes apart. Figure 3 shows the response of the same plant after repositioning the sporangiophore horizontally. The pictures were taken at 0, 15, 45, and 75 minutes after the direction of the sporangiophore was changed.

Measurements of this type were used to obtain the data of Table 1. The gravity-sensitive mutant (car-10) grows slower than the wild type. It begins to respond to gravity with only 2 or 3 minutes latency and has a much higher bending rate than the wild type. In contrast the wild type has a 20 to 30 minutes latency time.

It became of interest to make preliminary studies of the factors necessary for geotropic response and of competing or inhibiting factors. One should note that the rate of bending in response to light is many times higher than the rate of bending of either the wild type or of the car-10 mutant in response to gravity. However the rate of bending in response to light is independent of light intensity over 100-fold variation of light intensity whereas the response to gravity is faster if higher than 1 g force is employed. When light is employed from one direction, Phycomyces grows at an angle which is characteristic of an equilibrium between the geotropic and phototropic responses. However, gravity can only compete at low light intensities because high intensities of light inhibit the geotropic response in the wild type at a level of about 50 foot candles. The car 10 gravity sensitive mutant is at least 100 times more resistant to light indicued inhibition. Because of these effects of white light most of the experiments where gravity response was measured were conducted in red light. Red light was produced by white light sources and the application of appropriate filters so that the wavelengths below 5200 Å were excluded.

The following experiment sheds interesting light on the requirements for light in order to achieve response to gravity. In testing the effects of red light on the life cycle of the organism it was observed that when white

light was excluded from the car-10 mutant through stage 3 and it was left in red light throughout stages 4a and 4b then it could not respond to gravity but instead exhibited peculiar a growth which took the form of a randomly-oriented spiral. An example of this is shown in Fig. 4.

From this experiment it appeared that the organism may need the white light during stage 3 and 4a in order to show geotropic response in stage 4b and several experiments fully confirmed this. The organism grown in either weak or strong white light will exhibit geotropism in red light subsequently when it is in stage 4b. Conversely when the car 10 mutant is kept in red light throughout stage 3 and stage 4a and then allowed to absorb white light for a few minutes its geotropism response starts immediately. Observations such as these enabled us to conclude that illumination by white light is necessary sometime during stages 3 and 4a in order to activate geotropic response in the red light or in darkness. We assume that light is instrumental in some synthetic step and plan to follow up on this observation.

The absence of all visible light in many respects is quite similar to the growth situation where red light is present. However when all light is excluded immediately after the growth of the mycellium is complete and before stage 1 so that the entire sporangiophore develops in the dark then the sporangiophore cannot sense gravity at all, it will not spiral, it will instead grow in random directions in space, and it will produce branches with high frequency. Usually the branching occurs in such a manner that the "older branch" stops growing in stage 3 and gives rise to a daughter branch which also stops growing in stage 3, producing a third branch, etc. When such branched sporangiophores are exposed to

white light it is the newest branch that enters stage 4 and responds to gravity. Such branching sporangiophores photographed immediately after exposure to light following long period in darkness are shown in Fig. 5.

When the organisms are allowed to grow in a clinostat in the stage 4b under unilateral illumination at a rotation rate of 4 revolutions/min they grow along a straight line following the axis of the clinostat indicating that the presentation light time and gravity time are considerably longer than the rotation time. When the sporangiophores are not exactly in the axis of the clinostat but a few inches off-center, the rotation of the clinostat generates a small wind and the organism responds to this by bending aginst the wind which in this case coincides with the direction of rotation of the clinostat. The effect of very low wind velocities of the order of 0.2 mile per hour was measured in this manner.

Summary of the geotropic experiments. We have demonstrated that in the gravity-sensitive organism car-10 light is necessary to activate the geotropic response which actually occurs in red light or in the dark. In the complete absence of all light during all stages, the sporangiophores branch in stage 4b and grow in random directions. In the complete absence of white light but in the presence of red light they will grow in early stage 4 in random spirals. Thus grown in darkness, sporangiophores of *Phycomyces* act as though they were in the weightless state. Upon exposure to light they rapidly regain ability to respond to gravity.

II. Pilot experiment relating to the mechanism of the gravitational effect

It was known for some time that when a droplet of distilled water is placed on one side of the growing zone in stage 4b, the sporangiophore

rapidly bends to the opposite side (3). The rate of bending is higher than that achievable by either phototropic or geotropic means. In order to test this phenomenon further droplets differing in sucrose concentration were placed in appropriate position. When sucrose solution of greater than 0.6 M concentration was placed on one side of the growth zone of the sporangiophore in stage 4b the bending response stopped completely. At the same time the overall rate of growth also slowed down. A unilateral application of vasoline also produces a rapid bending away from the application. Figure 6 shows photographs of the Phycomyces response to distilled H_2O, 0.2 M sucrose, 0.6 M sucrose, and the vasoline application. Experiments of this type add to the avidence that the cell wall and the cell membrane may be involved in the bending response. It appears to us that due to osmotic relationships distilled water tends to move from the outside of the sporangiophore to the cell lumen through the wall and membrane and that perhaps distilled water causes an expansion of the cell wall. When solutions of high osmotic strengths are used, the movement should be reversed and the turgor pressure reduced. The reduced turgor pressure may explain whcy the growth rate shows and why the tropic bend fails to occur.

III. The effect of x-ray exposure on growth rate.

It has been known for many years since the pioneering work of Forssberg(4, 5) that a small dose of x rays will cause a temporary retardation of the rate of growth of the sporangiophores of Phycomyces followed by a spurt of more rapid growth. We have verified this observation by exposing stage 4b in the presence of white light to small doses of x rays. With a latency time of less than a minute the growth

rate immediately slows and is followed by the dynamic range of growth rates until the initial growth rate has re-established itself. Figure 7 reproduces observations at 3 different dose levels. Direct irradiation of the growth zone has a part in this process by radiation exposure of the micellium also makes a contribution. The radiation effects are best explained by assuming that radiation increases the permeability of the cell membrane to water and that a control mechanism is present that reestablishes the appropriate osmotic relationships following exposure.

It is interesting to note that the gravity-sensitive mutant car 10 shows a different response to ionizing radiation than the wild type. The response is somewhat faster, showing a greater overshoot following the initial growth-rate decline.

CONCLUSION

Phycomyces has many admirable properties that make it especially suitable for investigations concerning the basic nature of geotropism and of radiation effect. It would be interesting to compare the observations reported here to phenomena that may occur in a space ship in near weightlessness. We also plan to carry out biophysical and genetic experiments to further quantitate the molecular nature of the geotropic and radiation responses.

BIBLIOGRAPHY

1. Delbruck, M., et al., Phycomyces, Bacteriol. Rev., 33, 101-157 (1969).

2. Dennison, D. S., Gravity Receptors in Phycomyces, Gravity and the Organism, S. A. Jordon and M. J. Cohen, editors (University of Chicago Press, 1971). pp. 65-72.

3. Thimann, K. V., and Gruen, H. E., The Growth and Curvature of Phycomyces Sporangiophores. Beih. 2. zchweiz. forstv. 30, 237-263 (1960).

4. Forssberg, A., Growth-rate and biochemical changes in Phycomyces at low dose-levels of x-rays. Int. J. Rad. Biol. Suppl. 2 206 (1960).

5. Forssberg, A., The radiation induced reactions of Phycomyces blakesleeanus – pulsed transfer of cellular particles. Radiation Botany, Vol. 9, 391.

0 0 0 0 0 7 0 0 3 2 6

FIGURE LEGENDS

Fig. 1. Phycomyces life cycle and cell nomenclature.

Fig. 2. Normal negative-geotropic growth of car-10 in diffuse light.

Fig. 3. Geotropic response of car-10 following horizontal placement in nonphototropic red light. Exposures are at 0, 15, 45, 75 minutes.

Fig. 4. Nongeotropic growth of car-10 in nonphototropic red light. The disorientated growth begins in the early stage 4 sporangiophore.

Fig. 5. Nongeotropic branching of car-10 in complete darkness.

Fig. 6. Tropic responses to droplets of (a) distilled water (b) 0.2 M surcrose (c) 0.6 M sucrose, and (d) a unilateral application vasoline.

Fig. 7. Growth rate response of car-10 to x-irradiation.

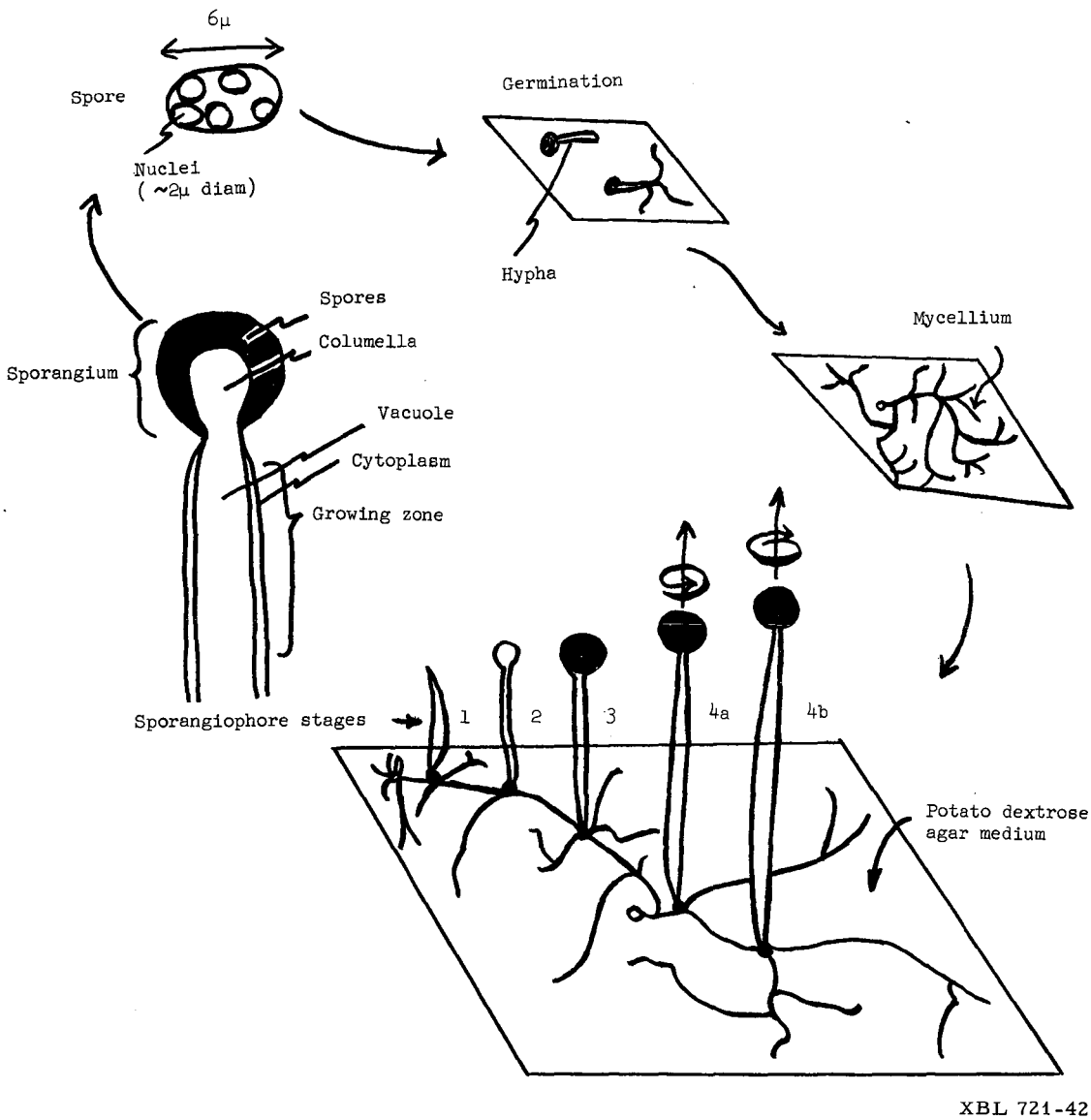
6μ
Spore
Nuclei
(~2μ diam)
Germination
Hypha
Mycellium
Spores
Columella
Sporangium
Vacuole
Cytoplasm
Growing zone
Sporangiophore stages
1
2
3
4a
4b
Potato dextrose
agar medium
XBL 721-42

Fig. 1

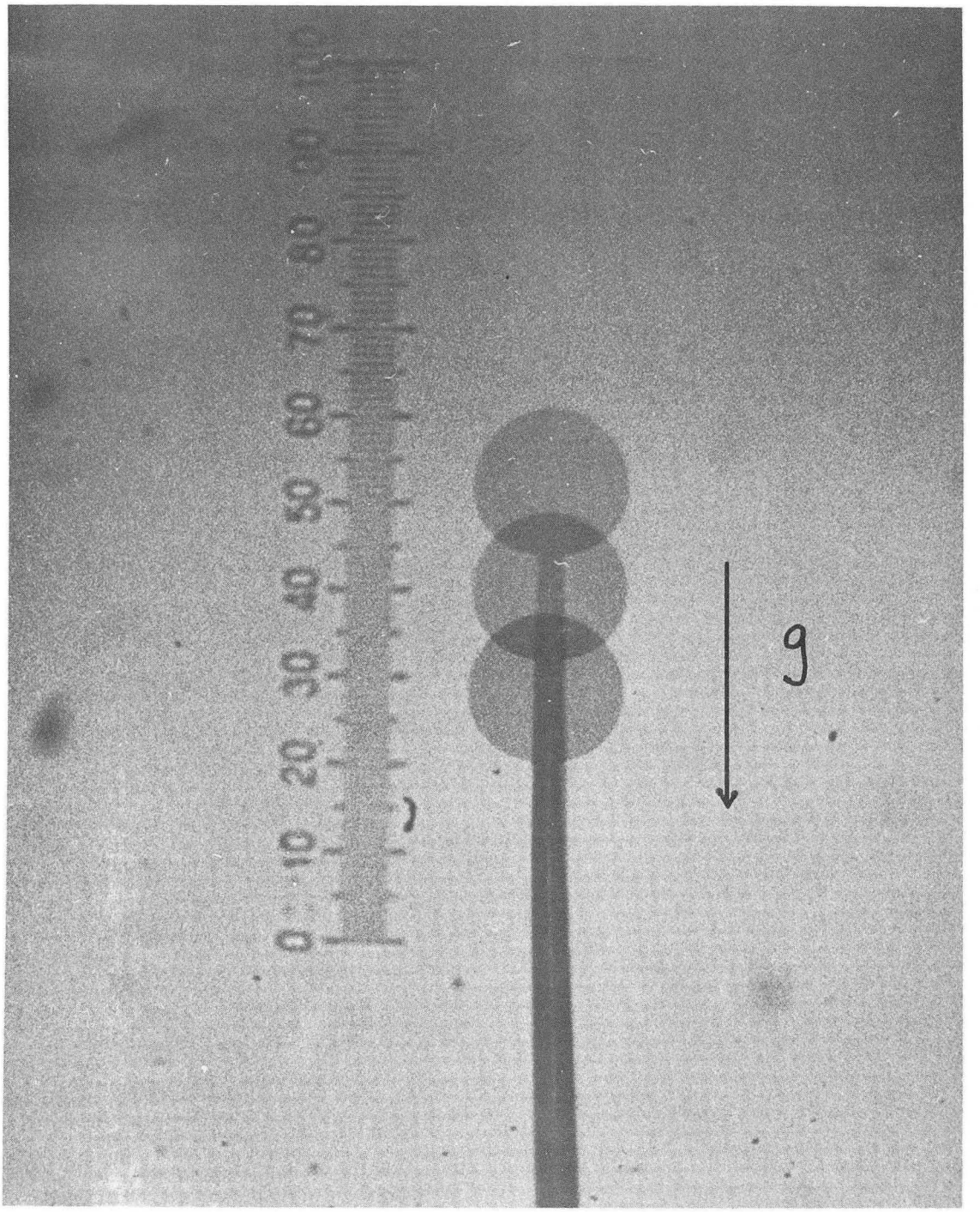

Fig. 2

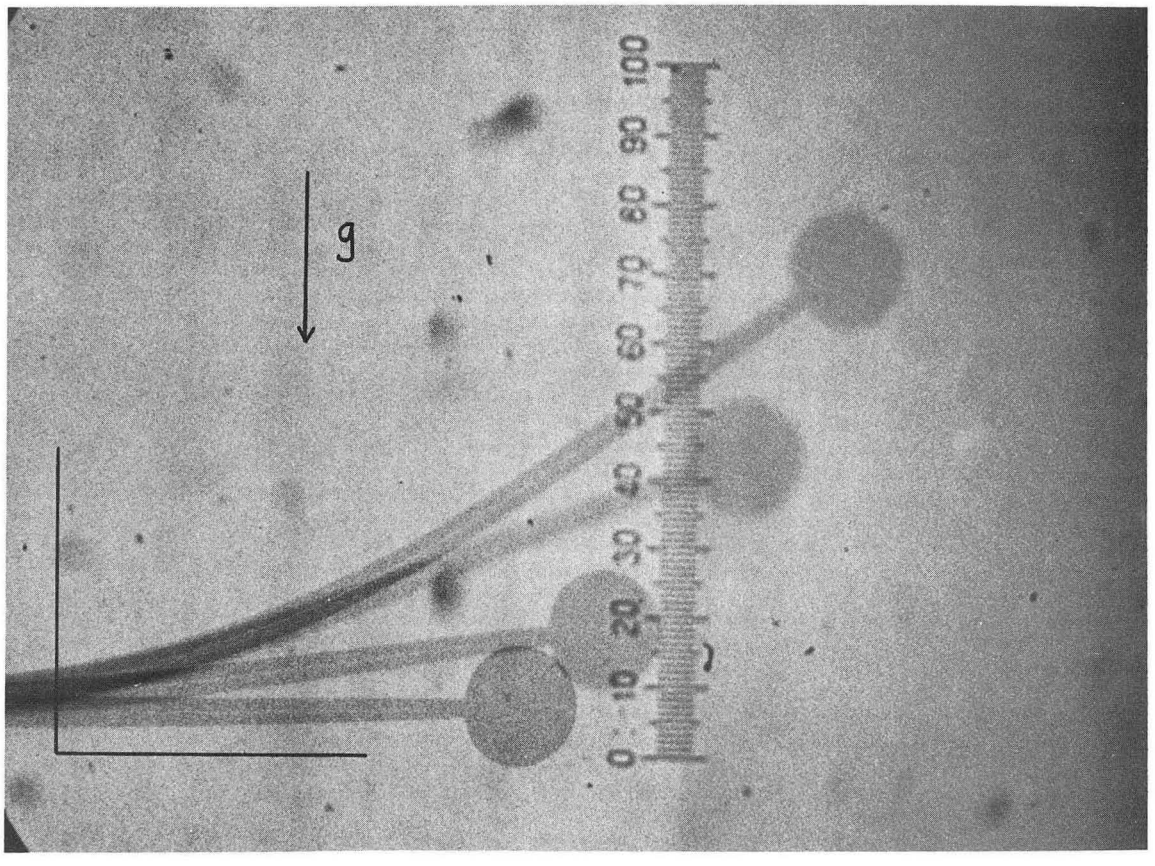

Fig. 3

0 0 0 0 3 7 0 3 8 2 7

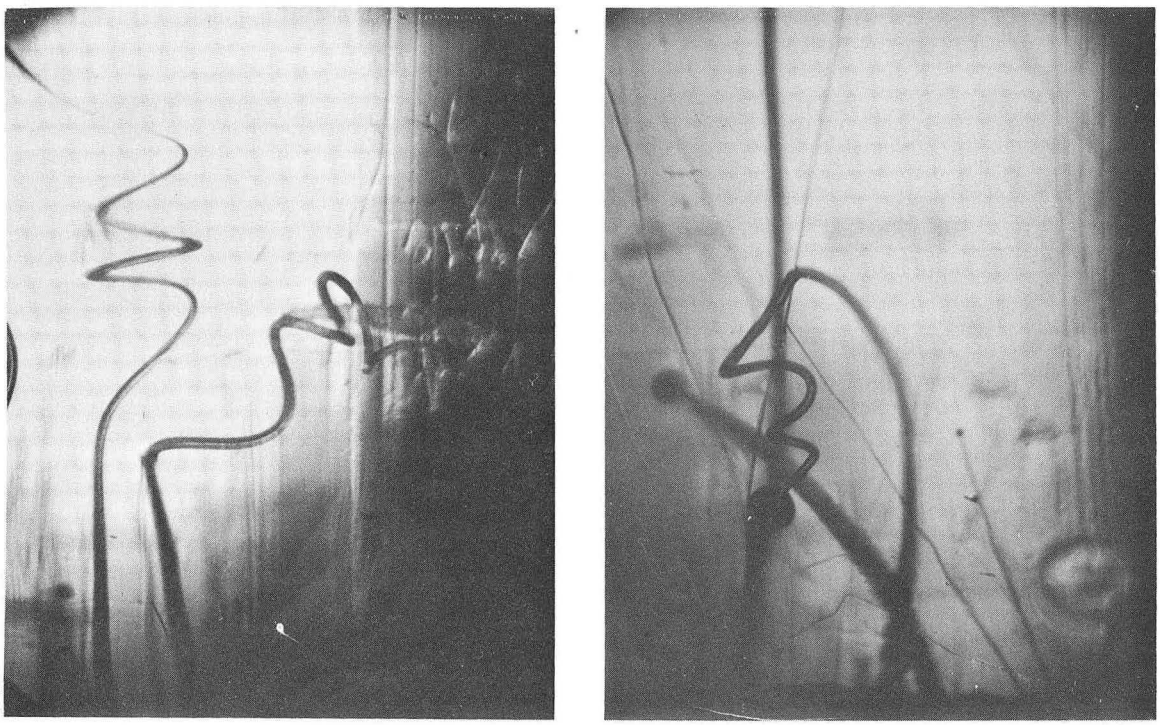

(a) (b)

Fig. 4

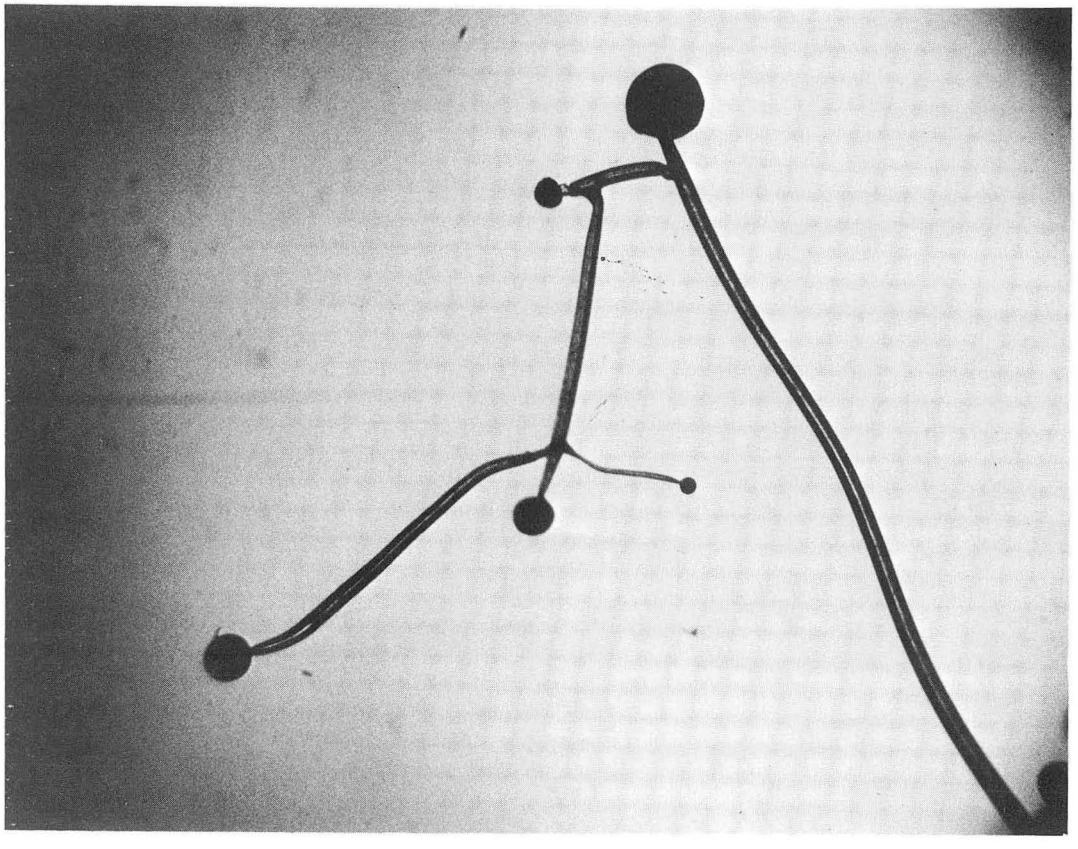

Fig. 5

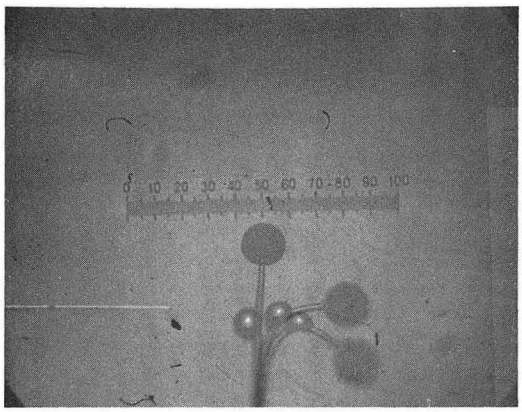

(a)

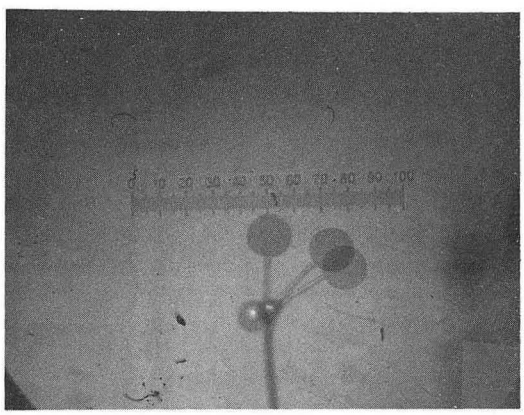

(b)

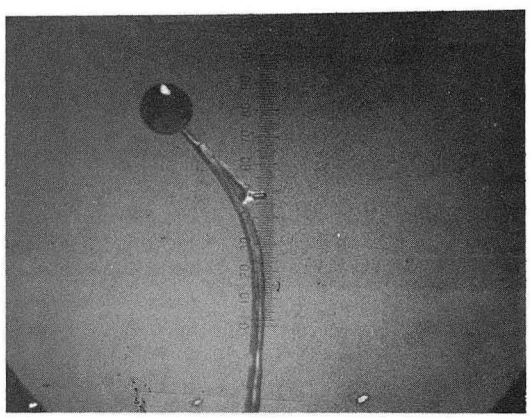

(d)

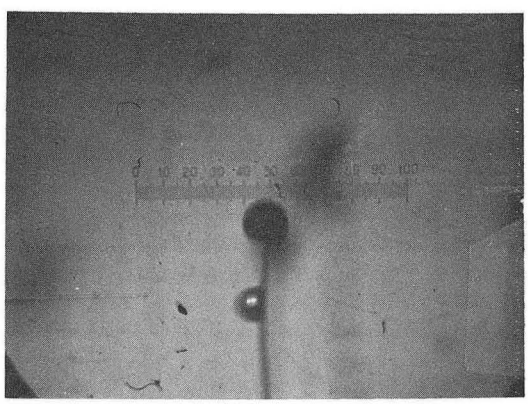

(c)

Fig. 6

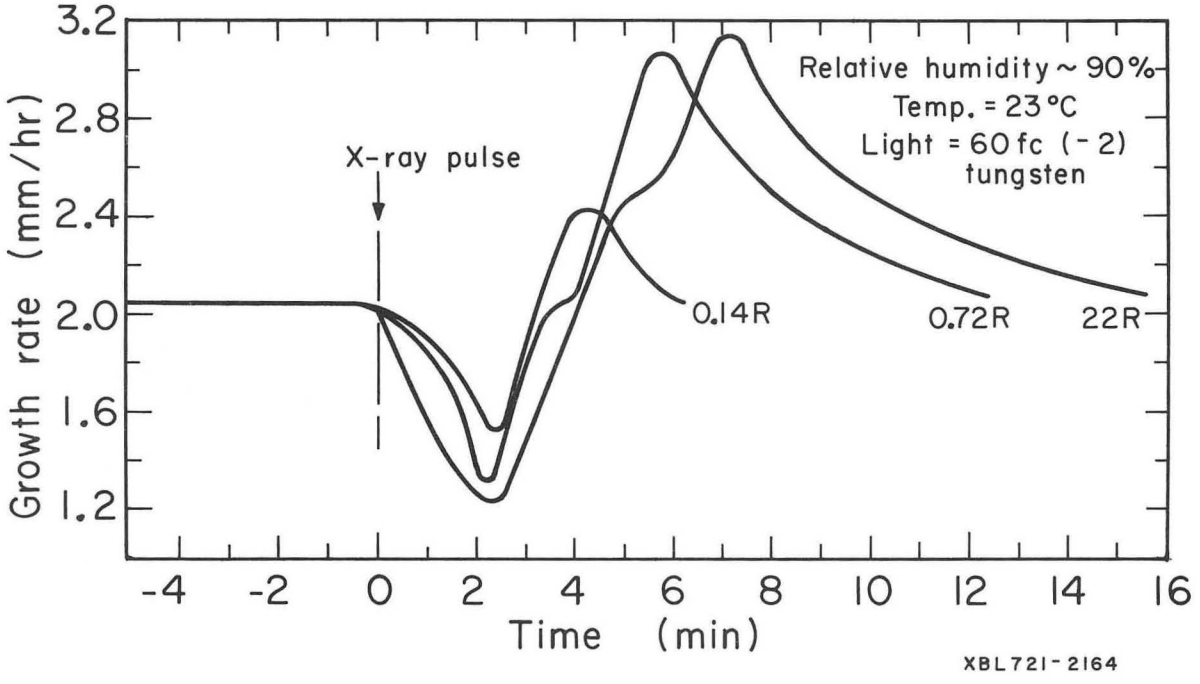
3.2
2.8
2.4
2.0
1.6
1.2
Growth rate (mm/hr)
X-ray pulse
Relative humidity ~ 90%
Temp. = 23 °C
Light = 60 fc (-2)
tungsten
0.14R
0.72R
22R
-4
-2
0
2
4
6
8
10
12
14
16
Time (min)
XBL721-2164

Fig. 7

PRELIMINARY RESULTS OF A SELECTION EXPERIMENT TO DECREASE RADIOSENSITIVITY OF THE FLOUR BEETLE, *TRIBOLIUM CONFUSUM*

William J. Heinze, Laurie Craise, and Cornelius Tobias
Donner Laboratory and Lawrence Radiation Laboratory
University of California
Berkeley, California 94720

Introduction

Genetic theory predicts that if there is phenotypic variation of a trait, and if part of this variation results from genetic variation, then this trait should respond to selection (Falconer, 1960; Pirchner, 1969). The percent hatchability of *Tribolium confusum* eggs is less following X-irradiation than non-irradiated control eggs, and the magnitude of the decrease is different in different stocks (Heinze, 1971). Therefore, the condition of phenotypic variability is met, and if radiosensitivity has a genetic base, then selection should be effective in increasing or decreasing radiosensitivity.

Instead of basing measurement of radiosensitivity on one dose of X-rays, five doses were used and a linear regression line was fit to the resultant data. The biological endpoint assessed was the slope of the regression line, and not the hatchability at any given dose. The use of the regression coefficient as an endpoint for genetic studies has been shown to be effective (Osborne and DeGeorge, 1959; Welch, 1969, 1970).

A difficulty arises, however, because the X-rays induce mutations (Muller, 1927, 1954) providing new genetic variation, and it is possible

that this new variation may oppose any change due to selection. Also the accumulation of non-lethal genetic damage, in particular chromosomal damage (Sax, 1952; Lane, 1951), might mask any gains made by selection by making the egg less viable.

Materials and Methods

Eight independent T. confusum stocks were established. From a given stock eggs were collected and a portion of the eggs were irradiated and placed in fresh flour and allowed to develop into adults. These adults became the parents of the next generation. The remaining eggs were divided into six groups, five were X-rayed,each at a different dose. The number of eggs hatching into larvae was counted, and all the eggs and larvae were then discarded.

A 24 hour collection period at 24°C was used for the eggs. The eggs were then immediately X-rayed through a 1.0 Al filter at 300 R/min (approximately 180 KV at 15 am). The groups which were to provide the parents of the next generation received 450 R. The groups which were to provide information on radiosensitivity received 0 R, 450 R, 600 R, 750 R, 900 R, or 1050 R.

To analyze the data with linear methods ($Y = a + bX$), a natural log transformation was used on the data points. First, each irradiated group value was standardized to its corresponding non-irradiated control value, and then a ln transformation applied. A linear regression line

was fit to the resultant data points for each stock. To test the hypothesis that the regression coefficient (slope) was not 0, a F-test was used. A significiant F-value indicates that most of the variation in hatchability is explained by the regression line. To compare the slope of one regression line against another a t-test was used. A significant t-value indicates that the slopes are different and therefore the lines are different; however, lack of significance does not indicate that the lines are the same even though the slopes are the same.

Results

Before selection was applied, the radiosensitivities of the 8 stocks (XRS-1,2,3,4,5,6,7, and XRS-Cont) were determined, and regression lines were fit (Table 1 and Figure 1). At the 0.05 level of significance, 4 out of 8 regression coefficients were smaller than 0 (Table 2). Also from Figure 1, it is apparent that there are phenotypic differences in radiosensitivity.

Following two generations of selection, radiosensitivity was again determined and new regression lines were fit (Table 3 and Figure 2). All regression coefficients were smaller than 0, most at the 0.005 level of significance (Table 4). After three generations of selection radiosensitivity was again determined and new regression lines were fit (Table 5 and Figure 3). All regression coefficients were again smaller than 0, most at the 0.005 level of significance (Table 6).

That the experimental treatment was effective in changing radiosensitivity can be seen in Figures 4 through 11. After two generations of selection, 6 out of 8 regression coefficients were different from their unselected progenitor's at the 0.005 level of significance (Table 7). The only stock clearly showing no difference was the non-irradiated control stock (XRS-Cont), as was expected. After three generations of selection all the regression coefficients were different from their unselected progenitor's at the 0.005 level of significance (Table 8), and 6 out of 8 had different slopes at the 0.05 level of significance (Table 9) from the previous generation.

Discussion

It is quite apparent that the experimental treatment has removed a large source of unwanted variation, so that the fitted regression lines are quite close to the actual experimental results. The better fit of the regression lines is due, in part, to the better pre-irradiation (small age variance, uniform handling, constant temperature, etc.), and due, in part, to the removal of weak individuals by previous irradiation. These stocks would be quite useful in synergism studies with X-rays and other treatments.

The expectation of decreased radiosensitivity following selection was not met, as all stocks showed increased radiosensitivity (Tables 1, 3, and 5). However, the difference between XRS-Cont and the other stocks in the third generation was smaller than in the second generation, indicating that selection may be having an effect. Calculations indicate

that a small response to selection per generation is expected, and therefore it is premature to judge after only three generations whether selection is effective. The possibility of inbreeding depression being the cause of the increased radiosensitivity is not very likely because of the large population size of adults in a given stock (approximately 500), and the few generations for possible inbreeding.

A likely explanation is that the stocks have X-ray induced point mutations and chromosomal damage which are lowering viability, hatchability, and productivity as well as increasing radiosensitivity; because the effects of these mutations are opposite to that of selection.

Another possibility is that there is genetic slippage (Pirchner, 1969). The stocks do better at the selection dose, but worse at the other doses, causing a steeper slope for the regression lines. The results of future generations will help determine whether selection is effective, and what is the cause of the increased radiosensitivities.

REFERENCES

Falconer, D., 1960. Introduction to quantitative genetics. The Ronald Press, New York.

Heinze, W., 1971. Unpublished experimental results.

Lane, G., 1951. X-ray fractionation and chromosomal breakage. Heredity, 5, 1-35.

Muller, H., 1927. Artificial transmutation of the gene. Science, 66, 84-87.

Muller, H., 1954. The nature of genetic effects produced by radiation. In Radiation biology, 351-473 (Alexander Hollaender, Ed., McGraw-Hill, New York).

Osborne, R. & F. DeGeorge, 1959. Genetic basis of morphological variation. Harvard, Cambridge.

Pirchner, F., 1969. Population genetics in animal breeding. W. H. Freeman, San Francisco.

Sax, K., 1952. The effect of fractional X-ray dosage on the frequency of chromosomal aberrations. Heredity, 6, 127-131.

Welch, Q., 1969. A genetic interpretation of variation in human growth patterns. Ph. D. dissertation, Univ. of California, Berkeley.

Welch, Q., 1970. A genetic interpretation of variation in human growth patterns. Behavior Genetics, 1, 157-168.

Table 1. Regression equations for G_0.*

Stock	Equation
XRS #1	$Y = -0.22 - 8.5 \times 10^{-4} X$
XRS #2	$Y = +0.03 - 7.0 \times 10^{-4} X$
XRS #3	$Y = -0.16 - 6.5 \times 10^{-4} X$
XRS #4	$Y = -0.23 - 5.7 \times 10^{-4} X$
XRS #5	$Y = +0.36 - 9.7 \times 10^{-4} X$
XRS #6	$Y = +0.22 - 13.1 \times 10^{-4} X$
XRS #7	$Y = +0.46 - 19.0 \times 10^{-4} X$
XRS-CONT	$Y = +0.47 - 18.4 \times 10^{-4} X$

*Y = percent hatchability

X = dose

Table 2. F-values for regression coefficients of G_0:
H_0: b = 0; H_1: b $\neq$ 0

Stock	b	F	Significance
XRS #1	-8.5×10^{-4}	9.684	$P < 0.05$
XRS #2	-7.0×10^{-4}	5.236	$P < 0.10$
XRS #3	-6.5×10^{-4}	2.631	$P < 0.25$
XRS #4	-5.7×10^{-4}	1.776	$P < 0.50$
XRS #5	-9.7×10^{-4}	3.552	$P < 0.25$
XRS #6	-13.1×10^{-4}	11.121	$P < 0.05$
XRS #7	-19.0×10^{-4}	44.041	$P < 0.005$
XRS-CONT	-18.4×10^{-4}	181.570	$P < 0.001$

0 0 0 0 3 7 0 0 8 3 1

Table 3. Regression equations for F_2.*

Stock	Equation
XRS #1	$Y = +0.88 - 27.9 \times 10^{-4} X$
XRS #2	$Y = +0.90 - 28.3 \times 10^{-4} X$
XRS #3	$Y = +0.79 - 27.6 \times 10^{-4} X$
XRS #4	$Y = +0.58 - 25.6 \times 10^{-4} X$
XRS #5	$Y = +0.79 - 28.6 \times 10^{-4} X$
XRS #6	$Y = +0.68 - 23.6 \times 10^{-4} X$
XRS #7	$Y = +0.10 - 15.9 \times 10^{-4} X$
XRS-CONT	$Y = +0.40 - 18.3 \times 10^{-4} X$

*Y = percent hatchability
X = dose

Table 4. F-values for regression coefficients of F_2: H_0: b = 0; H_1: b $\neq$ 0.

Stock	b	F	Significance
XRS #1	-27.9×10^{-4}	28.256	$P < 0.01$
XRS #2	-28.3×10^{-4}	72.183	$P < 0.005$
XRS #3	-27.6×10^{-4}	82.519	$P < 0.001$
XRS #4	-25.6×10^{-4}	110.085	$P < 0.001$
XRS #5	-28.6×10^{-4}	85.858	$P < 0.001$
XRS #6	-23.6×10^{-4}	65.112	$P < 0.005$
XRS #7	-15.9×10^{-4}	21.321	$P < 0.01$
XRS-CONT	-18.3×10^{-4}	93.672	$P < 0.001$

Table 5. Regression equations for F_3.*

Stock	Equation
XRS #1	$Y = +0.72 - 26.5 \times 10^{-4} X$
XRS #2	$Y = +0.96 - 30.0 \times 10^{-4} X$
XRS #3	$Y = +0.73 - 23.8 \times 10^{-4} X$
XRS #4	$Y = +1.17 - 31.6 \times 10^{-4} X$
XRS #5	$Y = +0.16 - 16.1 \times 10^{-4} X$
XRS #6	$Y = +1.04 - 33.6 \times 10^{-4} X$
XRS #7	$Y = +0.75 - 27.7 \times 10^{-4} X$
XRS-CONT	$Y = +0.72 - 25.7 \times 10^{-4} X$

*Y = percent hatchability
X = dose

Table 6. F-values for regression coefficients of F_3: H_0: b = 0; H_1: b $\neq$ 0.

Stock	b	F	Significance
XRS #1	-26.5×10^{-4}	54.499	$P < 0.005$
XRS #2	-30.0×10^{-4}	58.644	$P < 0.005$
XRS #3	-23.8×10^{-4}	178.702	$P < 0.001$
XRS #4	-31.6×10^{-4}	35.237	$P < 0.005$
XRS #5	-16.1×10^{-4}	78.765	$P < 0.001$
XRS #6	-33.6×10^{-4}	36.767	$P < 0.005$
XRS #7	-27.7×10^{-4}	117.379	$P < 0.001$
XRS-CONT	-25.7×10^{-4}	101.882	$P < 0.001$

Table 7. t-Values of comparison of regression coefficients of $G_0(b_0)$ to $F_2(b_2)$: H_0: $b_0 = b_2$; H_1: $b_0 \neq b_2$.

Stock	t	Significance
XRS #1	6.629	$P < 0.01$
XRS #2	9.541	$P < 0.001$
XRS #3	8.464	$P < 0.005$
XRS #4	8.114	$P < 0.005$
XRS #5	6.381	$P < 0.001$
XRS #6	4.330	$P < 0.05$
XRS #7	1.398	$P < 0.40$
XRS-CONT	0.043	$P < 0.90$

Table 8. t-Values of comparisons of regression coefficients of $G_0(b_0)$ to $F_3(b_3)$: H_0: $b_0 = b_3$; H_1: $b_0 \neq b_3$.

Stock	t	Significance
XRS #1	26.212	$P < 0.001$
XRS #2	9.359	$P < 0.001$
XRS #3	10.177	$P < 0.001$
XRS #4	7.642	$P < 0.005$
XRS #5	2.379	$P < 0.10$
XRS #6	6.095	$P < 0.01$
XRS #7	4.574	$P < 0.05$
XRS-CONT	5.103	$P < 0.01$

0 0 0 0 3 7 0 5 0 3 4

Table 9. t-Values for comparison of regression coefficients of $F_2(b_2)$ to $F_3(b_3)$: H_0: $b_2 = b_3$; H_1: $b_2 \neq b_3$.

Stock	t	Significance
XRS #1	8.065	$P < 0.005$
XRS #2	0.648	$P < 0.75$
XRS #3	2.181	$P < 0.10$
XRS #4	2.069	$P < 0.20$
XRS #5	7.051	$P < 0.005$
XRS #6	3.225	$P < 0.05$
XRS #7	5.559	$P < 0.01$
XRS-CONT	4.713	$P < 0.01$

FIGURE LEGENDS

Fig. 1. Dose responses of the XRS lines in the generation before selection (unit weighting, normalized to nonirradiated controls).

Fig. 2. Dose responses of the XRS lines following two generations of selection (unit weighting, normalized to nonirradiated controls).

Fig. 3. Dose responses of the XRS lines following three generations of selection (unit weighting, normalized to nonirradiated controls).

Fig. 4. Comparison of the dose responses of XRS I in three generations.

Fig. 5. Comparison of the dose responses of XRS II in three generations.

Fig. 6. Comparison of the dose responses of XRS III in three generations.

Fig. 7. Comparison of the dose responses of XRS IV in three generations.

Fig. 8. Comparison of the dose responses of XRS V in three generations.

Fig. 9. Comparison of the dose responses of XRS VI in three generations.

Fig. 10. Comparison of the dose responses of XRS VII in three generations.

Fig. 11. Comparison of the dose responses of XRS control in three generations.

0 0 0 0 3 7 0 0 3 3 3

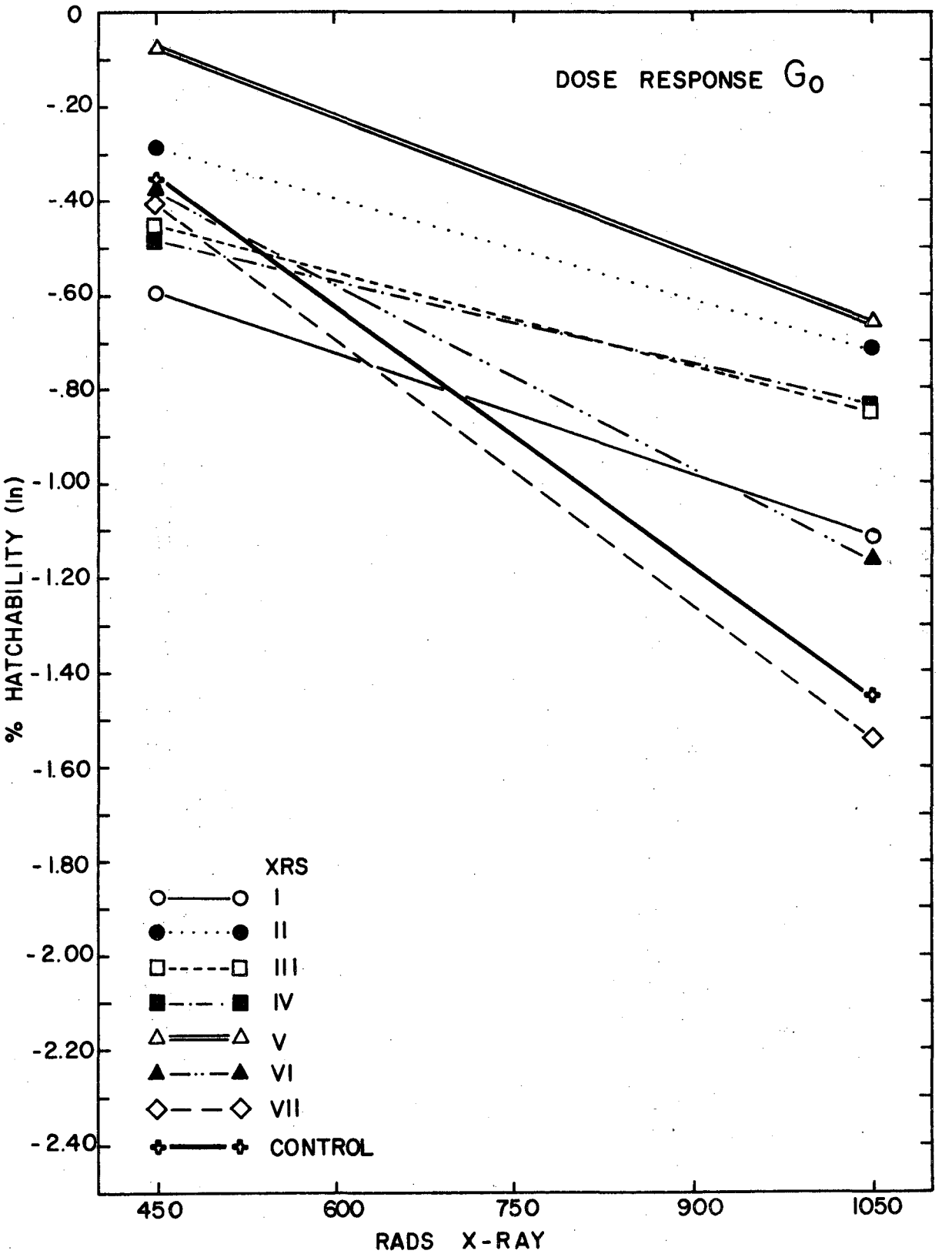

Fig. 1

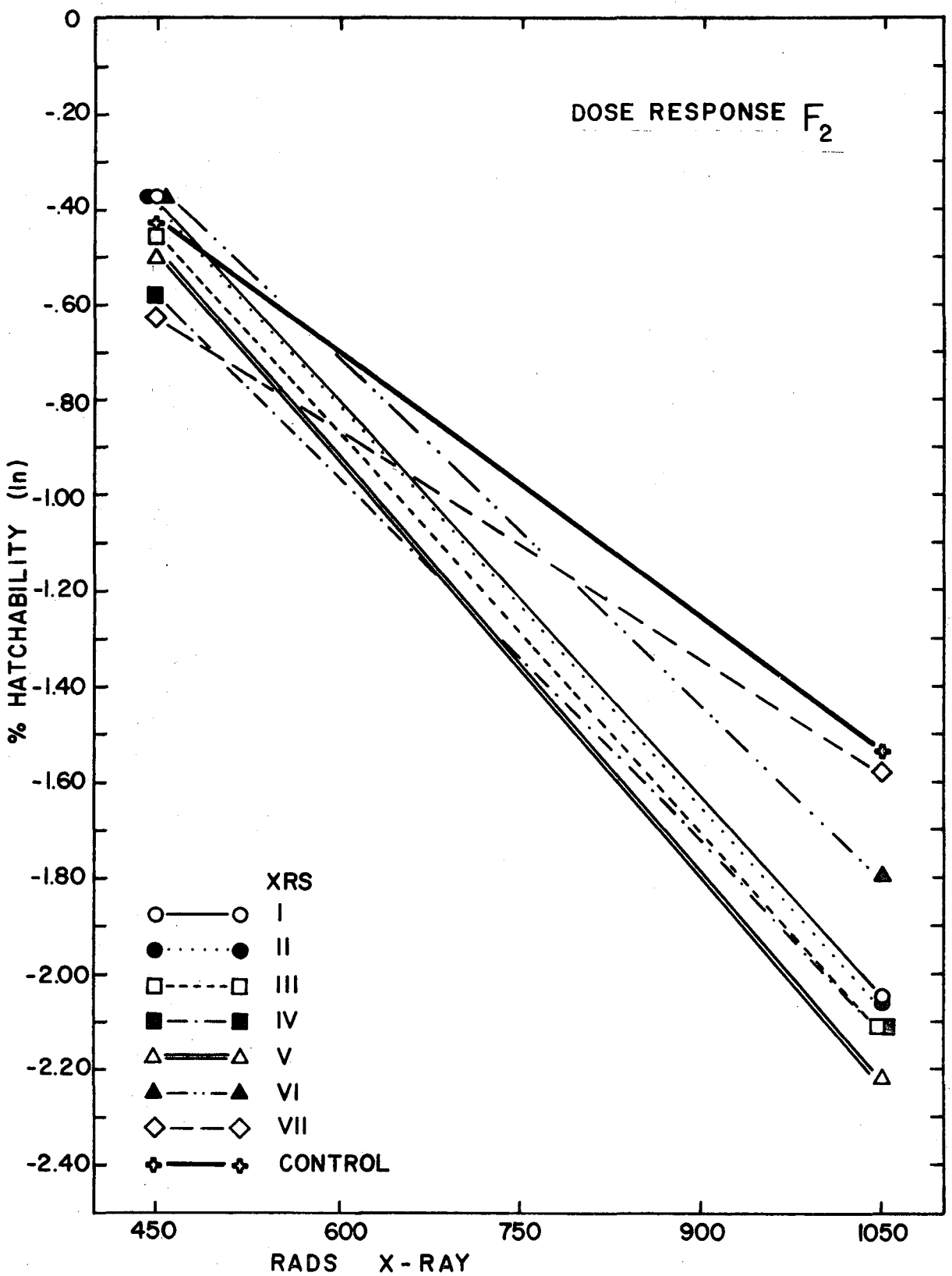
DOSE RESPONSE F_2
% HATCHABILITY (ln)
0
-.20
-.40
-.60
-.80
-1.00
-1.20
-1.40
-1.60
-1.80
-2.00
-2.20
-2.40
450
600
750
900
1050
RADS X-RAY
XRS
I
II
III
IV
V
VI
VII
CONTROL

Fig. 2

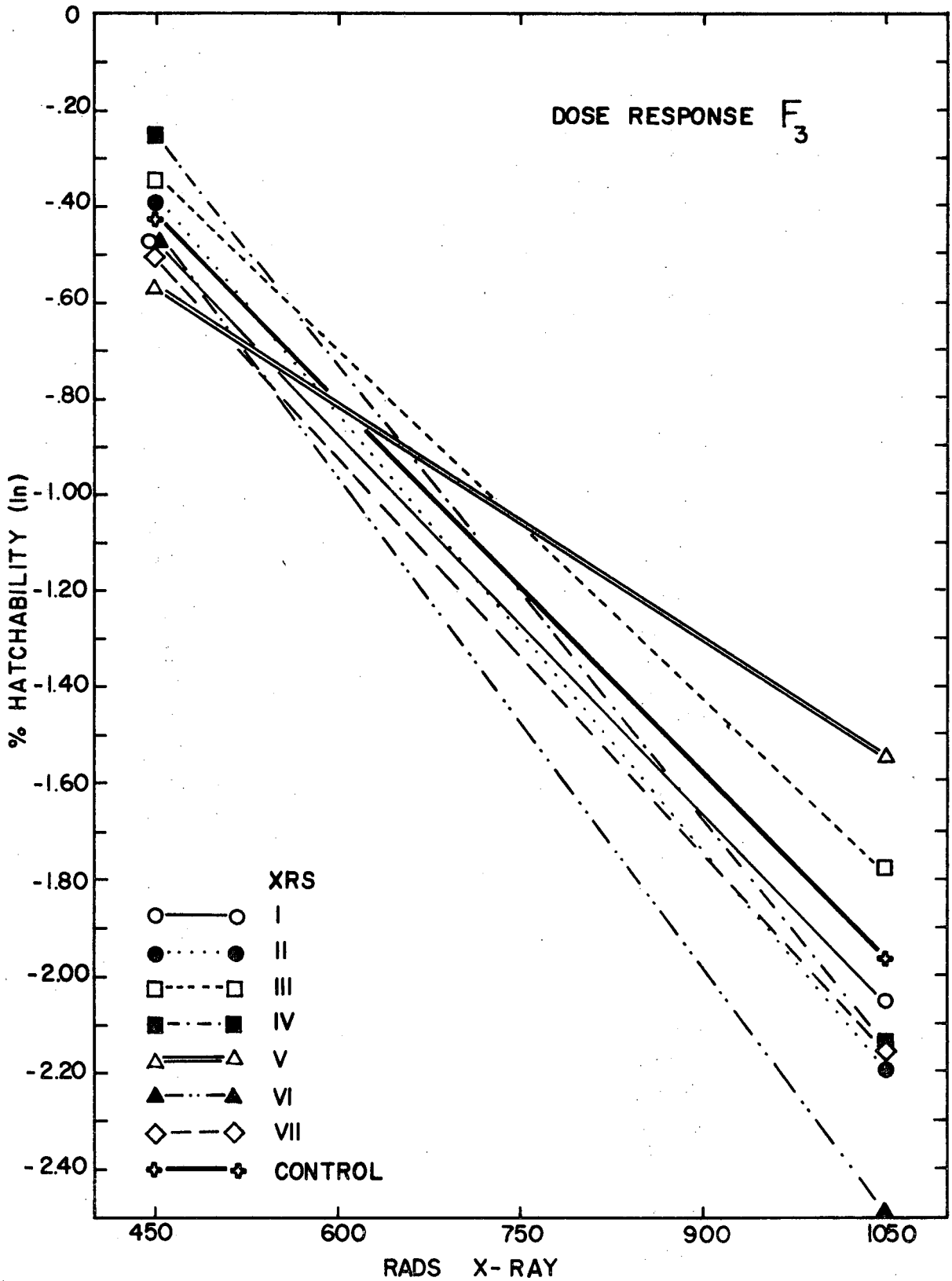
DOSE RESPONSE F_3
% HATCHABILITY (ln)
0
-.20
-.40
-.60
-.80
-1.00
-1.20
-1.40
-1.60
-1.80
-2.00
-2.20
-2.40
450
600
750
900
1050
RADS X- RAY
XRS
I
II
III
IV
V
VI
VII
CONTROL

Fig. 3

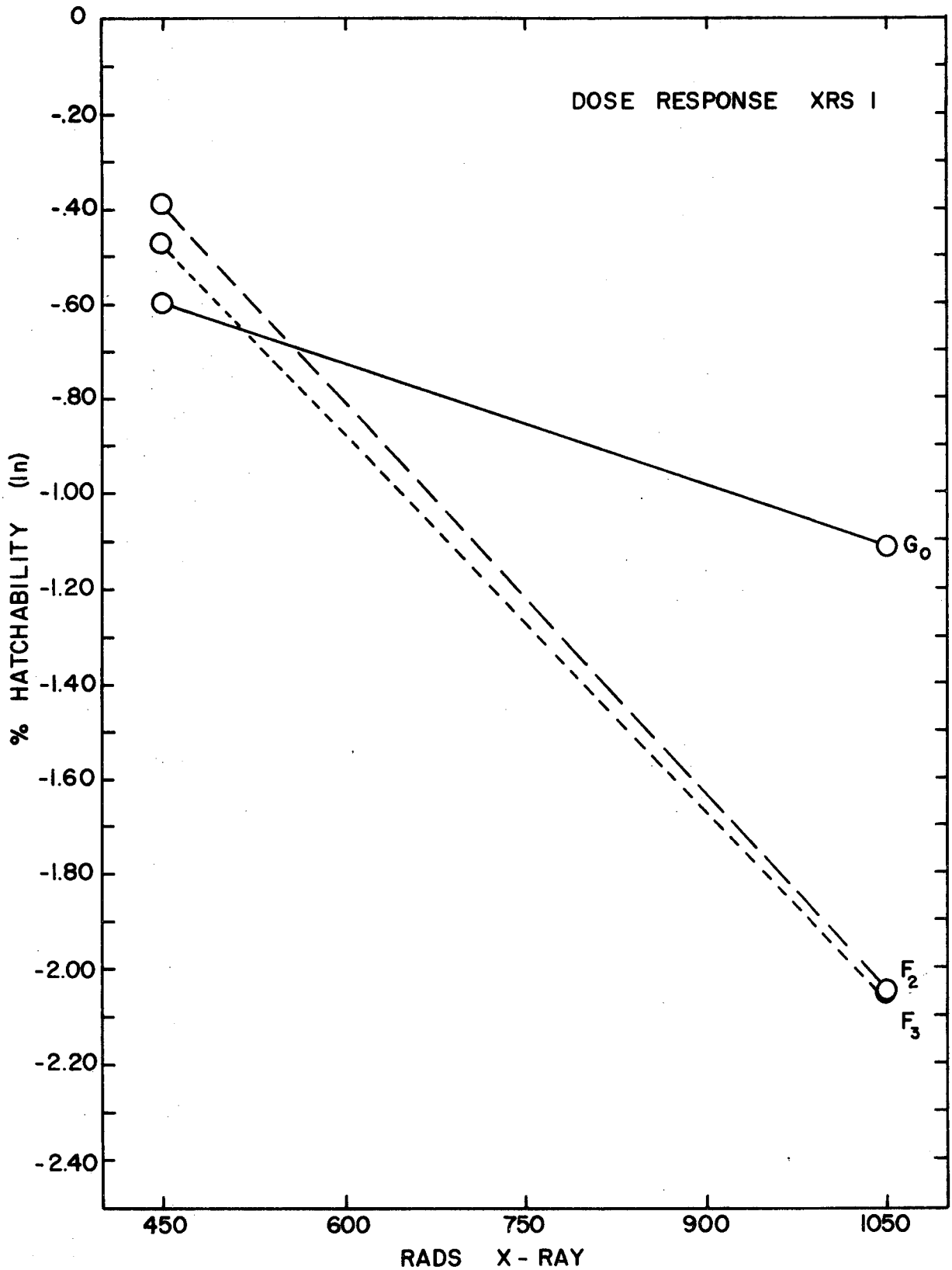
DOSE RESPONSE XRS I
% HATCHABILITY (ln)
0
-.20
-.40
-.60
-.80
-1.00
-1.20
-1.40
-1.60
-1.80
-2.00
-2.20
-2.40
450
600
750
900
1050
RADS X - RAY
G_0
F_2
F_3

Fig. 4

0 0 0 0 3 7 0 5 0 3 7

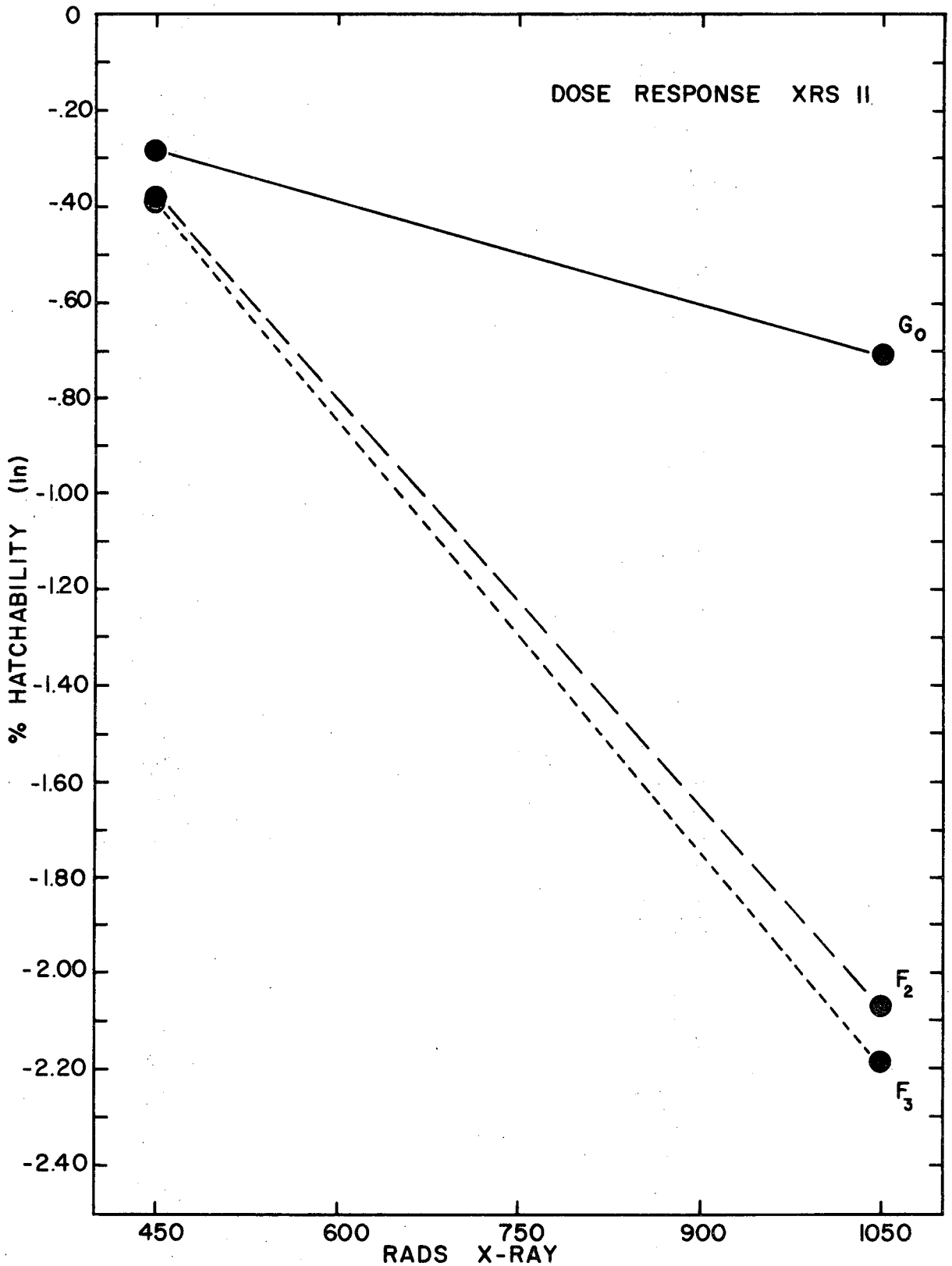

Fig. 5

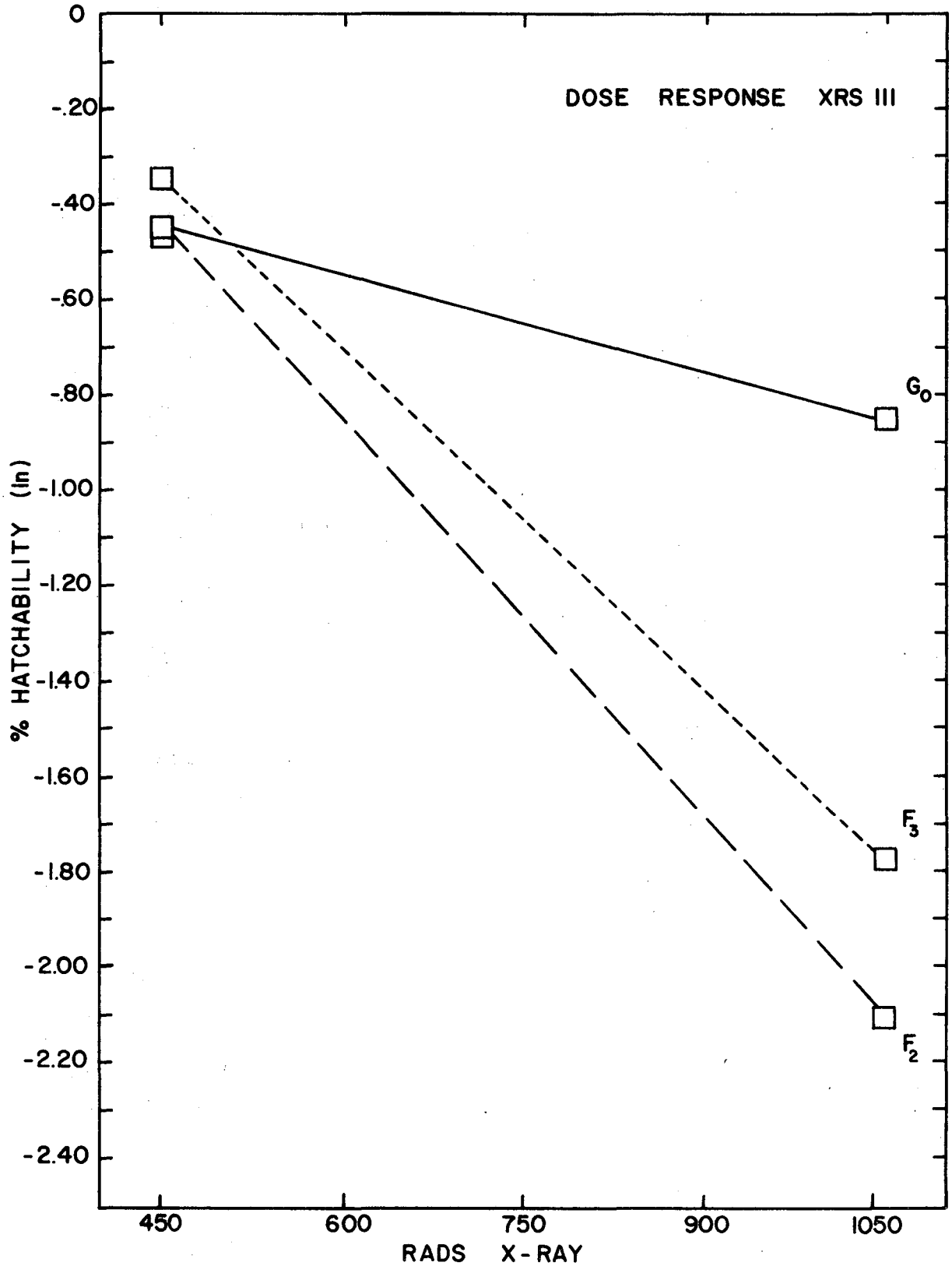
DOSE RESPONSE XRS III
% HATCHABILITY (ln)
0
-.20
-.40
-.60
-.80
-1.00
-1.20
-1.40
-1.60
-1.80
-2.00
-2.20
-2.40
450
600
750
900
1050
RADS X-RAY
G_0
F_3
F_2

Fig. 6

0 0 0 0 5 7 0 0 3 8

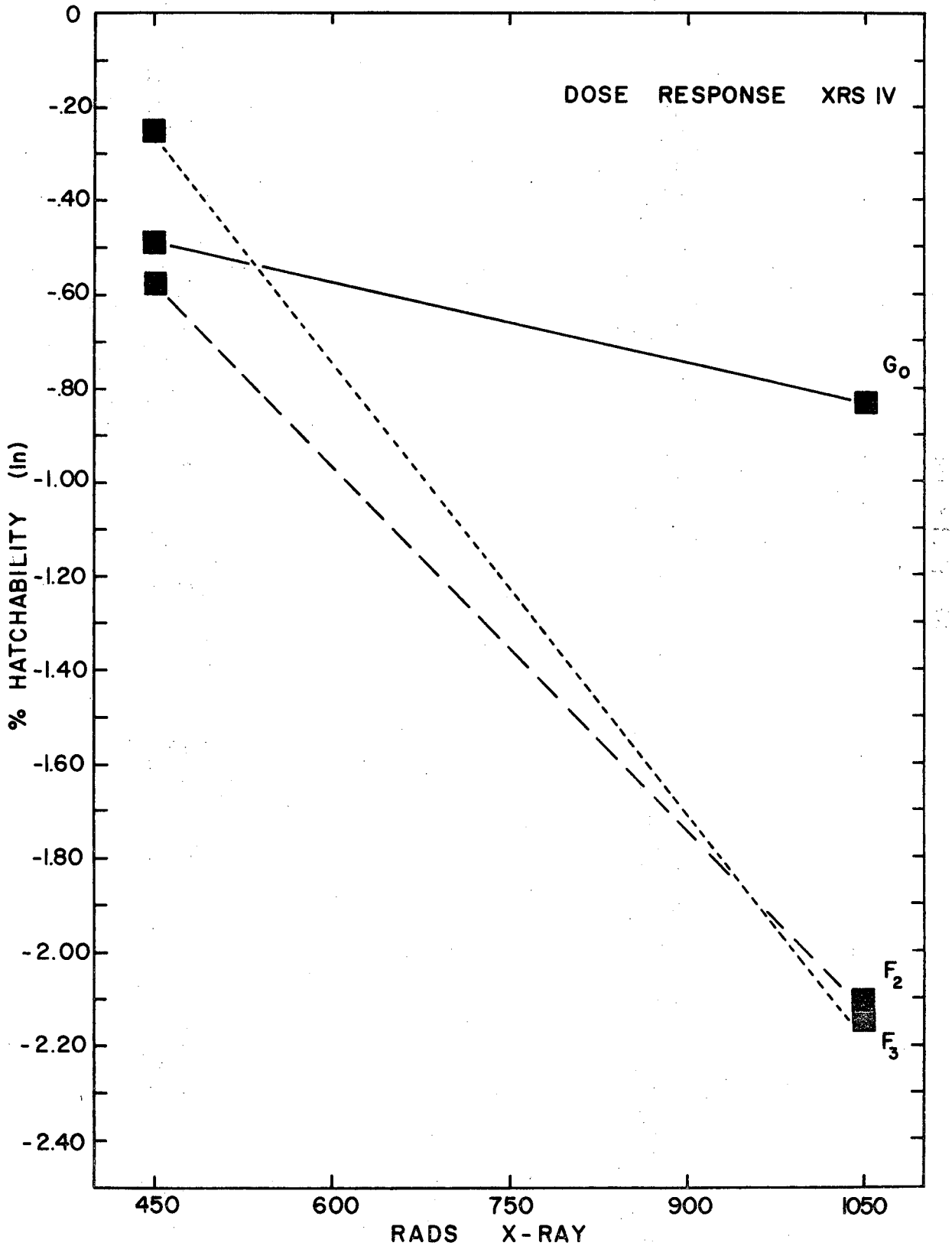

Fig. 7

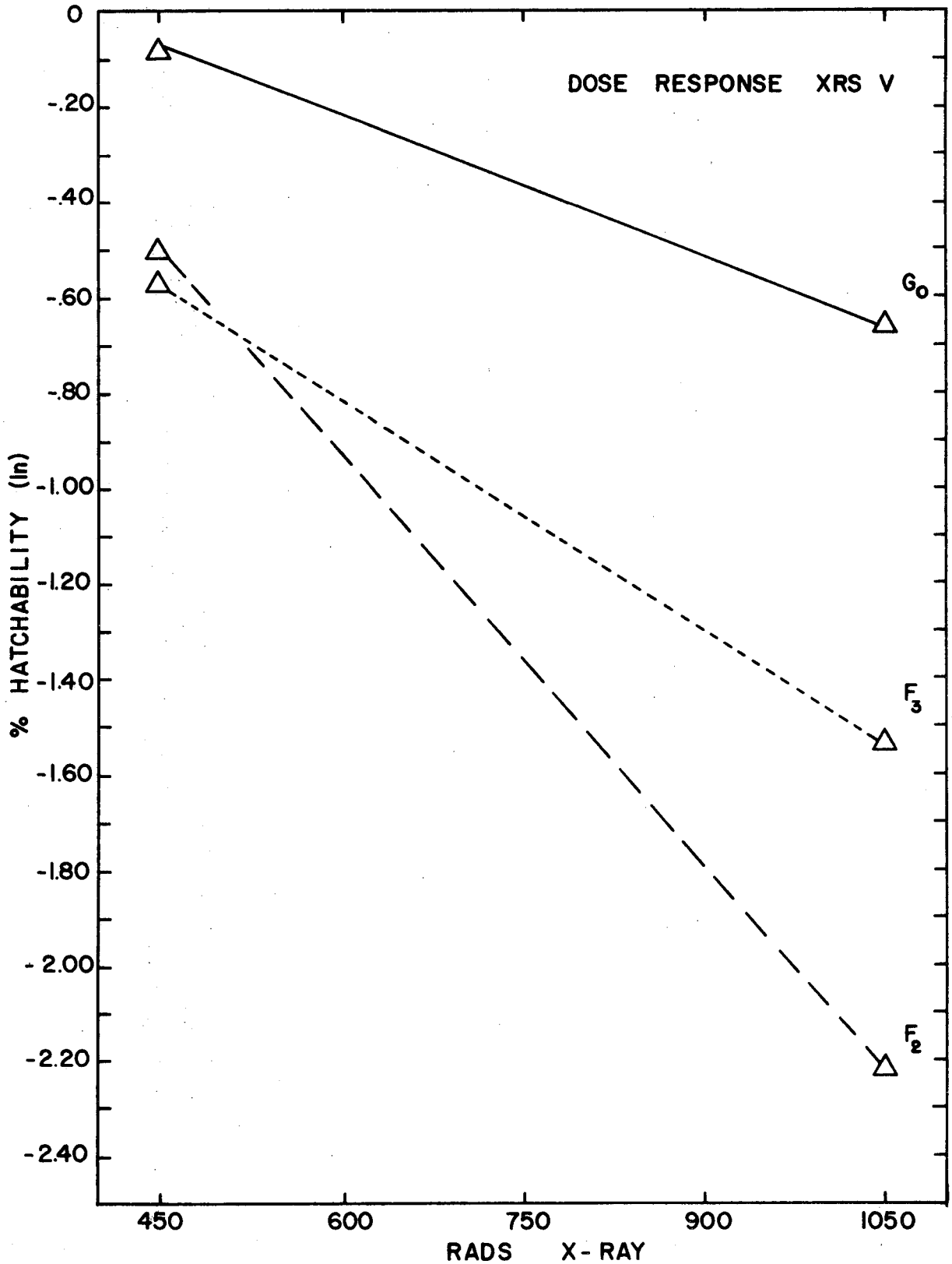
DOSE RESPONSE XRS V
% HATCHABILITY (ln)
0
-.20
-.40
-.60
-.80
-1.00
-1.20
-1.40
-1.60
-1.80
-2.00
-2.20
-2.40
450
600
750
900
1050
RADS X-RAY
G_0
F_3
F_2

Fig. 8

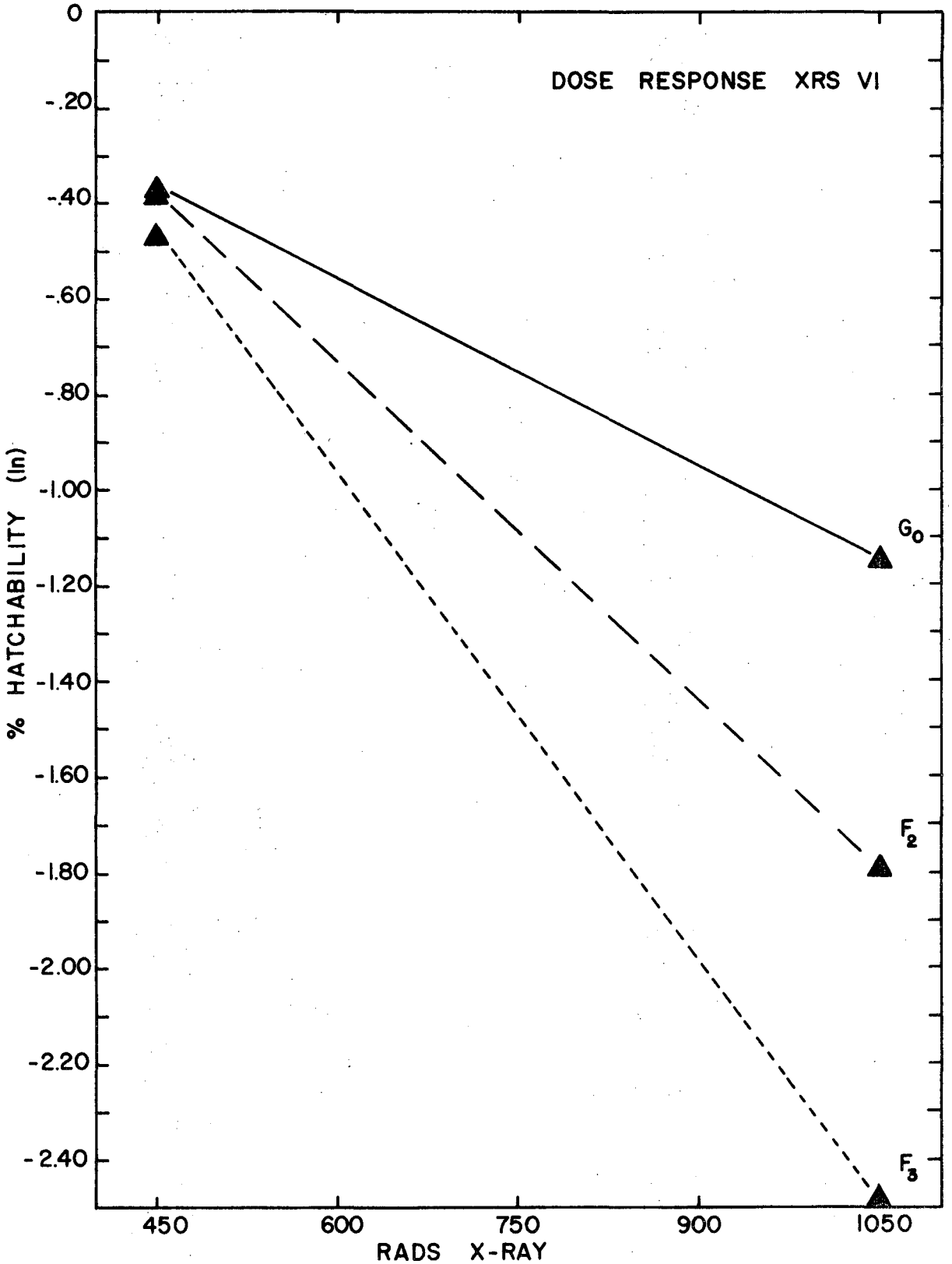
DOSE RESPONSE XRS VI
% HATCHABILITY (ln)
0
-.20
-.40
-.60
-.80
-1.00
-1.20
-1.40
-1.60
-1.80
-2.00
-2.20
-2.40
450
600
750
900
1050
RADS X-RAY
G_0
F_2
F_3

Fig. 9

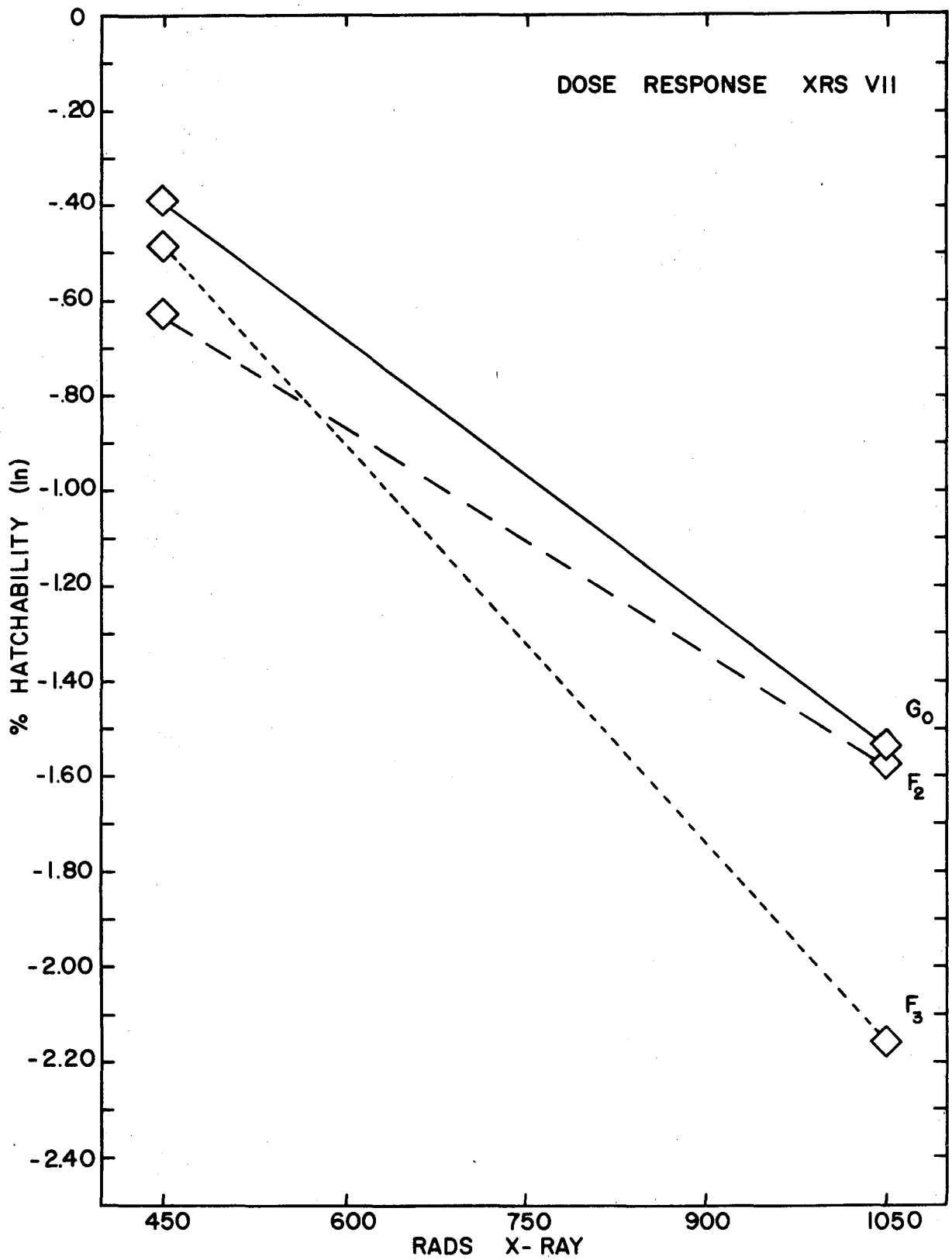
DOSE RESPONSE XRS VII
% HATCHABILITY (ln)
0
-.20
-.40
-.60
-.80
-1.00
-1.20
-1.40
-1.60
-1.80
-2.00
-2.20
-2.40
450
600
750
900
1050
RADS X- RAY
G_0
F_2
F_3

Fig. 10

0 0 0 0 3 7 0 3 8 4 0

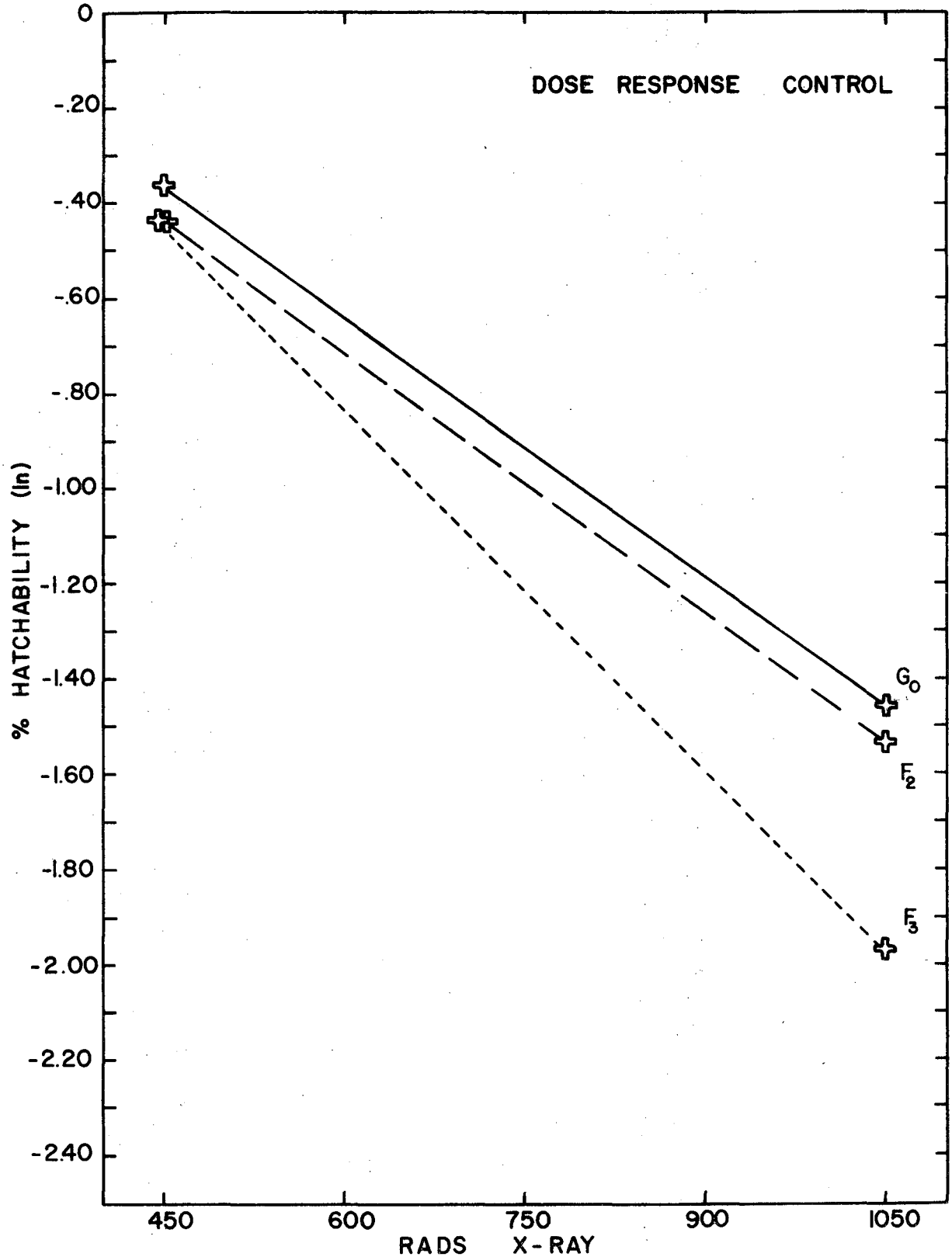

Fig. 11

0 0 0 0 3 7 0 0 8 4 1

RADIOBIOLOGY OF NEURONS IN CULTURE

RADIOBIOLOGICAL STUDIES WITH EXPLANTED CEREBELLAR TISSUE

A. Mamoon, W. Schlapfer, B. Gahwiler, and C. Tobias

Donner Laboratory, University of California, Berkeley, California 94720

and

J. Miquel and W. Haymaker

Ames Research Center, NASA
Moffett Field, California 94035

The estimation of biological effects of heavy primary cosmic rays on the nervous system is made exceedingly difficult by several factors. First, the instantaneous intensity of cosmic radiation is low; it is difficult and expensive to expose mammals to these rays for an adequate time interval. Balloon experiments have resulted in ambiguous results. Secondly, until very recently heavy particles with $Z \geqslant 2$ were not available at accelerators with sufficient energy so that the particles could penetrate the skull or some other part of the body to impinge on synaptic structures. Thirdly, nerve tissue is an exceedingly complex array of billions of cells. The most essential of these, the neurons, are in "G_0" state; they do not divide during the life-span of the animals. Methods to study nondividing cells and radiobiological techniques to measure these effects have not been developed sufficiently well to give unambiguous results. Finally, test such as electroencephalography and performance tests rely on simultaneous function of very large numbers of neurons and since the nervous system has functional redundance the tests may not possess sufficient sensitivity

to detect microlesions. Histopathologically, usually relatively large doses of x rays are necessary to demonstrate unambiguous deleterious effects. In spite of this, functionally, exceedingly small doses (less than one rad) of radiation can be detected by specialized receptor systems and there are claims that relatively small doses of radiation (e.g. a few rads) have lasting effects on conditional reflexes. Radiation greater than 25 rad can change the electroshock seizure threshold in rats in a permanent manner.

In an attempt to understand radiation effects on nerve tissue in a quantitative manner, we have initiated a series of studies on mammalian neurons explanted and existing over a period of several weeks in tissue culture. Methods were found to grow these cultures in a thin layer, such that they became suitable for exposure to low energy heavy particles accelerated at the Hilac. One set of exposures have been performed to 204 MeV argon beams in 1971, before the accelerator was shut down for alterations. It will function again in early 1972, this time at kinetic energy of 7.5 MeV/nucleon and it will be capable of accelerating very heavy ions, including krypton (34) and xenon (54). With the availability of heavy ion beams of several Bev kinetic energy at the Bevatron, it will soon become feasible to expose thicker cultures to nitrogen and perhaps to neon beams. The brains of a group of pocket mice have already been exposed to slowed 270 MeV/nucleon nitrogen beams. In this report we shall briefly summarize the techniques and preliminary results and indicate some of the unsolved problems.

Methods

Cultures from rat cerebellum: Explants (about 1 mm^3 in volume and 1 mm thick) from newborn (1-3 day old) rat cerebella were used. The explants were embedded in a plasma clot and incubated at 36° C in roller tubes. The explants were fed with medium compound of: 25% heat inactivated calf serum, 25% balanced salt solution, and 50% basal Eagle's medium. The medium was enriched with glucose up to a net concentration of about 6 mg/ml. Cultures were fed weekly. Blood vessels and any pre-existing myelin degenerated upon explantation. The techniques and references are described in detail in (1) and (2).

Morphology and function of the cerebellar cultures: Probably because of loss of nutrition, via the blood circulation, and anoxia, the cultures initially exhibit pathological alterations. Many cells die. During the first few days signs of degeneration are prevalent. Cell debris and numerous macrophages can be seen. In the roller tube culture, however, within about ten days the surviving cells appear to be approaching normal morphology.

After about three weeks the central portion of the cultures flatten out to about 100 μM in thickness. In this portion of about 1-mm^2-cross section, eventually about 100 Purkinje cells and about 10,000 glial cells and microneurons develop a neural net made up from the cell bodies and axonal, dendritic and glial processes. In addition, other cell types such as macrophages and ependymal cells are often also present. The central region becomes transparent to light and it is possible to examine

cells by the use of phase microscopy (Fig. 1a, b, c) individually and to apply glass microelectrodes to them in order to measure their electrical activities.

At the periphery of the 1 mm^2 central region one finds a mound of cells, probably glia and microneurons wandering to the culture edge. Still further out (sometimes at 3 to 5 mm distance) a network of dendrites, axons, glial processes and migrating cells is steadily expanding.

The cells in the central region were examined morphologically by standard staining methods (Fig. 2a, b) and by electron microscopy. The neurons appear to have normal morphology and are spread in a monolayer (Fig. 3). Abundant myelination is present in most cultures by two weeks and many synapses are present. The cultures metabolize glucose.

Such cultures live for approximately eight weeks in the Laboratory (no effort was made to attain a "maximum" life span). After several weeks they begin to show standard signs of aging (e.g. generalized vacuolization) and eventually degenerate. The cultures are also susceptible to contamination since no antibiotics are used in the feeding medium.

Because of the monolayer nature of the cultures, we can change the nutritional milieu <u>during</u> an experiment.

<u>Comparison to other techniques:</u> We believe that currently ours is among the first laboratories where functional cerebellar monolayers have been achieved. Roller tube cultures fed with medium used by Hild (3), which is different from ours, are generally thicker than a monolayer. Cultures by the Maximow technique (4) are several cell

layers in thickness, which makes it difficult to identify the source of recorded electrical activity. Rose chamber cultures (5) are difficult to use for microelectrode work and usually have variable thickness. Many others have attempted to isolate single neurons or to grow "pure" neural cultures as in the case of neuroblastoma isolates. Proliferating glial cultures are also obtainable. However, as far as is known to the authors, in none of these cases has electrical communication or synapse formation between neighboring cells been demonstrated.

Spontaneous electrical activity: External microelectrodes placed against the soma of one of a large neuron, usually a Purkinje cell, record spontaneous action potentials. In a normal culture the majority of the cells have such action potentials. We have described these previously and only summarize them here.

1. At constant environmental conditions the average firing rate from the same neuron is constant. In order to realize appropriate conditions, a thermostated microscope substage was built (see following paper).

2. Increase in temperature doubles the rate of firing by neurons in about 9° C. In the physiological range (e.g. between 20 and 37° C) the changes in rate of firing are reversible. Temperature changes are discussed.

3. We have analyzed the time pattern of spontaneous neuron activity. Three types of patterns are found:

a. Time intervals between subsequent pulses are random and the time interval spectrum is exponential, except for a small anomaly at small time intervals. The frequency distribution is approximately a Poisson distribution.

b. The impulses follow a periodic pattern; these neurons have pacemaker activity.

c. The impulse distribution is nonrandom and deviates from the Poisson distribution. Autocorrelation studies reveal two or more preferred frequencies. The distribution usually has impulse trains, bursts, and relatively long silent periods. By statistical analysis of the data, we have shown (Schlapfer, Mamoon, Tobias, in prep.) that there is a delayed time correlation between pairs of neurons located near each other. We regard such pairs of neurons as "communicating". The communication in the case of Purkinje neurons is probably not direct, since they do not synapse with each other, but is mediated by microneurons and other cellular components.

4. At present we do not have good microscopic criteria to tell from the morphology of the living culture whether or not its cells are "communicating". The environmental conditions for development and maintenance of communicating cultures appear to be more stringent than those for Poisson or pacemaker activity. Cell density in the cultures is also important. There are usually more active and communicating neurons at the central portion of the cultures if the density of neurons and of glia and microneurons is high. Such activities decrease at the periphery of the cultures.

Agents causing irreversible alterations in neuron activity pattern: Temperature changes are also accompanied by changes in electrical activity patterns (see next two papers by Gahwiler et al.) Above physiological temperature limits (at about 45° C) the neuron activity is

permanently abolished. Micro-laser pulses to the soma of a single neuron at appropriate energy levels can abruptly change the firing pattern. Changes in ionic concentration of mono and divalent cations and many drugs can also alter the electrical activity pattern. Radiation has an immediate as well as a delayed effect. Extracellular electrical stimulation also has immediate as well as delayed effects.

Radiation Studies

A great deal of research has been carried out with heavy ions on proliferating mammalian cell populations. It was determined that accelerated light-heavy ions inhibit colony formation whenever they pass through the cell nucleus and there is some evidence that medium heavy ions can sometimes cause this effect even if they pass through the cell missing the nucleus.

Some neurons in the brain are quite large and possess large nuclei. The nuclei of pyramidal cells and of Purkinje cells have diameters up to 20 μ, whereas microneurons have much smaller nuclei of 4-6 μ. One of our eventual aims is to measure "interaction cross sections" for heavy ions that cause significant deleterious effects in these neurons. Since neurons do not divide we must find criteria other than colony formation for the effect. Initially we are testing three such criteria. These are:

a. Development of neural nets following radiation.

b. Alterations of neuronal communication following radiation.

c. Change in longevity in neurons and glia as evidenced by altered permeability and abnormal histological changes.

Development of Neural Nets Following Radiation

Methods: Rat cerebellar explants were expected right after dissection from the newborn animal to one of the following radiations: 145 kvp x rays, 36 MeV helium ions (Hilac), 54 MeV helium ions (88" cyclotron) and 30 MeV deuterium ions (88" cyclotron). Doses varied from 400-4000 rads. LET of these radiations vary from about 3 keV/μM to about 20 keV/μM. Cultures that developed from control (sham irradiated) as well as irradiated explants were examined at 15 days postirradiation.

Results (Ref. 1): There was a noticable decrease at the high doses in the net area of the culture as evidenced by a reduction in its diameter. Furthermore, at the central area of the culture decreases in cell density were apparent; these decreases were attributed to decreased numbers of glial cells and microneurons. The density of small cells decreased from a level of about $8000/mm^2$ in the control cultures to about 1/10 of that value, $800/mm^2$ in the cultures that received 4000 rad, without appreciable decrease in the density of Purkinje cells, that remained at about $100/mm^2$. Probably as a consequence of the reduced number of glia, appreciable reduction in the myelinization of axons was noticeable already at the lowest dose level, 400 rad. Myelinization was assessed by microscopy in polarized light. Only 50% of the explants (compared to the controls) exhibited myelinization after a dose of 1727 ± 115 rads (mean $\pm$ 1SD). No recovery of myelination was observed in amyelinated cultures during an observation period of one month. The small difference in LET between the different radiations used did not prove to be significant.

The spontaneous electrical activity of irradiated cultures was compared to that of normal cultures at the 15 day period post explantation. Vigorous spontaneous activity was detected in all radiated cultures, with the rate of impulses observed at single cells sometimes higher than in controls. However, practically all the electrical activity was random (Poisson type) or of the pacemaker type. In unmyelinated cultures, often no "preferred" activity pattern or cell to cell communication was found (Schlapfer, Mamoon, Tobias, in prep.) From these findings it would appear that the cultures exposed to radiation at the time of explantation did not properly develop excitatory and inhibitory synapses.

Radiation exposure of cerebellar cultures to accelerated argon ions: A group of fully differentiated cultures, five-weeks old, were exposed to a beam of accelerated argon ions at the Hilac. At that time the cultures had an average thickness of 50 μ. The ions had an energy of approximately 5.1 MeV/nucleon and an LET of approximately 2000 keV/μ at the culture surface, and a range in tissue about 65 μ. Dose levels varied between 7500 rad and 60,000 rad. Prior to irradiation, the cover slips bearing the cultures were transferred under sterile conditions to plastic petri dishes that had very thin mylar covering and fed with medium. Immediately before irradiation, the medium was removed by suction and then replaced after completion of the irradiation. Ten cultures were used per each dose. Controls were sham irradiated. The cultures were then transferred back into the roller tubes and further incubated. At one week postirradiation, the cultures were examined by phase contrast microscopy and then fixed and stained by standard staining methods. Controls and irradiated samples were examined for glycogen

deposits, damage to Niss1 substance and myelin. Loss of large cells as well as small cells was estimated by making an average count of the large cells and mean density of small cells in some cultures before and after irradiation.

The most obvious effects from argon ions at the histological level was increased accumulation of glycogen (Fig. 4) in Purkinje cells and in glia. The fraction of cells where glycogen was demonstrated was abnormal at all dose levels tested and could be fitted by a linear dose-effect relationship, with the rate of appearance of cells with glycogen being 2.87% per 1000 rad (Fig. 5). Only 5% of the controls exhibited demonstrable glycogen granules.

Many of the Purkinje cells also developed abnormal patterns in the distribution of Niss1 substance (chromatolysis) (Fig. 6). The data are not sufficiently accurate to show whether or not this relationship is linear with dose; the average rate of increase in chromatolytic cells at one week postirradiation was 1.42% per thousand rad (Fig. 5). Many small cells, including glia and microneurons, were lost from the culture during the one week postirradiation period, presumably due to pyknosis (Fig. 7a, b) and lysis. The dose effect relationship is shown on (Fig. 8). Of all cell types in the culture Purkinje cells were most resistant to lysis, as shown in (Fig. 9).

These findings were in harmony with the view that all cell types sustained some form of membrane and/or nucleic acid injury due to the argon particles and that histologically the effects of premature aging were seen. In a few cases where moderately irradiated cultures were maintained for more than a week, the inflicted damaged observed at one-week postirradiation seemed to have progressed. Similar obser-

vations were reported by Masurovsky (6) after irradiating rat spinal ganglia with 40 krad X-rays. Long-term study of radiation damage is planned with the heavy beams of the Hilac concurrently with studying the damage produced by equal doses of X-rays. Preliminary experiments with X-irradiation, seem to produce nearly comparable damage, at one week postirradiation, with the intermediate doses of argon particles used. Not many experiments, however, have been done from which to draw definite conclusions. When exposed to hypotonic solutions cells in irradiated cultures seemed to exhibit increased osmotic fragility; however this effect was difficult to quantitate. Further studies are planned with the heavy beams of the Hilac.

Attempts to Observe Immediate Effects of Radiation on Spontaneous Electrical Activity of the Cerebellar Cultures.

Having established that the electrical activity of single neurons has Poisson, Pacemaker and Communicative modes it seemed worthwhile to attempt to find what, if any, immediate effect radiation may have on these activities. This work was started in late Fall 1971 and it is still being continued. The findings reported here must be regarded as preliminary and subject to possible future revision.

The procedure was as follows: Taking a normal culture 14- to 21-days old, a microelectrode is placed on a single neuron from the center of the culture and throughout the experiment electrical activity is being recorded from this neuron. The temperature is kept constant, and balanced salt solution is replenished from time to time via a syringe feed system. The experiment usually is carried out over a period of several hours.

The electrical impulses generated by the neuron under observation are amplified, passed through a pulse height discriminator, and a time interval histogram between successive pulses is prepared by a "computer of average transients" (C. A. T.). The spectral distribution on inter-spike intervals are analyzed before and after exposure of the whole culture to bursts of x rays.

It was clearly established that Pacemaker or Poisson activity of single neurons is exceedingly resistant to radiation: immediate changes occur only if the dose approximates 100,000 rad.

Some effects were noted on neurons that were normally in the "Communicative" mode. This effect may be described as causing a

gradual transition over a period of 2 to 3 hours from the Communicative to the Pacemaker-Poisson modes. We illustrate the effects observed by reproducing the observations from two different experiments in Figs. 10 and 11.

Figure 10 has both differential and integral spike interval spectra. The effects are more clear cut in the integral spectra. These are supposed to be represented on the semilog plots as straight lines of negative slope if the activity is Poisson and deviating from straight lines if it is "communicating". Initially two sets of control spectra were taken. The integral spectra appear to be composed from two or three exponentials, indicating the communicative mode and the two control spectra superimposed exceedingly well. A dose of 500 rad of x ray was given in a period of about two minutes. All the following integral spectra are nearer and nearer a single exponential and a general change in the slope is also seen (about 1/2 hour following the first dose another 5000 rad were added).

Figure 11 show differential interspike interval distribution in another experiment. Four spectral curves are shown, each the average of four distributions, showing normal cells prior to exposure, after 500 rad and after additional doses of 1000 rad and 5000 rad. The whole experiment lasted about three hours and a total of about 100,000 impulses were counted from the same neuron during this interval. The nonrandom behavior of the unirradiated cells is characterized by early, rapid bursts shown by the presence of many short intervals and long silent periods. The four successive curves gradually approach a pattern somewhat characteristic of Pacemakers.

Unfortunately, the significance of these data at present is only suggestive and much more work needs to be done to establish the significance of these findings. A problem exists with controls: each cell ceases to be a control when it receives the first dose of radiation. Mechanical injury to the cell by the tip of the electrode and other effects, not too well defined at present, can also cause transition to the Poisson or Pacemaker states and in a few isolated examples we cannot be certain of the specific causes.

Summary and Discussion

The utility of thin layer cerebellar explants for studies of the development and function of a network of neurons and supporting cells is clearly established.

We have identified spontaneous neuronal impulse patterns which appear to exist in the absnece of informational communication, that is Poisson and Pacemaker patterns. We have also demonstrated that there is a "communicative" state of neurons in culture, when the spike interval distribution does not follow simple Poisson or harmonic behavior. Radiation exposure of explants from newborn rat cerebellum damages glia and microneurons and prevents development of myelinated axons and appears to interfere with electrical "communication" between neurons at high doses.

Recently we have initiated electron microscopy of the cultured neurons and are developing additional cytological methods for demonstrating abnormal permeability of the cell membranes. Both of these approaches promise to increase the sensitivity of detecting radiation damage. Radiation by argon ions of cultures when they are several

weeks old causes a variety of well known pathological developments, including chromatolysis, the appearance of intracellular glycogen and lysis of glia and microneurons. Purkinje cells are quite resistant to radiation: at least 30,000 rad is necessary if they are to lyse within the first week post exposure. The general appearance of radiation effects is equivalent to that of membrane injury and aging response.

Some recent, incomplete experiments suggest that a dose of 500 rad of x rays--or more--causes neurons in "communicative" states to revert into Poisson neurons or Pacemakers. Immediate suppression of Poisson or Pacemaker activity requires dose levels of the order of 100,000 rad.

The authors feel that the technique of studying radiation effects on neurons in culture has much to offer, and that they must understand normal behavior patterns of neurons in parallel with obtaining information on radiation effects. The tools available from the Bevatron, that is beams of penetrating heavy ions will be suitable for work with cell cultures.

It appears desirable to develop heavy ion microbeams also, perhaps at the Hilac so that exposure of portions of individual neurons becomes feasible under the microscope. Simultaneously it will be possible to record electrical activity from the same neuron.

Since different portions of the nervous system have characteristic morphology and specific types of electrical communication, it might be useful to initiate explant cultures of various anatomical regions, e. g. of hypothalamus, cerebrum, retina, hippocampus, etc. The value of pure cultures of glial cells and of neurons from neuroblastoma tumors

are also obvious. We already have culture isolates of these two cell types, and J. Leith in our laboratory has initiated neuron cultures from rat embryos as well.

References

1. Mamoon, A.: Effects of ionizing radiations on myelin formation in rat brain cultures. UCRL-19481 (1969).

2. Schlapfer, W. T.: Bioelectric activity of neurons in tissue culture: synaptic interactions and effects of environmental changes. UCRL-19393 (1969).

3. Hild, W., and Tasaki, I.: Morphological and physiological properties of neurons and glial cells in tissue culture. J. Neurophysiol. 25: 277-304 (1962).

4. Crain, S. M.: Development of "organotypic" bioelectric activities in central nervous tissues during maturation in culture. Internat. Rev. of Neurobiol. 9: 1-43 (1966).

5. Rose, G.: A separable and multipurpose tissue culture chamber. Texas Rep. Biol. Med. 12: 1074-1083 (1954).

6. Masurovsky, E. B., Bunge, M. B.; and Bunge, R. P. Cytological Studies of organotypic cultures of rat dorsal root ganglia following x-irradiation in vitro. I. Changes in neurons and satellite cells J. Cell Biol. 32: 467-496 (1967). II. Changes in Schwann cells, myelin sheaths, and nerve fibers. J. Cell Biol. 32: 497-518 (1967).

0 0 0 0 3 7 0 3 3 4 8

FIGURE CAPTIONS

Fig. 1a. Newborn rat cerebellum explaint after one week of incubation. Notice edge of explant and outgrowing small cells that have many processes. Phase.

Fig. 1b. Large nerve cells (Purkinje cells) from a 4-week-old culture from rat cerebellum. Notice large nucleus and very distinct nucleolus. Phase.

Fig. 1c. Myelinated axon in a 55-day-old culture from rat midbrain. Left part of picture: axon viewed in phase. Right part of picture: same axon in polarized light showing myelin birefringence.

Fig. 2a. Bodian stained nerve cell in a Hilac control culture showing apparently normal nerve cell with neurofibrils inside cell soma and dendrites. Bar represents 10 μ.

Fig. 2b. Cresyl violet stained nerve cells in a Hilac control culture fixed one week from time of experiment, showing apparently normal Nissl substance pattern. Bar represents 10 μ.

Fig. 3. Hilac control culture viewed in phase one week post experiment. Notice many apparently normal large nerve cells. Bar represents 50 μ.

Fig. 4. ^{40}A irradiated culture that was fixed and stained for glycogen one week post irradiation. Notice that not all nerve cells show glycogen. 20,000 rad. Bar represents 20 μ.

Fig. 5. Incidence of glycogen deposits in nerve cells and their chromalolysis with ^{40}A radiation dose. Irradiated and control (sham irradiated) cultures were all fixed and stained one week post irradiation.

Fig. 6. Cresyl violet stained nerve cells in ^{40}A irradiated cultures fixed one week post irradiation (30,000 rad). Bar represents 10 μ.

Fig. 7a. Same as above except dose was 15,000 rad. Notice the darkly stained (pyknotic) small cells. Bar represents 20 μ.

Fig. 7b. Same as above except dose was 30,000 rad. Notice Pyknotic cells and decrease in small cell density. Bar represents 20 μ.

Fig. 8. Change in density of surviving small cells (glia and small nerve cells) with ^{40}A dose. All cultures were fixed and stained one week post irradiation.

Fig. 9. Purkinje cell loss with ^{40}A radiation dose. Notice that nerve cell survival apparently remains unchanged until above a dose of 30,000 rad. All cultures were fixed and stained one week post irradiation.

Fig. 10. Differential and integral time interval spectra of impulses generated by a neuron over a time interval of about 2-1/2 hours. Initially the neurons were in a "communicative" state. The differences are most easily noticeable in the integral curves.

Control 1 and 2: The integral curves have at least two exponential components. Notice that the two control curves superimpose very well. A radiation dose of 500 rad of 150 kvp X-rays was administered.

0 0 0 0 3 7 0 3 8 4 9

Rad 1 and 2: The integral curves are nearer to exponential. There are fewer small time intervals and fewer large time intervals. An additional dose of 1000 rad was given.

Rad 3, 4, 5, and 6: The integral curves are approximating exponential behavior, that is Poisson distribution. The average time intervals increased: the average rate of impulses slowed compared to the control.

Temperature was kept at 33° C.

Fig. 11. Differential time interval spectra are shown for spontaneous electrical impulses from the same neuron, tested over a period of about three hours. Each curve is based on more than 20,000 pulses.

a. Average of four "control" runs, prior to radiation exposure. More events with very short time intervals (bursts) and more with long intervals (silent periods) than any of the distributions following radiation doses.

b. Average of four runs immediately following 500 rad.

c. Average of four runs immediately following an additional 1000 rad.

d. Average of four runs immediately following an additional 500 rad.

Temperature was kept at 36° C.

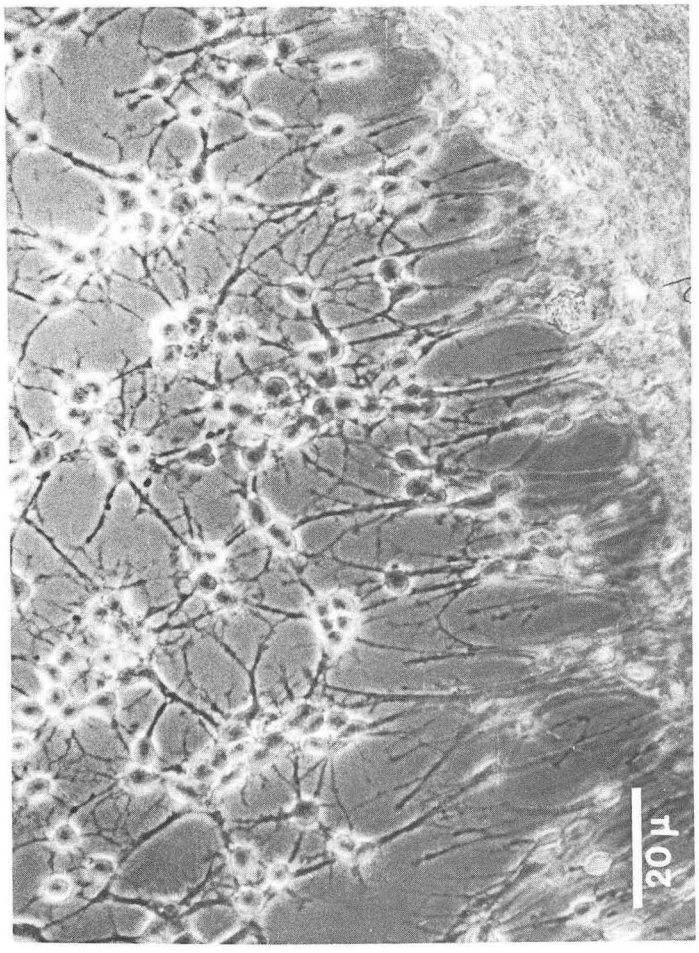

Fig. 1(a)

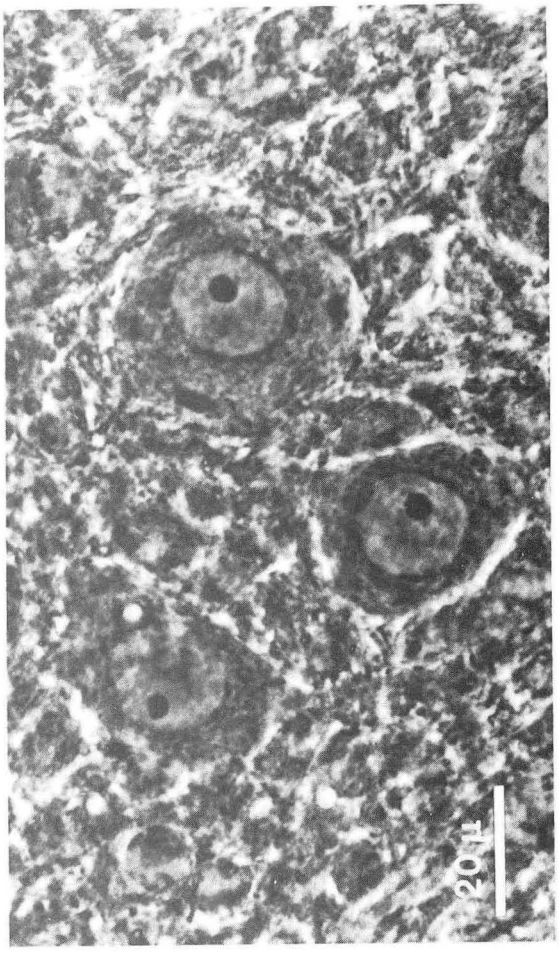

Fig. 1(b)

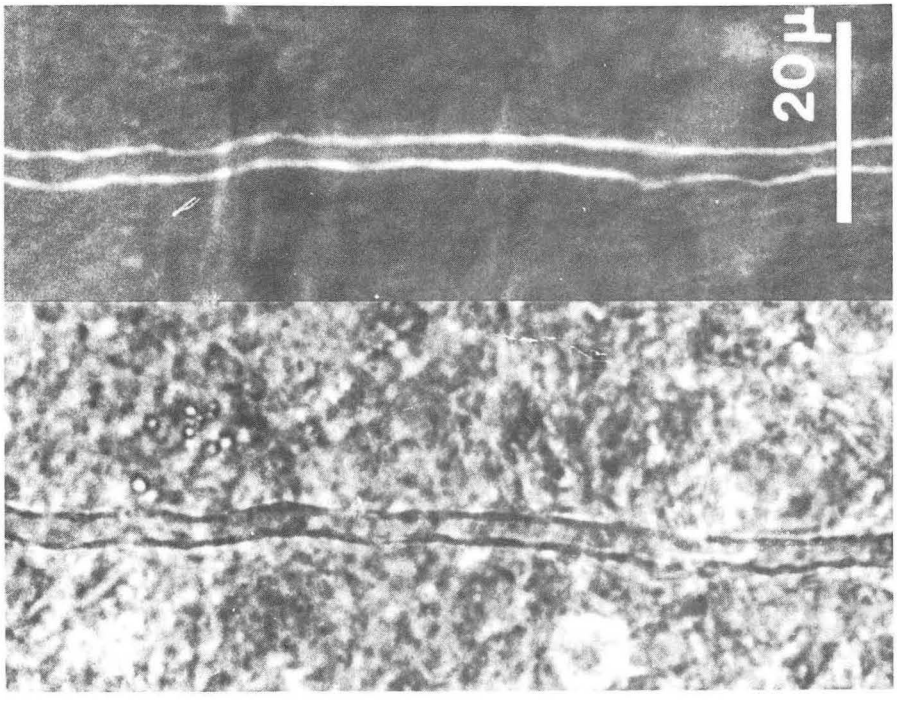

Fig. 1(c)

0 0 0 0 3 7 0 3 3 5 0

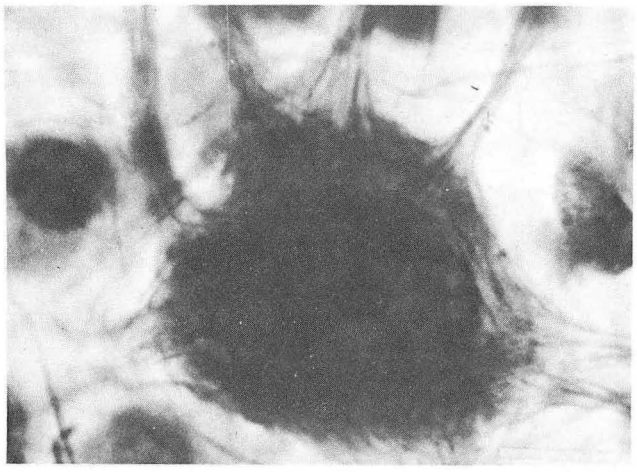

Fig. 2(a)

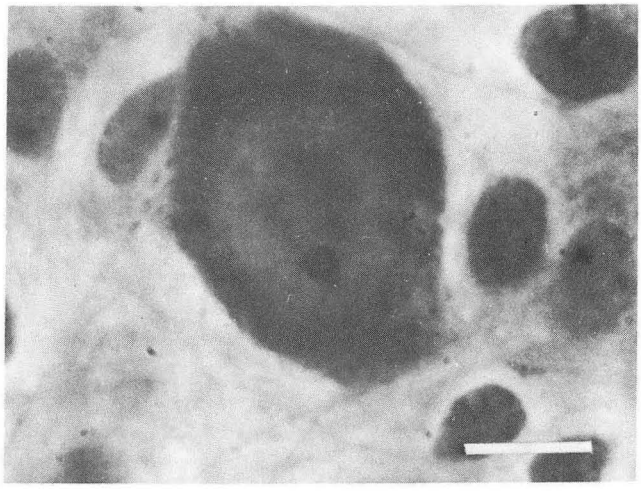

Fig. 2(b)

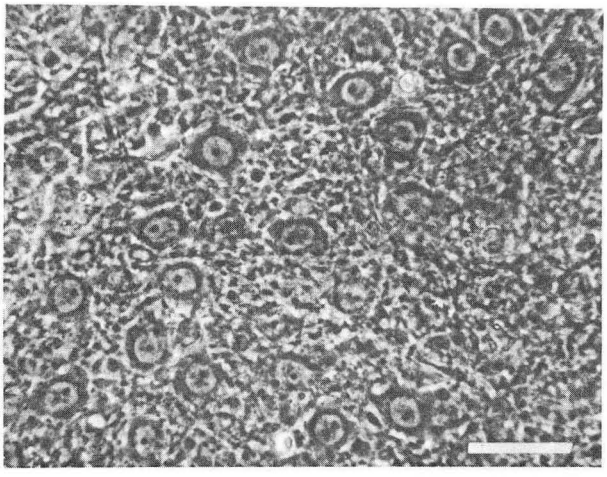

Fig. 3

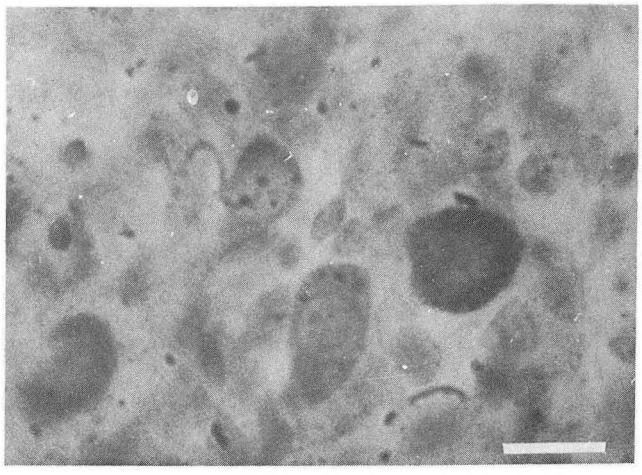

Fig. 4

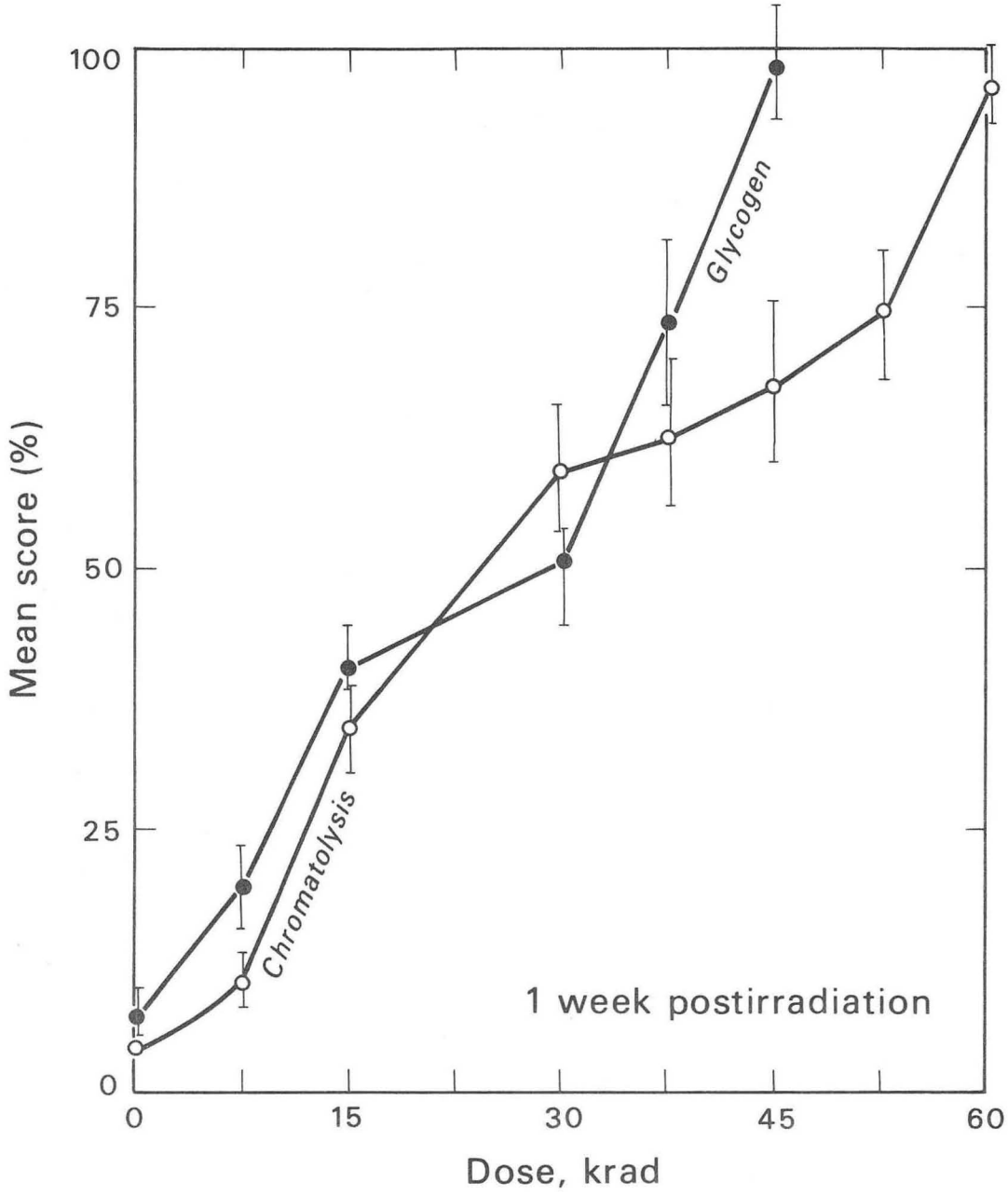

DBL 711 5642

Fig. 5

0 0 0 0 3 7 0 3 8 5 1

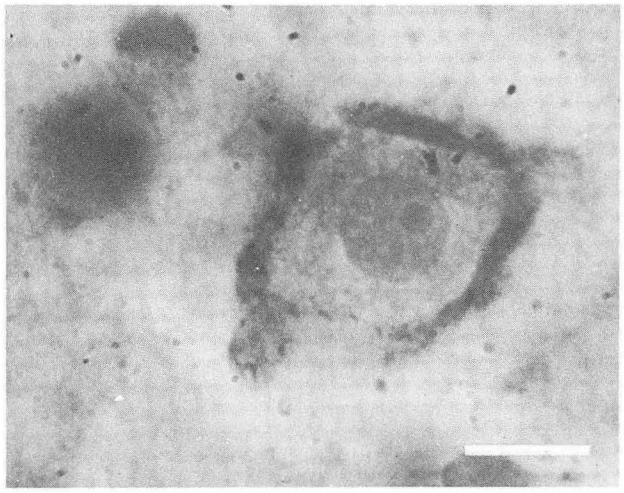

Fig. 6

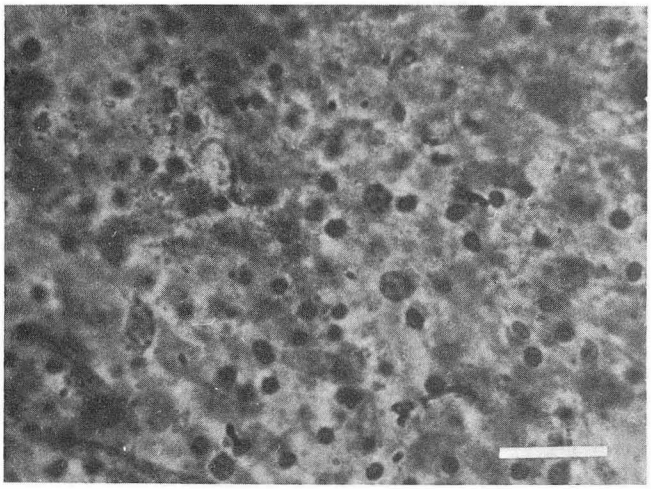

Fig. 7(a)

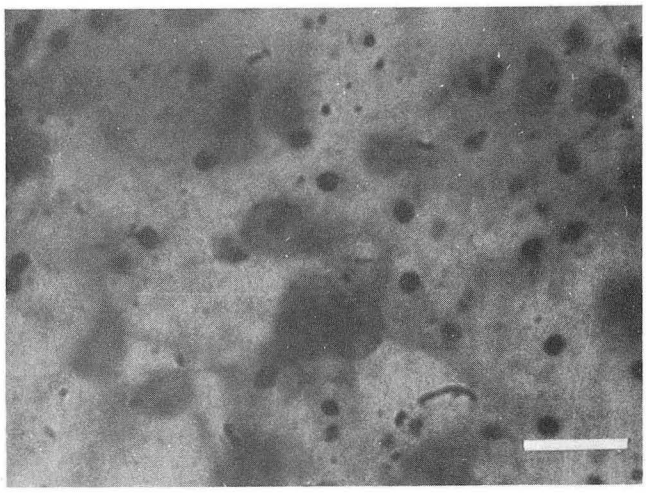

Fig. 7(b)

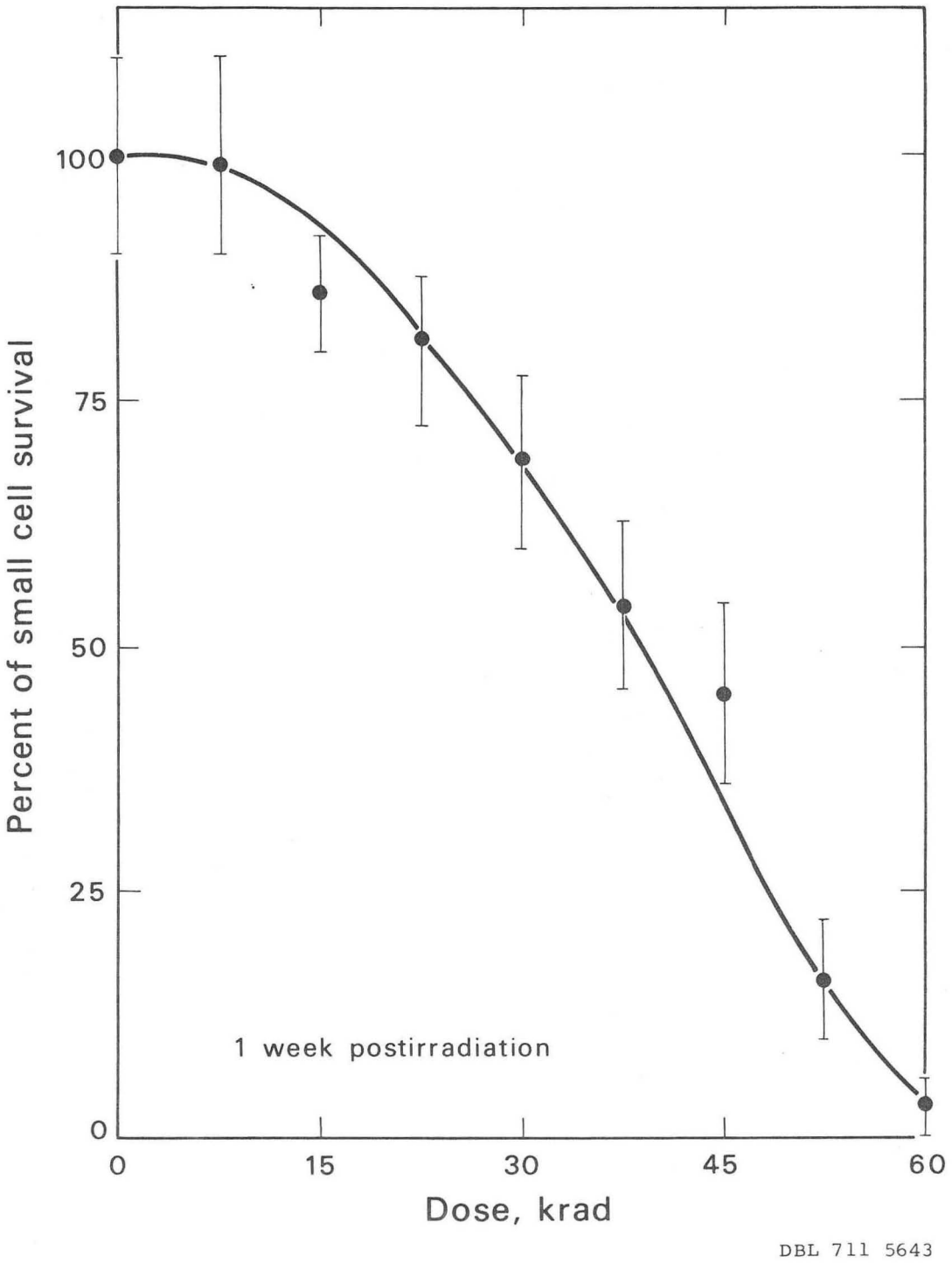
100
75
50
25
0
Percent of small cell survival
1 week postirradiation
0
15
30
45
60
Dose, krad
DBL 711 5643

Fig. 8

0 0 0 0 3 7 0 0 8 5 2

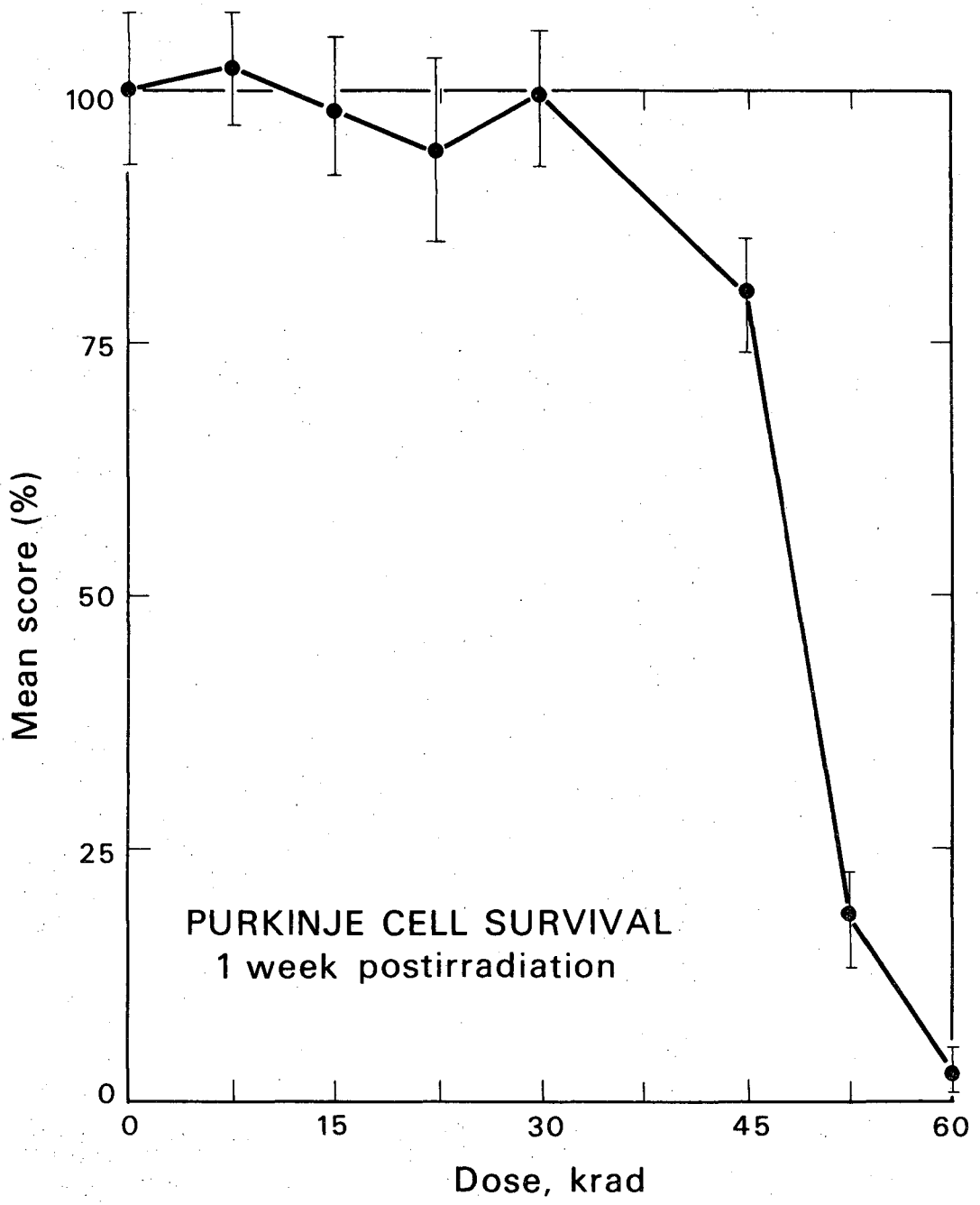

DBL 711 5641

Fig. 9

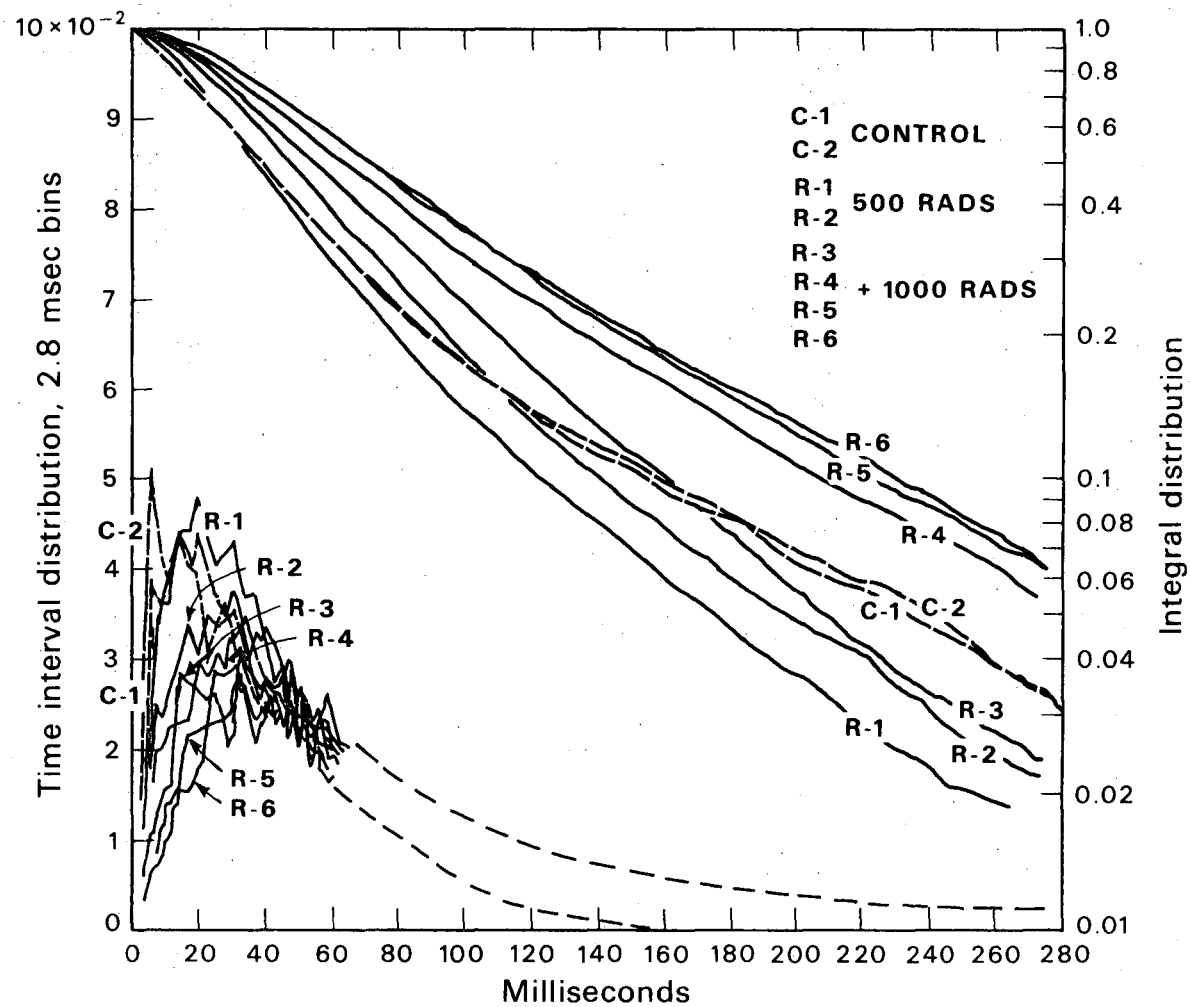

DBL 721-5134

Fig. 10

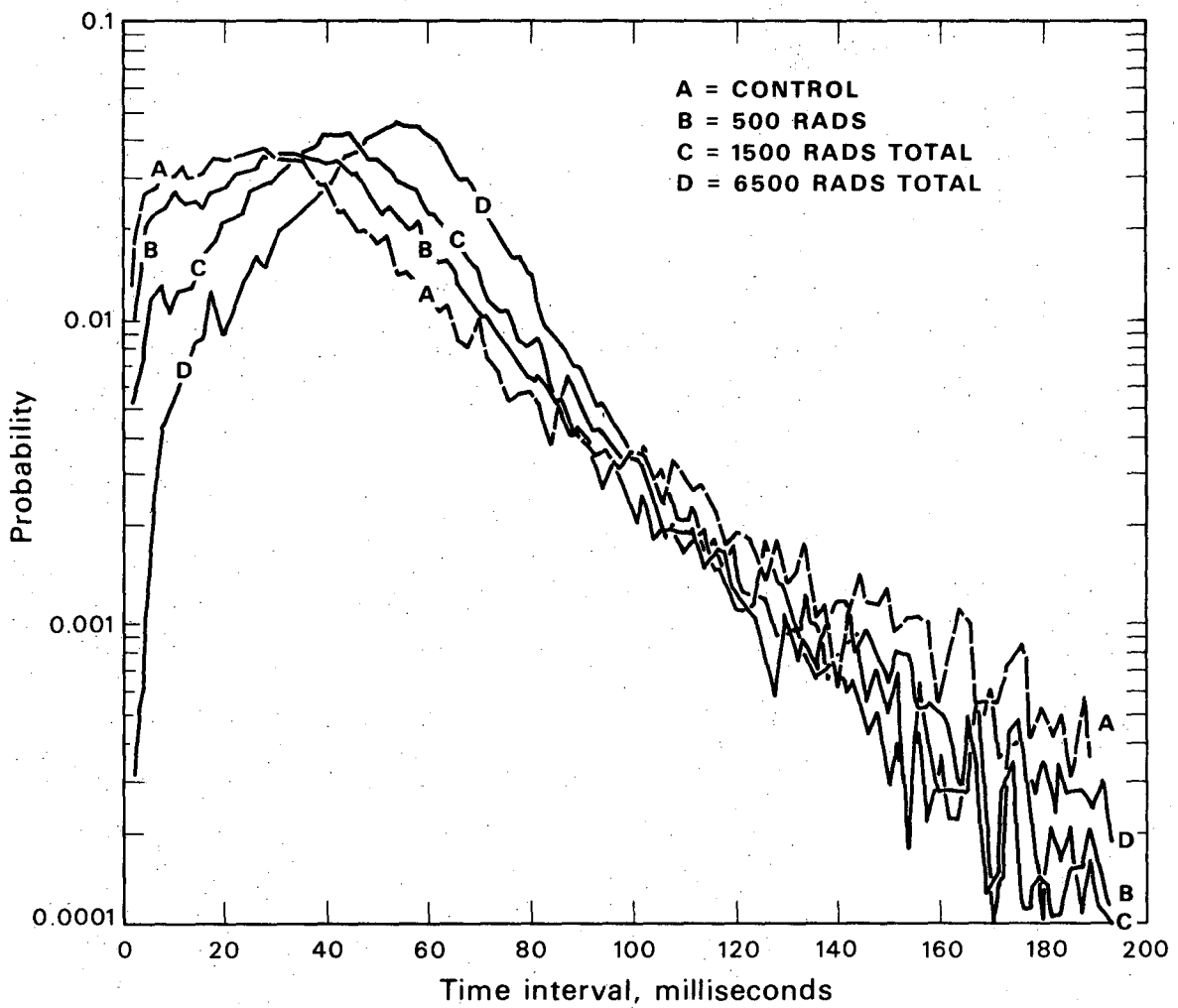

DBL 721-5135

Fig. 11

0 0 0 0 3 7 0 0 0 3 4

Temperature-Controlled Micro-Chamber for Electrical Recording from Nerve Tissue Cultures

B. H. Gahwiler, A.-M. Mamoon, and C. A. Tobias

Abstract

A device to control the temperature of a micro-chamber for electrophysiological recording from nerve tissue cultures is described. The temperature can be altered between 0°C and 50°C and kept constant within ±0.2°C.

Accurate control of the physical and chemical environment is most important in terms of the reproducibility of the patterns of bioelectric activity recorded from cultured nerve tissue. In many cases, it is not only necessary to control these parameters, but one is often also interested in changing them in a reasonably short time. We developed a device which enables us to control the temperature of the bathing solution within ±0.2°C and to change it rapidly in a range from 0 to 50°C.

Materials and Methods

Nerve Tissue Cultures of rat cerebellum are grown on glass coverslips and incubated in roller tubes at 36.5°C in a Rollertherm incubator.[2,3] For the electrophysiological analysis, the cultures are transferred to a small chamber which fits between the objective and condenser of a microscope. The bathing chamber is similar to that used by Hild and Tasaki[1] and consists of a glass base and two thin Perspex strips bearing a coverslip as roof of the chamber. Through the open sidewalls of the chamber microelectrodes can be inserted. Balanced salt solution is perfused through openings in the Perspex mounts and held in place by surface tension. Visual inspection of the culture is performed with a phase contrast microscope which is mounted on a movable baseplate for independent

positioning. The microscope stage is completely removed.

Temperature Control

The problem of how to control the temperature of the bathing solution (approximately 0.7 ml) without impairing visual control of the culture was solved with the setup shown schematically in Fig. 1. Two thermoelectric modules (Melcor Inc., Trenton, New Jersey) are attached to the glass plate of the culture chamber by the intermediary of a thin copper plate. This plate serves as thermal contact and has an opening to allow optical inspection with the microscope. The thermoelectric modules (TEM) have to be far apart (Fig. 1) because of the dimensions of the light condenser which has to fit in between them. The TEM is a device working on the Peltier principle and consists of 12 semiconductor elements. These modules transfer heat from one side to the other depending upon the polarity of the current applied. To prevent excessive heating of the bottom plate of the TEM during cooling of the chamber, water cooling coils are provided.

The experimental arrangement for controlling the temperature of the chamber is shown in Fig. 2. The actual chamber temperature is sensed with two thermistors and fed into a control bridge. The voltage produced when the bridge becomes unbalanced is amplified and applied to the TEM. The power input to the TEM is proportional to the error voltage of the unbalanced bridge and the gain factor of the amplifier is computed by dividing the voltage required to change the temperature the full range by the allowed error voltage representing the error in the temperature demanded ($50^{o}C/0.1^{o}C = 500$). To obtain a fast temperature change without

any overshooting, two thermistors have to be used because the bathing solution is reaching equilibrium with a certain delay caused by the distance between the solution and the TEMs. One thermistor is located in the bathing solution, the second one is glued on the copper plate close to a TEM. It is very important to avoid temperature overshooting since it could be harmful to the cells.

Results

Independent of the two thermistors the temperature is measured with a thermocouple and plotted with a chart recorder. The thermocouple is located at one end of the chamber and is therefore measuring a different value than the actual temperature at the place of the culture. Corrected for this difference (approximately 0.5°C, depending upon the temperature) the temperature of the culture can be measured with an accuracy of ±0.3°C and kept constant within ±0.2°C.

In Fig. 3 the performance of the system when changing the temperature can be seen. The gradient of the temperature change is dependent upon the maximum current applied to the TEMs. To prevent interference of ac signals with the electrophysiologic recordings we used car batteries and limited the current to 10 A.

Because of the open sidewalls some solution evaporates during an experiment and has to be replaced. We provided, therefore, the perfusion system with a small reservoir (Fig. 1) where the solution is brought up to approximately the right temperature. Although adding solution from the reservoir does not change the temperature of the chamber, complete replacement of the chamber solution has a definite effect and is indicated

by an arrow in Fig. 3 (the volume of the reservoir is 0.4 ml, the volume of the chamber 0.7 ml).

Acknowledgements

The authors are particularly grateful to Mr. A. Windsor who designed the electronic control unit and to Messrs. Frank T. Upham, Pete Dowling and William Worthington and John Flambard for their helpful technical assistance. One of the authors (B.H.G.) has been supported by a grant of the Swiss Academy of Medicine; A.M.M. was partially supported by a NASA-Ames grant.

0 0 0 0 3 7 0 0 8 5 6

References

1. Hild, W. and Tasaki, I: Morphological and physiological properties of neurons and glial cells in tissue culture. J. Neurophysiol. 25: 277-304 (1962).

2. Mamoon, A. M.: Effects of ionizing radiations on myelin formation in rat brain cultures. Ph.D. Thesis, University of California, Berkeley, 1969.

3. Schlapfer, W. T.: Bioelectric activity of neurons in tissue culture: Synaptic interactions and effects of environmental changes. Ph.D. Thesis, University of California, Berkeley, 1969.

Figure Captions

Fig. 1. Schematic drawing of the temperature control set up used for electrophysiologic studies on nerve tissue cultures. The coverslip bearing the culture is mounted, with the culture facing downwards, on a bridge mount. A copper plate serves for better contact between the glass plate and the thermoelectric modules. Cooling coils are provided for protection of the thermoelectric modules.

Fig. 2. The temperature of the chamber is sensed with two thermistors and the voltage produced when the bridge becomes unbalanced is amplified and applied to the thermoelectric modules. Temperature alterations are obtained by changing the resistance of one branch of the bridge.

Fig. 3. Performance of the temperature control set up as recorded with the thermocouple when unbalancing the bridge. Refillment of the solution lost by evaporation does not change the temperature of the chamber since the solution in the reservoir was already at the right temperature. Complete exchange of the bathing solution does, however, change the temperature of the chamber as indicated by an arrow.

0 0 0 0 3 7 0 0 8 5 7

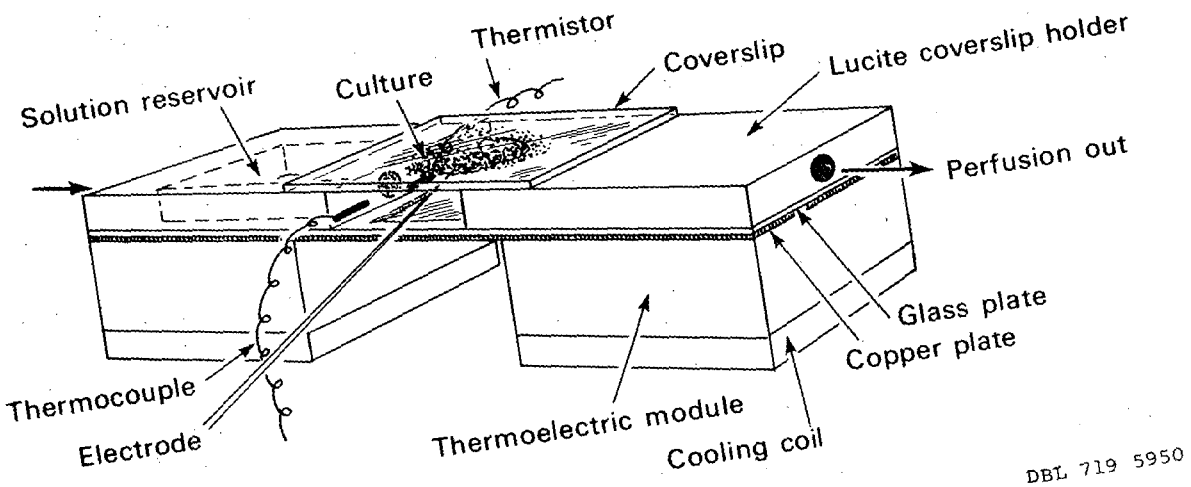

Fig. 1

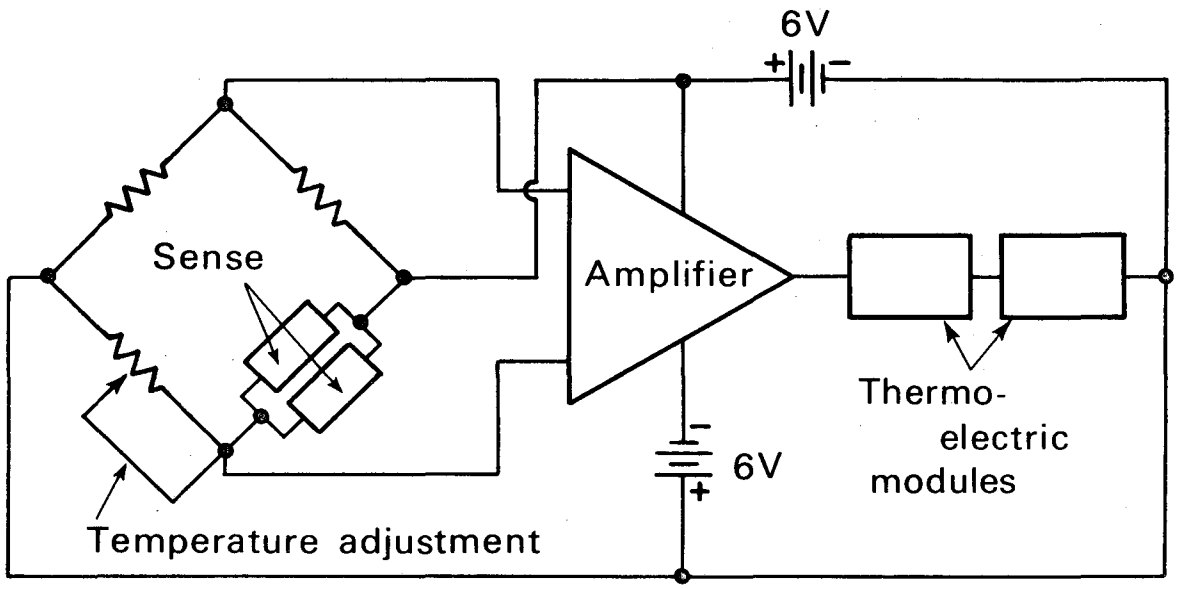

DBL 719 5951

Fig. 2

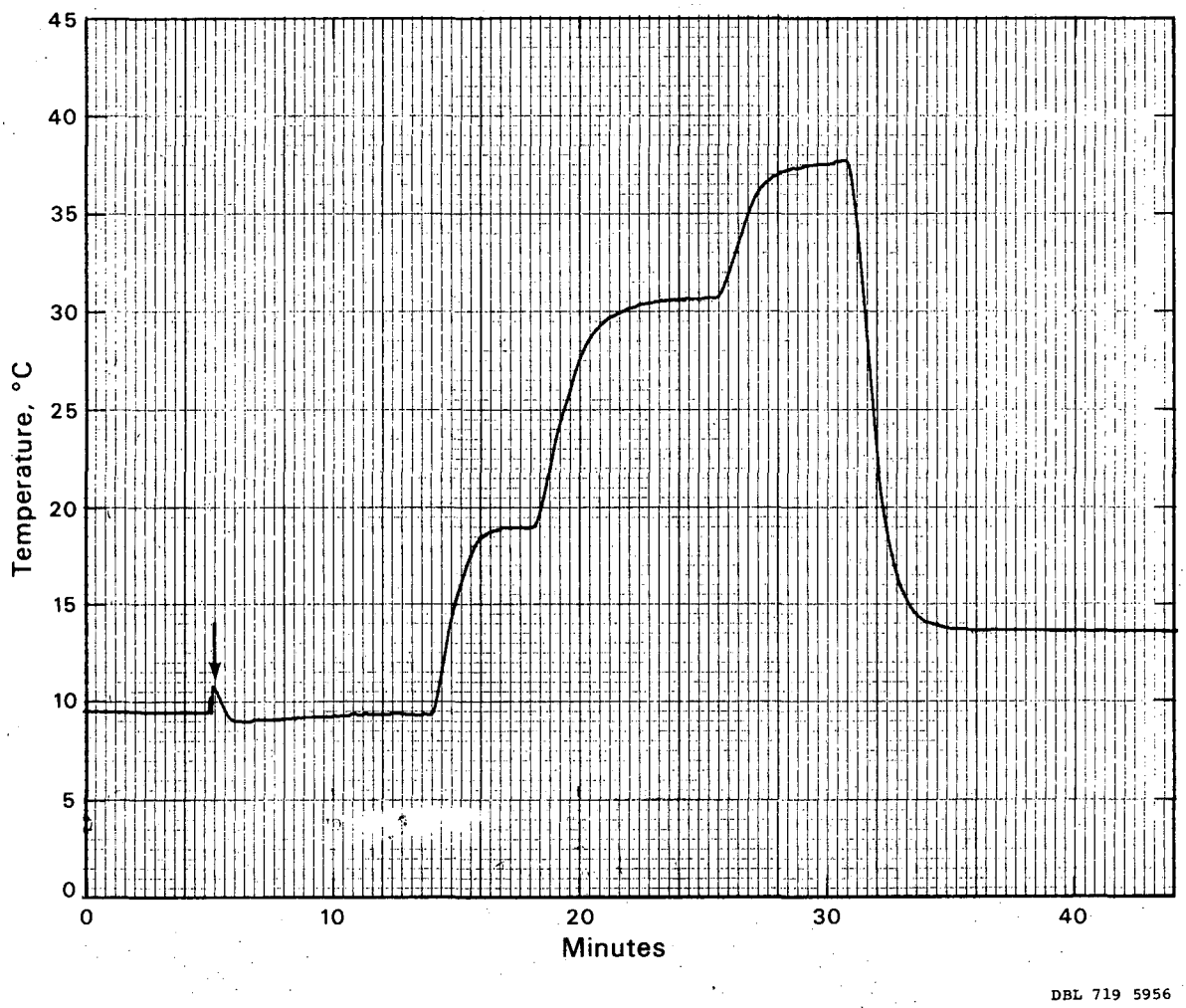
45
40
35
30
25
20
15
10
5
0
Temperature, °C
0
10
20
30
40
Minutes
DBL 719 5956

Fig. 3

Effects of Temperature on Spontaneous Bioelectric Activity of Cultured Nerve Cells

B. H. Gahwiler, A.-M. Mamoon, W. Schlapfer, C. A. Tobias, Donner Laboratory, University of California, Berkeley, 94720

The spontaneous bioelectric activity as recorded extracellularly from large nerve cells (Purkinje cells and Golgi type cells, 25μ to 35μ diameter) of cultured rat cerebellum has been investigated by several workers[5,8]. Changes in temperature affect the duration of action potentials and influence the frequency of the spontaneous activity[6,10], but no attempts have been made to study these effects over a large range of temperature.

Temperature represents an important physiological variable since the question of reversibility as well as the extreme values of temperatures at which spontaneous activity still occurs are of general interest. In cultured nervous tissue, spontaneous bioelectric activity can be recorded from a single neuron during many hours, and the temperature of the preparation altered over a large range ($0^{o}C$ - $50^{o}C$) within a short time (minutes).

Explants from the cerebellum of 2 to 4 day old rats (Sprague-Dawley, Simonsen albino) were grown on glass coverslips in a plasma clot which was formed by chicken plasma and chicken embryo extract. The cultures were maintained in Falcon plastic tubes placed in a Rollertherm incubator at $37^{o}C$[9]. The nutrient medium contained 50 percent Basal Medium Eagle, 25 percent Hanks Balanced Salt Solution, 25 percent Calf Serum and glucose (5.5 mg/ml) and was exchanged

weekly. Solution pH was kept between 7.4 and 7.5 by a flow of 5 percent CO_2 in air.

For studies of bioelectric activity the coverslip bearing the culture was placed with the culture facing downwards on a bridge mount. Microelectrodes were inserted through the open sidewalls of the chamber which was filled with 0.7 ml Hanks Balanced Salt Solution held by surface tension. The microscope with stage completely removed was fixed to a movable base plate for independent positioning and scanning of the culture. The temperature of the solution bathing the culture was monitored by a thermistor and could be varied between $0^{o}C$ and $50^{o}C$ and kept constant within $\pm 0.2^{o}C$ by means of a pair of thermoelectric modules (Melcor, Trenton, New Jersey) described earlier[4].

Action potentials were recorded extracellularly with micropipettes (4μ to 6μ tip diameter) which had a resistance of 10 MΩ to 20 MΩ when filled with Hanks Balanced Salt Solution. A platinum or Ag-AgCl wire was inserted into the microelectrode and connected to a high input impedance amplifier. The solution was grounded via a large platinum wire. The signals were fed into a multichannel analyser and tape recorder for further analysis of the data.

Effects on Average Spike Frequency. The average spike frequency of large nerve cells was measured after 10 to 20 days *in vitro* and plotted against the temperature in Fig. 1. The results of 13 measurements from 10 cultures are shown. Each line refers to recordings from the same neurone. The results of 25 more neurones which were examined later fit into the envelope (drawn in Fig. 1)

that marks the extreme values.

Most neurons stopped firing between 20°C and 10°C, but some cells were still spontaneously active at 5°C. These nerve cells apparently responded in a different way to alterations in temperature below and above about 18°C (Fig. 2). It is unclear whether such cells represent a special type with a different temperature response or whether this behavior could not be observed in other neurons because they stopped spontaneous bioelectric activity at about the critical temperature of 18°C for some other reason.

Spontaneous activity could still be recorded at a temperature as low as 5°C and stopped irreversibly in all cultures between 42°C and 43°C. The average spike frequency at 37°C of the 38 neurons tested amounted to 1000±30 percent spikes/min, the mean standard deviation of the frequency measured at 37°C of the single cell being ±5 percent. The temperature of 37°C was chosen as reference point because the cultures were kept at this temperature in the incubator and after transfer to the bathing chamber all measurements were started at this temperature.

To check for the reversibility of the effects observed, the temperature was often lowered and raised many times. There was in no case a significant steady state hysteresis. However, recovery time after temperature change increased at low temperatures and was always obtained with a significant time lag compared to the thermal equilibrium of the bathing chamber.

Effects on Duration of Spike. The shape of the action potentials corresponded well with *in vivo* recordings[3]. Biphasic and triphasic

extracellular action potentials were observed, biphasic potentials with an initial negative deflection being the most frequently recorded. Sometimes, however, positive-negative giant spikes could be seen. Because of their larger amplitude, only these spikes were included in this study. The duration of the pulse was arbitrarily measured at half height of the positive phase. The observed effects are illustrated in Fig. 3 and a temperature-duration curve from one such neuron is shown in Fig. 4 suggesting constant Q_{10} values over the range tested in this study. The Q_{10} for this process varied little and had a mean value of 1.8 ± 0.2 (20 neurones in 12 cultures tested).

Effects on Discharge Pattern. The time between two spikes was measured using a ramp generator triggered at each incoming input and the so converted time-amplitude signal was fed into a pulse height analyser. Two time interval histograms recorded at 37° and $31^{o}C$ from the same neurone are shown in Fig. 5. The alterations in pattern are reversible and reproducible for the same neuron but differ greatly from neuron to neuron .

There is considerable variation in how neurons respond to altering the temperature (Fig. 1). Different cell type and different number of synapses are factors that could conceivably contribute to a greater variation in results.

Recordings were made from large nerve cells that were recognized as Purkinje cells by their size, shape and the form of the origins of dendritic arborization. Nevertheless, it is possible that in some cases we were recording from Golgi cells. Since the number of Golgi

cells is only slightly above 10 percent of Purkinje cells[2], this should not have influenced the results greatly.

Each cerebellar neuron receives an unknown number of synaptic inputs from other nerve cells of the cerebellar cortex that discharge spontaneously *in vivo*[2] as well as *in vitro*[12]. The existence of synapses in the cultures used in this investigation has been shown by electrophysiological methods[10].

Since different responses to changes in temperature have been found while recording from two neurons simultaneously in the same culture, fluctuations in physiological parameters such as partial pressure of O_2 and CO_2 or pH are very unlikely to be responsible for the variability of the response.

The effect of temperature on the duration of nerve or muscle action potentials was previously studied[7, 11, 1]. The Q_{10} values reported in these papers indicate the temperature dependence of different phases of the action potential. They cannot, therefore, be compared with the Q_{10} value obtained by our method of extracellular recording which does not provide a direct measure of transmembrane potential. Empirically, a clear linear relation between temperature and pulse duration may serve in further studies as a convenient measure of changes in the behavior of the membrane to alterations in temperature.

The reproducibility of the response to the precisely controlled temperature alterations shows the value of nerve tissue culture as a model in exploration of an important parameter of nerve functions. This contrasts sharply with the data provided by time interval

histograms (Fig. 5) which indicate how little we know about the generation of spontaneous bioelectric activity of these cultures. The study of the patterns of the spontaneous discharges as recorded from isolated Purkinje cells may reveal more about the mechanism of the spontaneous spike generation and the nature of the synaptic inputs.

We thank Dr. A. B. Steinbach for his careful reading of this manuscript and his helpful suggestions, and to P. G. Banchero who designed the time height converter for the pulse height analyser. Thanks to Roseanne Stevens for her skillful help in preparing the cultures. One of the authors (B.H.G.) is very grateful to the Swiss Academy of Medicine for supporting this work; A.M.M. was partially supported by a NASA-Ames grant.

0 0 0 0 3 7 0 5 3 6 1

Summary

Spontaneous discharges of Purkinje cells in rat cerebellum cultures were recorded extracellularly in the range from 5°C up to 43°C. Raising the temperature from 10°C to 37°C increased the average spike frequency by a factor of about 20. The lengthening of the spike showed a Q_{10} = 1.8±0.2. Spike interval histograms changed considerably with temperature. All effects observed were reversible, even when the preparation was held for a long time (30 minutes) at low temperatures.

References

(1) Coraboeuf, E. and Weidmann, S., Temperature Effects on the Electrical Activity of Purkinje Fibers, Helv. Physiol. Acta 12 (1954) 32-41.

(2) Eccles, J. C., Ito, M. and Szentagothai, J., The Cerebellum As A Neuronal Machine. Springer-Verlag New York Inc., 1967, p. 60.

(3) Eccles, J. C., Llinas, R., and Sasaki, K., The Action of Antidromic Impulses on the Cerebellar Purkinje Cells, J. Physiol. (Lond.) 182 (1966) 316-345.

(4) Gahwiler, B. H., Mamoon, A. M., and Tobias, C. A., Temperature-Controlled Micro-Chamber for Electrical Recording from Nerve Tissue Cultures, LBL-528 (1971).

(5) Hild, W. and Tasaki, I., Morphological and Physiological Properties of Neurons and Glial Cells in Tissue Culture, J. Neurophysiol. 25 (1962) 277-304.

(6) Hild, W., Electrophysiological Phenomena Observed in Single Neurons and Neuroglial Cells in Cultures of Central Nervous Tissue, M. M. Brazier (Ed.), Brain Function II, UCLA Press, Los Angeles, 1964, p. 109-134.

(7) Hodgkin, A. L. and Katz, B., The Effect of Temperature on the Electrical Activity of the Giant Axon of the Squid, J. Physiol. (Lond.) 109 (1949) 240-249.

(8) Lumsden, C. E., Nervous Tissue in Culture. In The Structure and Function of Nervous Tissue, Vol. 1, G. H. Bourne (Ed.), Academic Press, New York, 1968, p. 67-140.

(9) Mamoon, A. M., Effects of Ionizing Radiations on Myelin Formation in Rat Brain Cultures, Ph. D. Thesis, University of California, Berkeley, 1969.

0 0 0 0 3 7 0 5 8 6 2

(10) Schlapfer, W. T., Bioelectric Activity of Neurons in Tissue Culture Synaptic Interactions and Effects of Environmental Changes, Ph. D. Thesis, University of California, Berkeley, 1969.

(11) Schoepfle, G. M. and Erlanger, J., The Action of Temperature on the Excitability, Spike Height and Configuration, and the Refractory Period Observed in the Responses of Single Medullated Nerve Fibers, Ann. J. Physiol. 134 (1941) 694-704.

(12) Tyska, E., Jr., Growth and Bioelectric Activity in Cultured Rat Cerebellum, Ph. D. Thesis, University of California, Berkeley, 1971.

Figure Captions

Fig. 1. Response of the spontaneous firing of Purkinje cells to alterations in temperature. Each curve refers to measurements from a single neuron, the measurement being at inflections of the lines. The temperature of 37°C was chosen as reference value. The results of measurements from 12 neurons in 10 cultures are presented.

Fig. 2. Average frequency of spontaneous bioelectric activity at different temperatures. Extracellular recordings from 4 Purkinje cells in different cultures still showing spontaneous activity at low temperatures.

Fig. 3. Extracellular action potentials. Same scale for all pictures. Positive deflection upwards. Culture 14 days *in vitro*.

Fig. 4. Pulse duration as measured at half height of the positive phase. Recordings from the same neuron at different temperatures. The Q_{10} for this process showed a mean value of 1.8 ± 0.2.

Fig. 5. Time interval histograms for spike trains recorded from the same neuron at different temperatures. Upper histogram: temperature 37°C, sampling time 2 minutes. Lower histogram: temperature 31°C, sampling time 7 minutes.

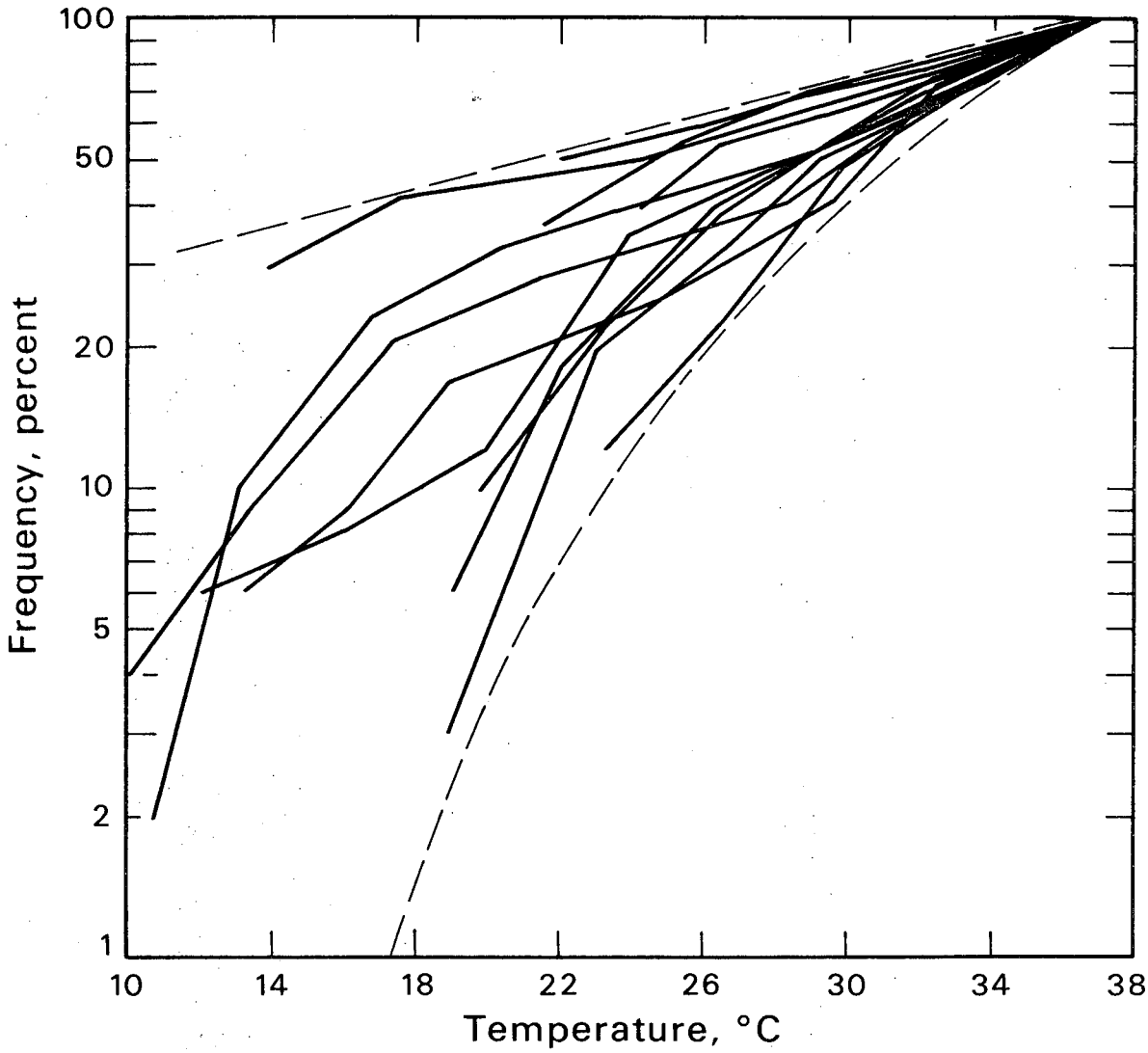

DBL 719 5952

Fig. 1

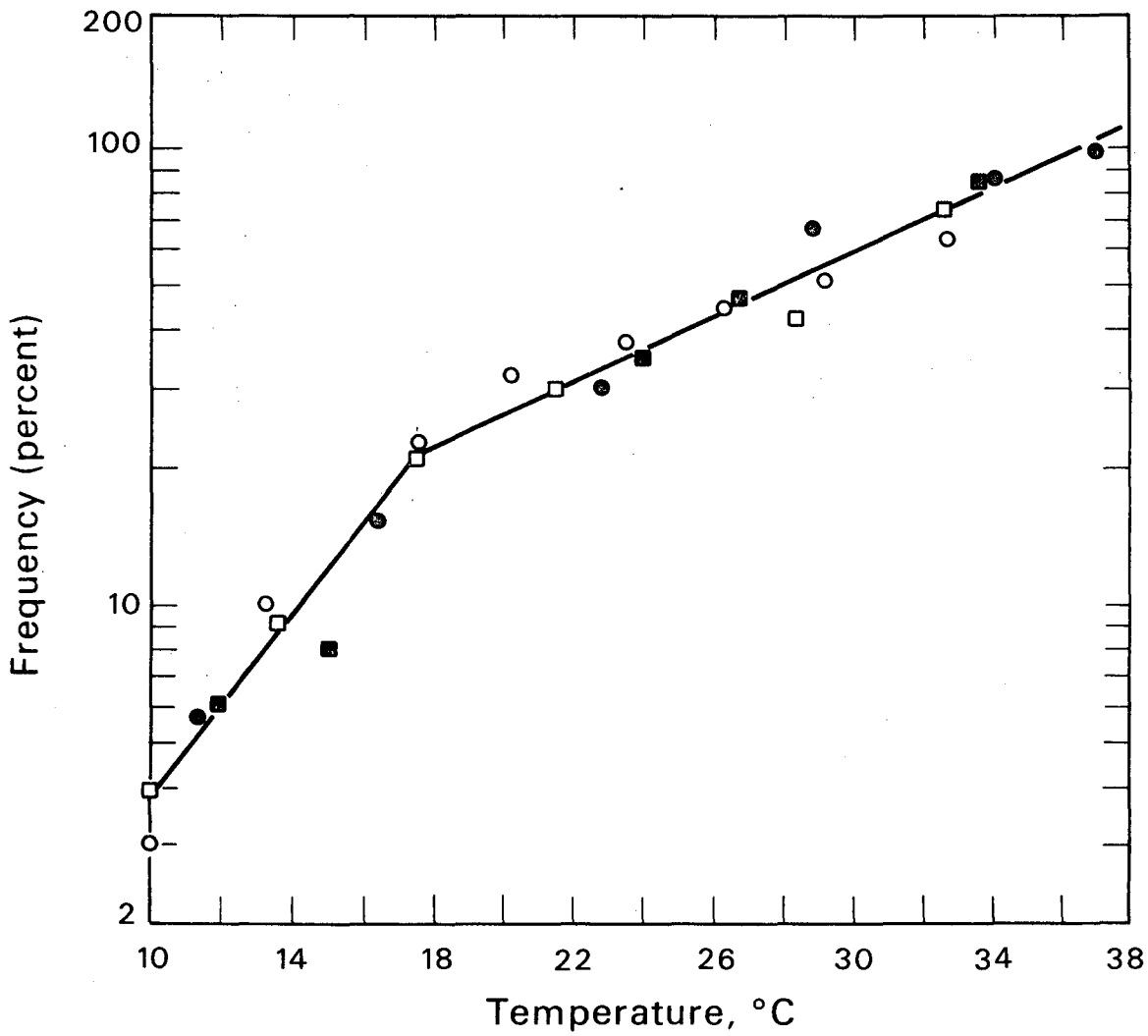

DBL 719 5955

Fig. 2

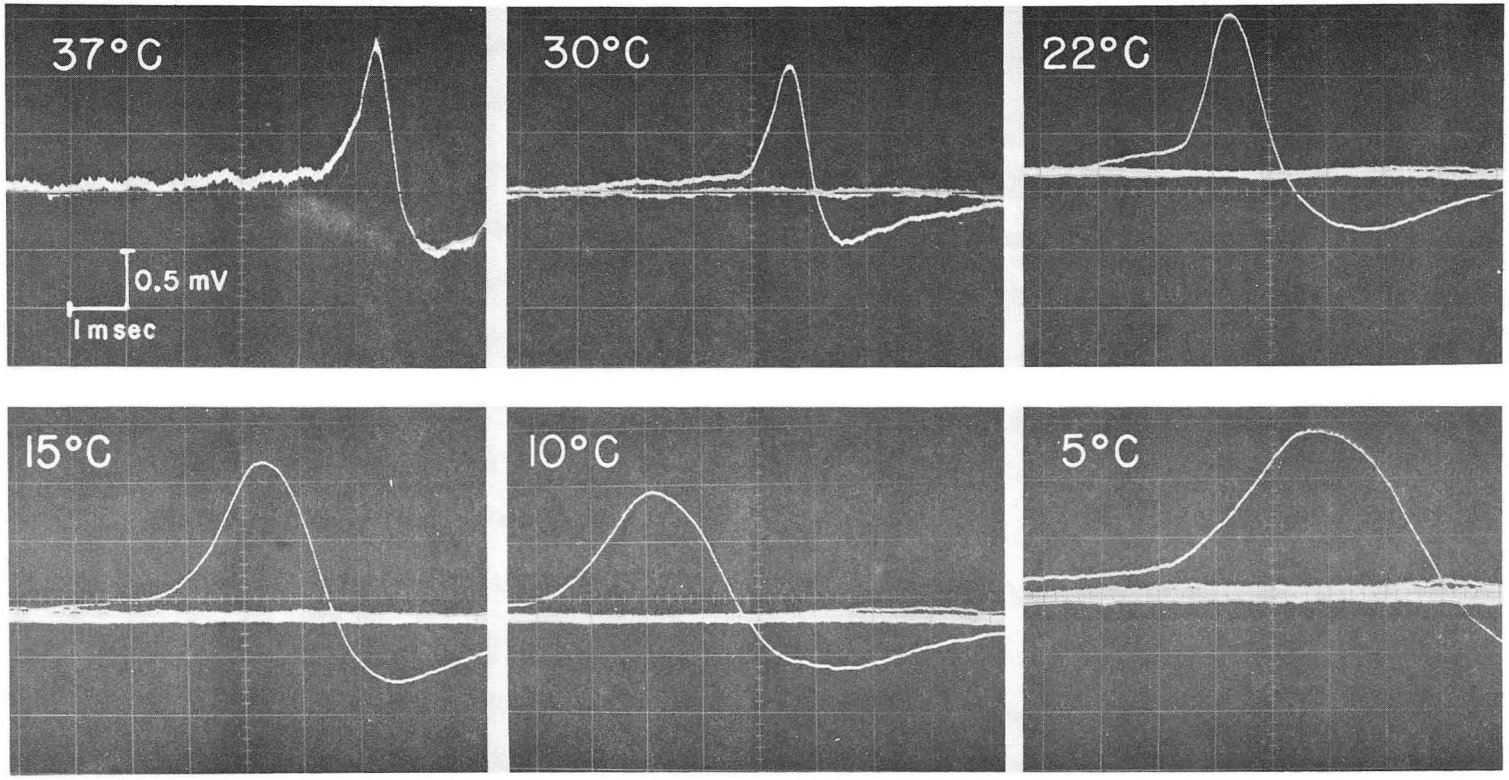

Fig. 3

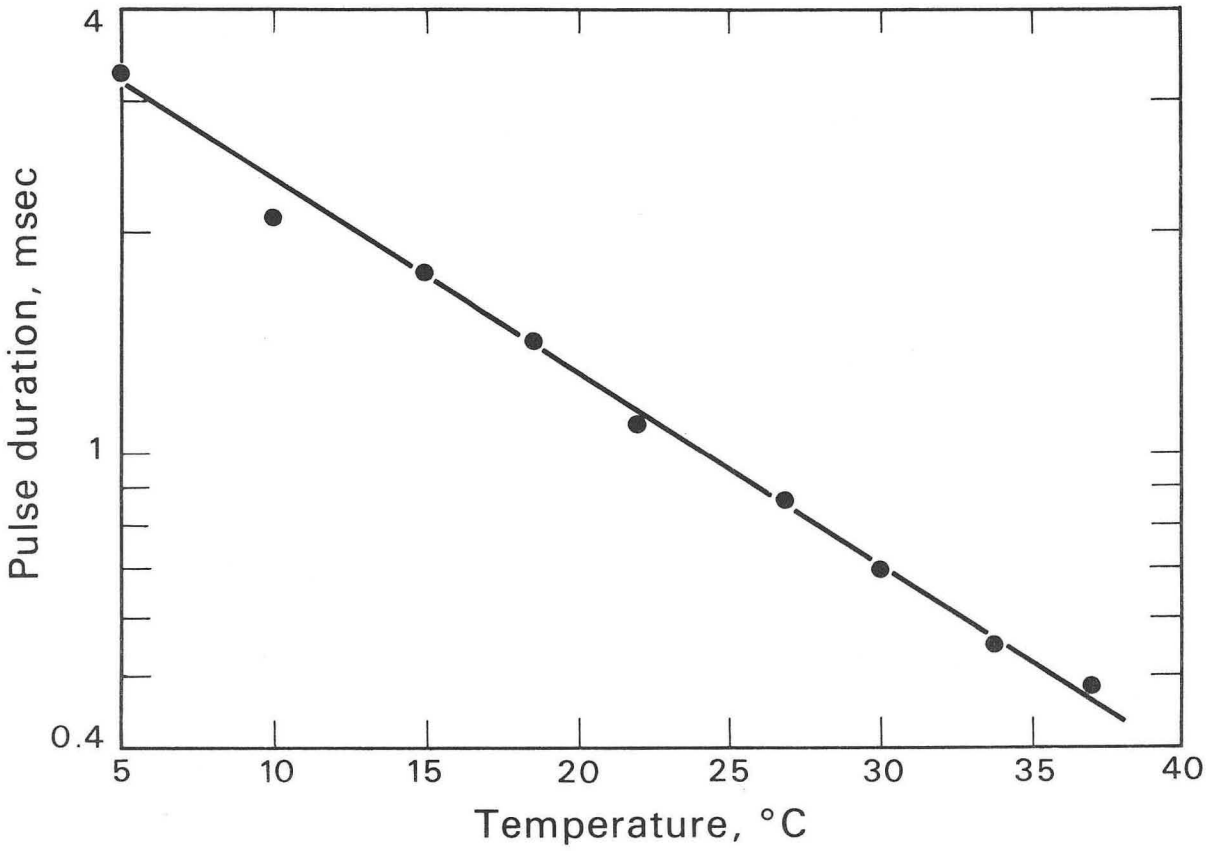

DBL 719 5953

Fig. 4

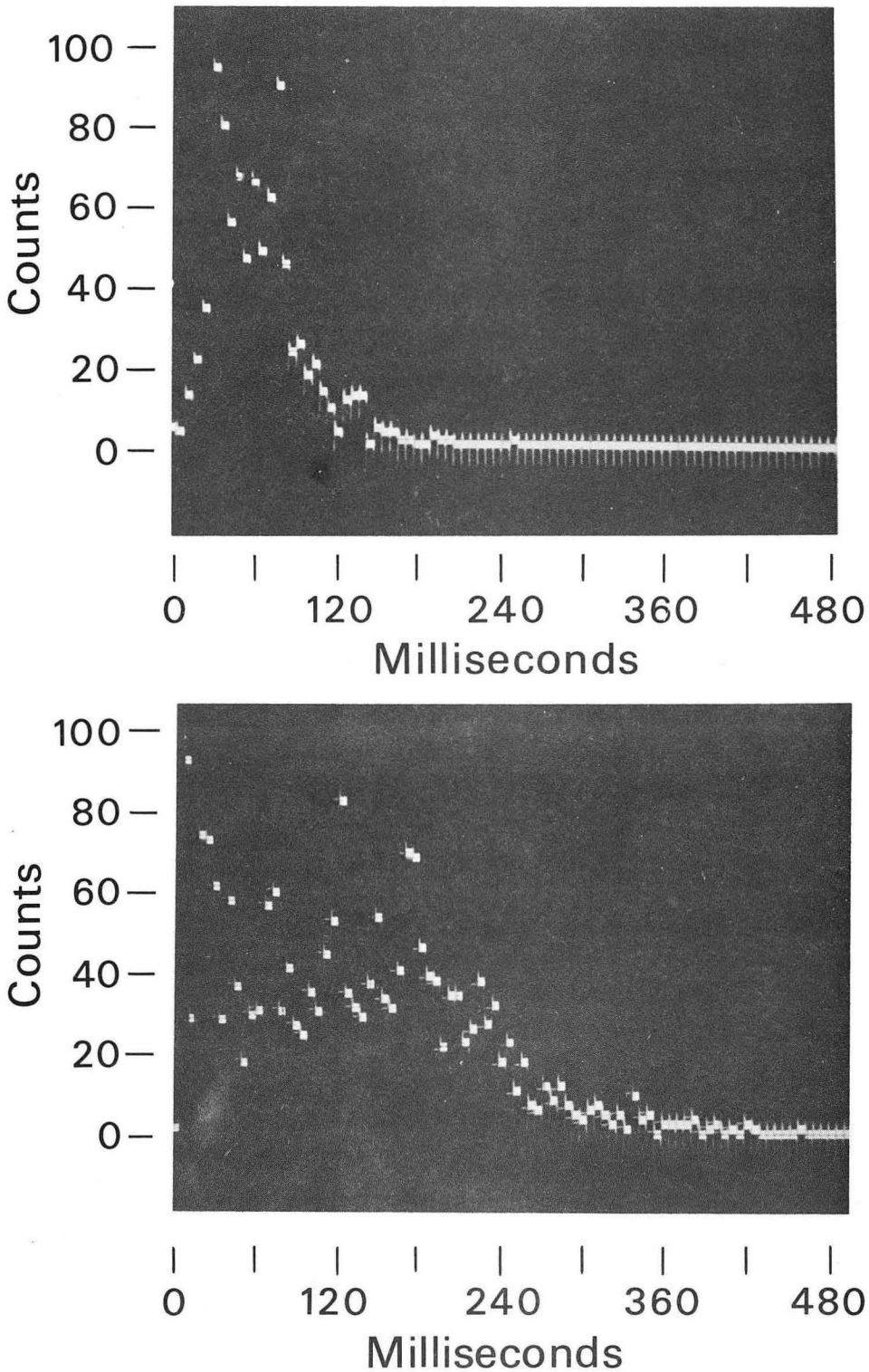
100
80
60
40
20
0
Counts
0
120
240
360
480
Milliseconds
100
80
60
40
20
0
Counts
0
120
240
360
480
Milliseconds

Fig. 5

0 0 0 0 3 7 0 3 8 6 5

NEURONAL REAGGREGATION--A MODEL SYSTEM FOR INVESTIGATION OF RADIATION EFFECTS ON NONDIVIDING CELLS

J. Leith and W. Schilling

Lawrence Berkeley Laboratory
University of California
Berkeley, California 94720

January 1972

INTRODUCTION

The acute and longterm effects of ionizing radiation on cellular populations that have the capacity to undergo cellular division and multiplication are relatively easily studied. However, quantification of the effects of radiation on nondividing cellular populations, such as the adult central nervous system, is still largely lacking. Most studies of such radiation effects are primarily morphological in nature and require relatively high doses of radiation, at which levels actual cell killing is the primary result. We are attempting to develop an assay system for radiation effects on neurons that appears to be able to yield quantitative dose-response relationships for the effects of radiation on neuronal cells. Specifically, we are studying the effects of radiation on dissociated embryonic mouse neural cells which have been allowed to reaggregate in vitro into presumptive neural structures. It has been shown (1,2) that neuronal isocortical and hippocampal cells dissociated from embryonic mouse brain will reaggregate in vitro to form specific organotypic structures similar to the in vivo structures that would have developed had the embryonic brain been allowed to develop to its full extent in vivo. A significant point about the neuronal reaggregation is that cells of different

types sort out (i. e., reaggregate) in very specific relationships to other cell types; they do not simply clump randomly. It appeared to us therefore that such a specific system of in vitro cell specialization and differentiation could perhaps be a sensitive system for studying radiation effects on neuronal cells.

This aggregation technique for mouse brain cells has been used (3,4) to show that the dissociated and aggregated cells will yield results similar to the naturally developing in vivo mouse brain. In particular, the levels of activity of choline acetyltransferase, acetylcholinesterase, and glutamate decarboxylase increase in vitro much as they would in vivo; this same observation can also be made for synaptic formation, as well as the cyclic AMP levels after norepinephrine stimulation.

MATERIALS AND METHODS

Fetuses were obtained from a C57B1/6J stock obtained from the Jackson Laboratories, Bar Harbor, Maine. The gestation time is 19 to 20 days in this strain. Females estimated to be 17 to 18 days pregnant were anesthetized with Nembutal (sodium pentobarbital 35 mg/kg). The abdomen was opened aseptically, and fetuses were removed to sterile petri dishes. The fetuses were decapitated, the skull opened, and the meninges were removed. The brain tissues were then dissected and placed into a small volume of sterile calcium-magnesium-free isotonic salt solution containing 0.1% glucose (CMF). In some experiments, tissues were placed in CMF that contained a small amount of antibiotic (Pen-strep, 50 units/ml: 50 mg/ml) to see if the antibiotic interfered with subsequent reaggregation. Mouse cerebral cortex, hippocampus and cerebellum were examined.

0 0 0 0 3 7 0 3 8 6 6

Tissues were placed in 1 ml of 0.3% trypsin (Worthington Biochemical Co.) in CMF solution for 20 to 25 min. They were then washed 3 times with warm CMF; the CMF was removed, and 1 ml of medium was added. The tissue was then dissociated into single cells by repeatedly drawing it in and out of a capillary pipette. Cell counts were performed with a hemocytometer, and dissociated cells were placed in 10-or 25-ml Erlenmeyer flasks with 1.3 to 3.0 ml of medium.

The medium used was that described by Moscona (5) for reaggregating cultures: Eagle's basic medium with 0.1% glutamine, 10% horse serum, 2% chick embryo extract, and supplemental glucose added (as 5% dextrose in water) to a total glucose concentration of 600 mg/100ml. Cultures were gassed with 4% CO_2 in air, sealed with rubber caps, and placed on a rotating shaker (2.25-cm rotation diameter, 70 rpm) at 37°C. Cultures were fed every four days by adding 0.5 ml of fresh medium to the flask. The number of cerebral cortical and hippocampal cells seeded was approximately 6.0×10^6/flask, and the number of cerebellar cells seeded was 3.0×10^6 cells/flask. Cultures were maintained from 6 to 12 days in the rotary cell-suspension system.

In one experiment, an attempt was made to preserve the formed aggregates as explant cultures. At 12 days after seeding, the aggregates were harvested and placed in 5.0-cm-diameter petri dishes. Initially, 0.4 ml of chicken plasma (Baltimore Biological Laboratories) was added to the dish; the aggregates were dispersed into the chicken plasma, and then 0.4 ml of chicken embryo extract was added to make a plasma clot. The clot was allowed to harden for one-half hr, and then 1.5 ml of the basic medium used for the rotary system was added.

Cultures were then maintained in a CO_2 incubator, to be examined for further differentiation as an explant.

RESULTS

In Fig. 1, an initial suspension of trypsin-dissociated cells from mouse cerebral cortex is shown. In all experiments, a 90% viability measure of the dissociated cells (as indicated by trypan blue exclusion) was found. These cells have an average diameter of about 8 microns.

In Figs. 2 and 3, small aggregates of cerebral cortical cells are shown at 1 day after seeding into the suspension culture system. It may be easily seen (particularly in Fig. 3) that the aggregates are composed of many cells.

Figure 4 is a phase-contrast photomicrograph of two large reaggregates after 12 days in suspension culture. The diameter of these is approximately 0.3 mm. Figure 5 is a low-power photomicrograph of these aggregates after 12 days in suspension culture when seeded as an explant culture in a plasma clot.

No effects from antibiotics were found on reaggregation of mouse brain cells.

DISCUSSION

There are important considerations concerning the possibility of using this system as an indicator of radiation damage. From a certain number of originally seeded individual brain cells (say 10^6), one may expect a certain number of large aggregates (say 100 to 150) at 8 to 12 days after seeding. With this type of end point, the observed yield may be easily described, and it appears to us that effects of radiation may produce dose-response relationships similar to, for example, endogenous

0 0 0 0 3 7 0 3 8 6 7

spleen colony experiments (6), skin cell survival (7) or intestinal cell survival (8, 9), although in this instance, for a nondividing cell population. Such experiments are currently being performed using a Cobalt-60 gamma-ray source. Doses of 100, 500, and 1000 R have been administered to neuronal cultures.

REFERENCES

1. DeLong, R. G., Histogenesis of Fetal Mouse Isocortex and Hippocampus in Reaggregating Cell Cultures, Develop. Biol., 22: 563-583 (1970).
2. DeLong, G. R., and Sidman, R. L., Alignment Defect of Reaggregating Cells in Cultures of Developing REELER Mutant Mice, Develop. Biol., 22: 584-600 (1970).
3. Seeds, N. W., Biochemical Differentiation in Reaggregating Brain Cell Culture., Proc. Nat. Acad. Sci. USA, 68: 1858-1861 (1971).
4. Seeds, N. W., and Gilman, A. G., Norepinephrine Stimulated Increase of Cyclic AMP Levels in Developing Mouse Brain Cell Cultures. Science, 174: 292 (1971).
5. Moscona, A. A., In: Cells and Tissues in Culture, B. M. Willmer, Ed. (Academic Press, New York, 1965), p. 483.
6. Till, J. E., and McCulloch, E. A., A Direct Measurement of the Radiation Sensitivity of Normal Mouse Bone Marrow Cells, Radiat. Res., 14: 213-222 (1961).
7. Leith, J. T., Schilling, W. A., and Welch, G. P., Survival of Mouse Skin Epithelial Cells After Heavy-Particle Irradiation, Int. J. Radiat. Biol., 19: 603-609 (1971).
8. Withers, H. R., and Elkind, M. M., Dose Survival Characteristics of Epithelial Cells of Mouse Intestinal Mucosa, Radiol., 91:998-1000 (1968).
9. Withers, H. R., and Elkind, M. M., Microcolony Survival Assay for Cells of Mouse Intestinal Mucosa Exposed to Radiation, Int. J. Radiat. Biol., 17: 361-367 (1970).

0 0 0 0 3 7 0 0 0 6 8

FIGURE LEGENDS

Fig. 1. Low-power photomicrograph of the initial suspension of trypsin-dissociated embryonic neuronal cerebral cortical cells in a hemocytometer. Bar indicates 100 microns.

Fig. 2. Photomicrograph of neuronal aggregate one day after placement in gyrorotary suspension culture system. Bar indicates 100 microns.

Fig. 3. Photomicrograph of neuronal aggregate one day after placement in gyrorotary suspension culture system. Bar indicates 100 microns.

Fig. 4. Phase-contrast photomicrograph of neuronal aggregates after 12 days in gyrorotary suspension culture system. Bar indicates 100 microns.

Fig. 5. Low-power photomicrograph of neuronal aggregates as placed in a plasma clot 12 days after initial seeding and maintenance in the gyrorotary suspension culture system.

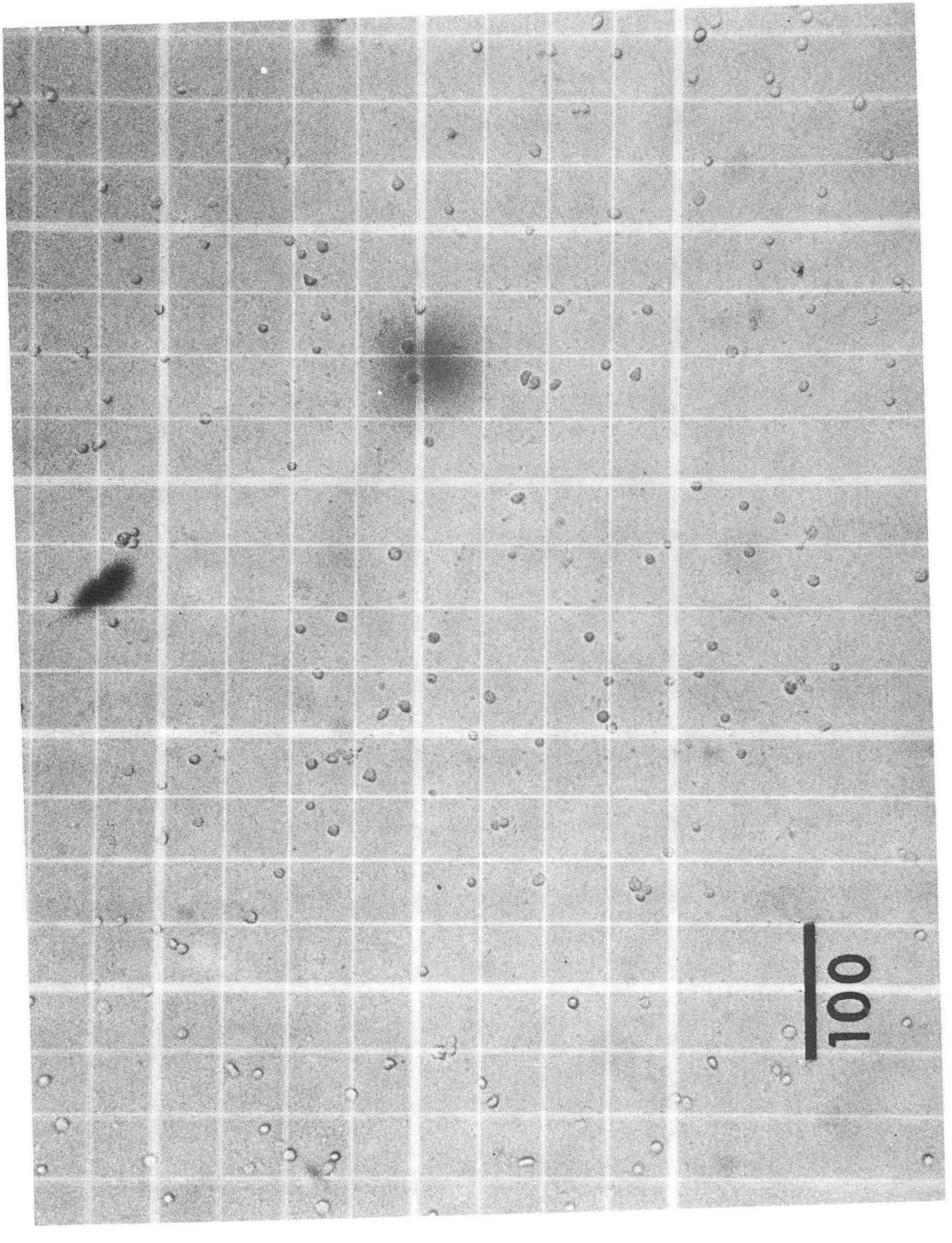

Fig. 1

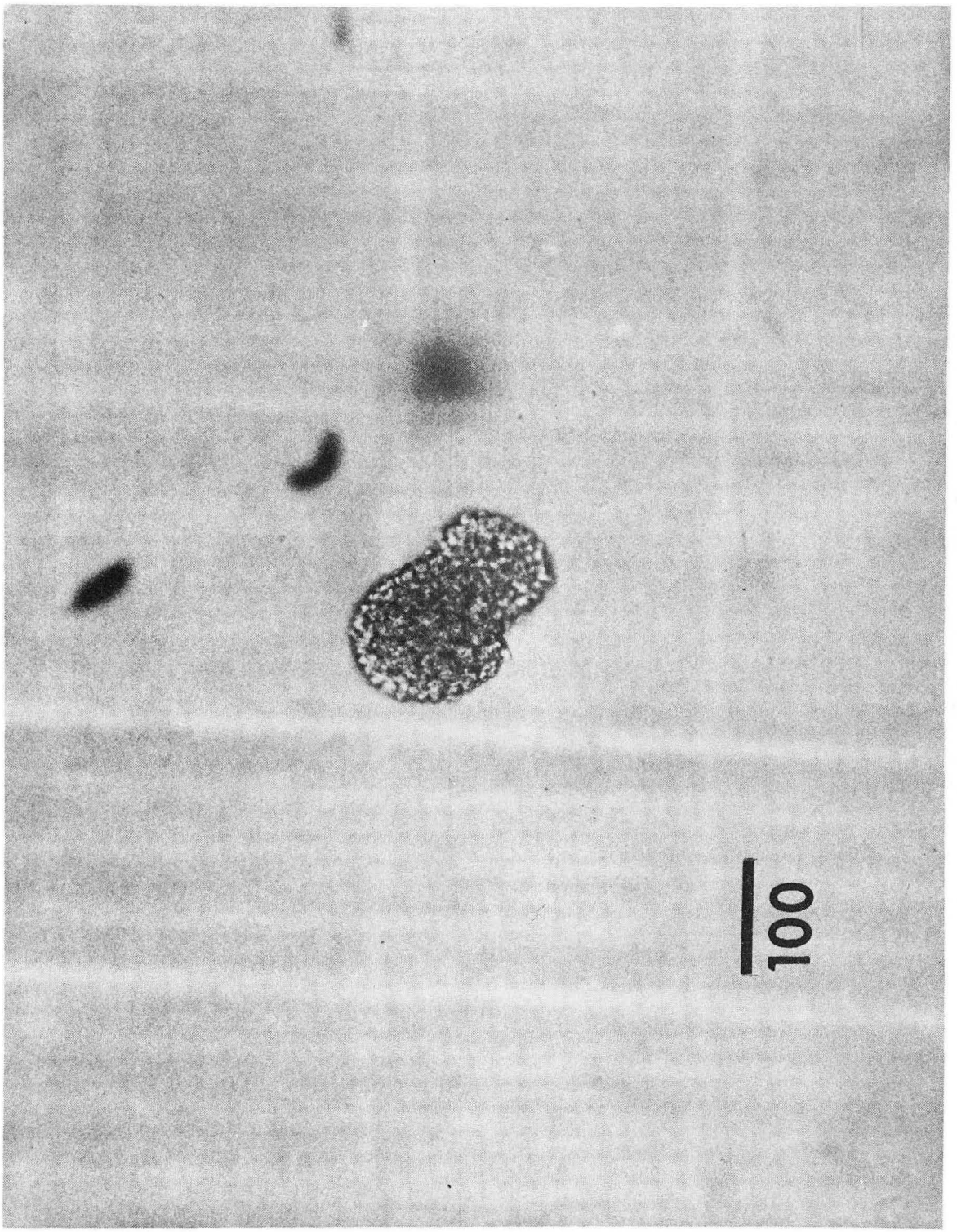

Fig. 2

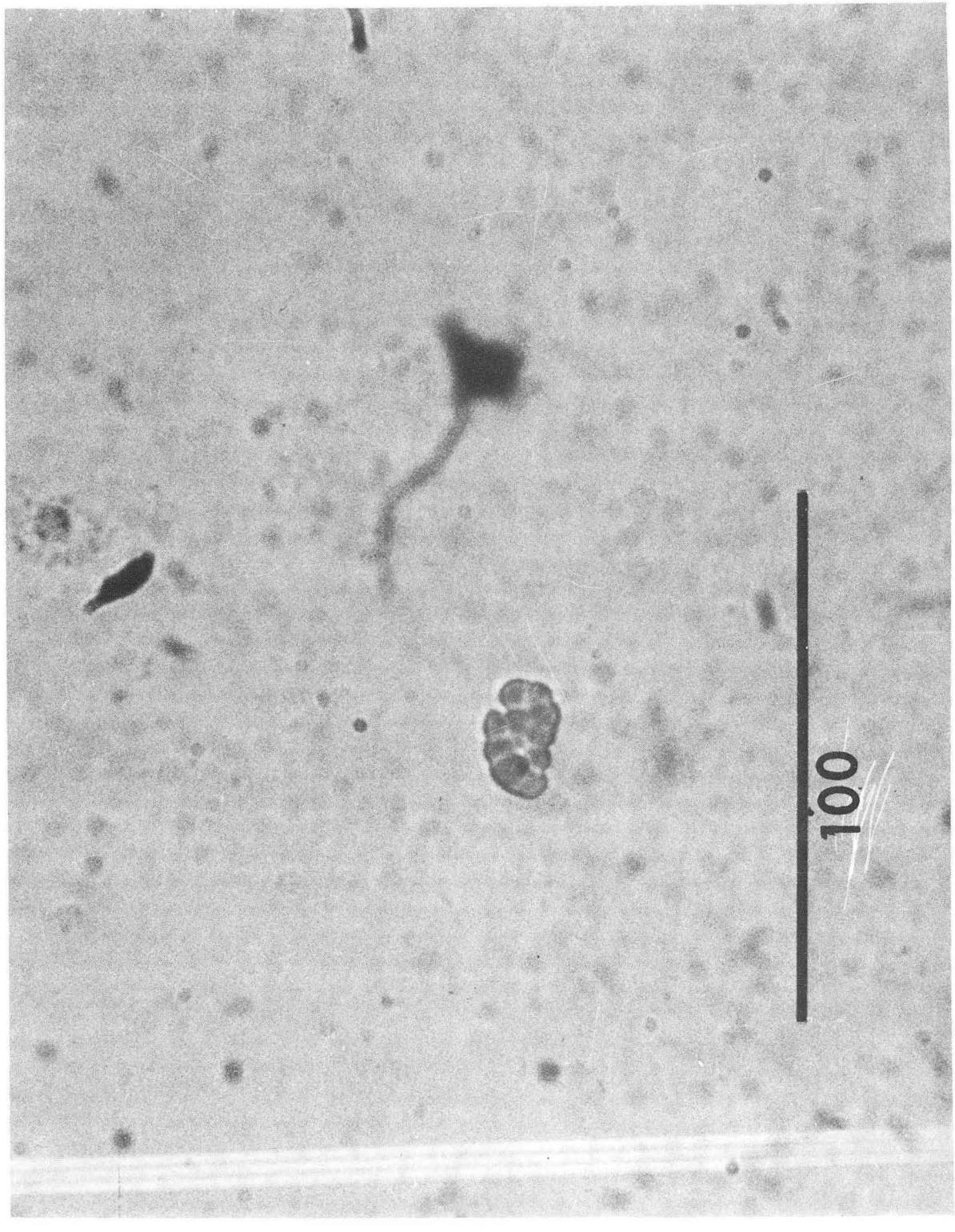

Fig. 3

0 0 0 0 3 7 0 3 8 7 0

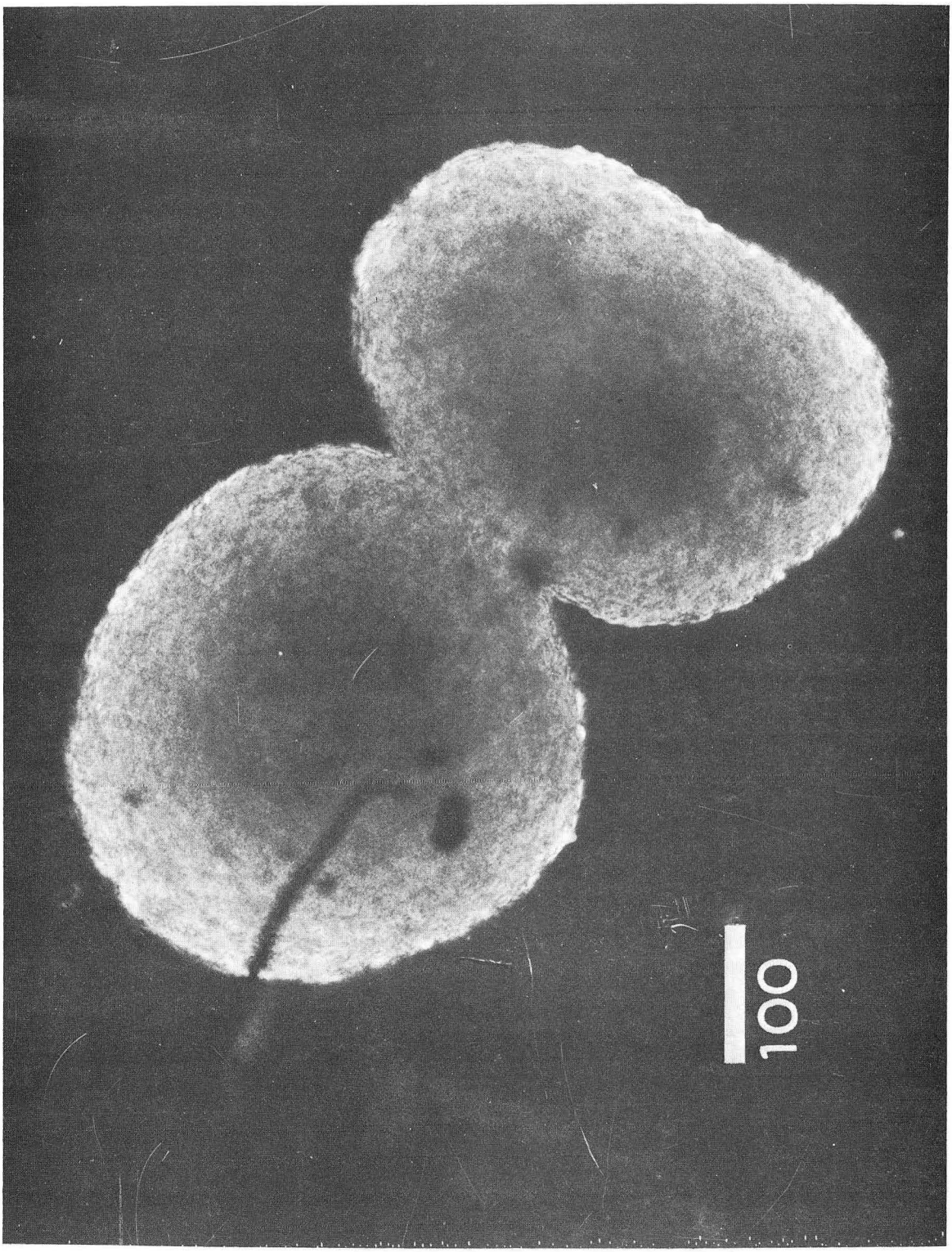

Fig. 4

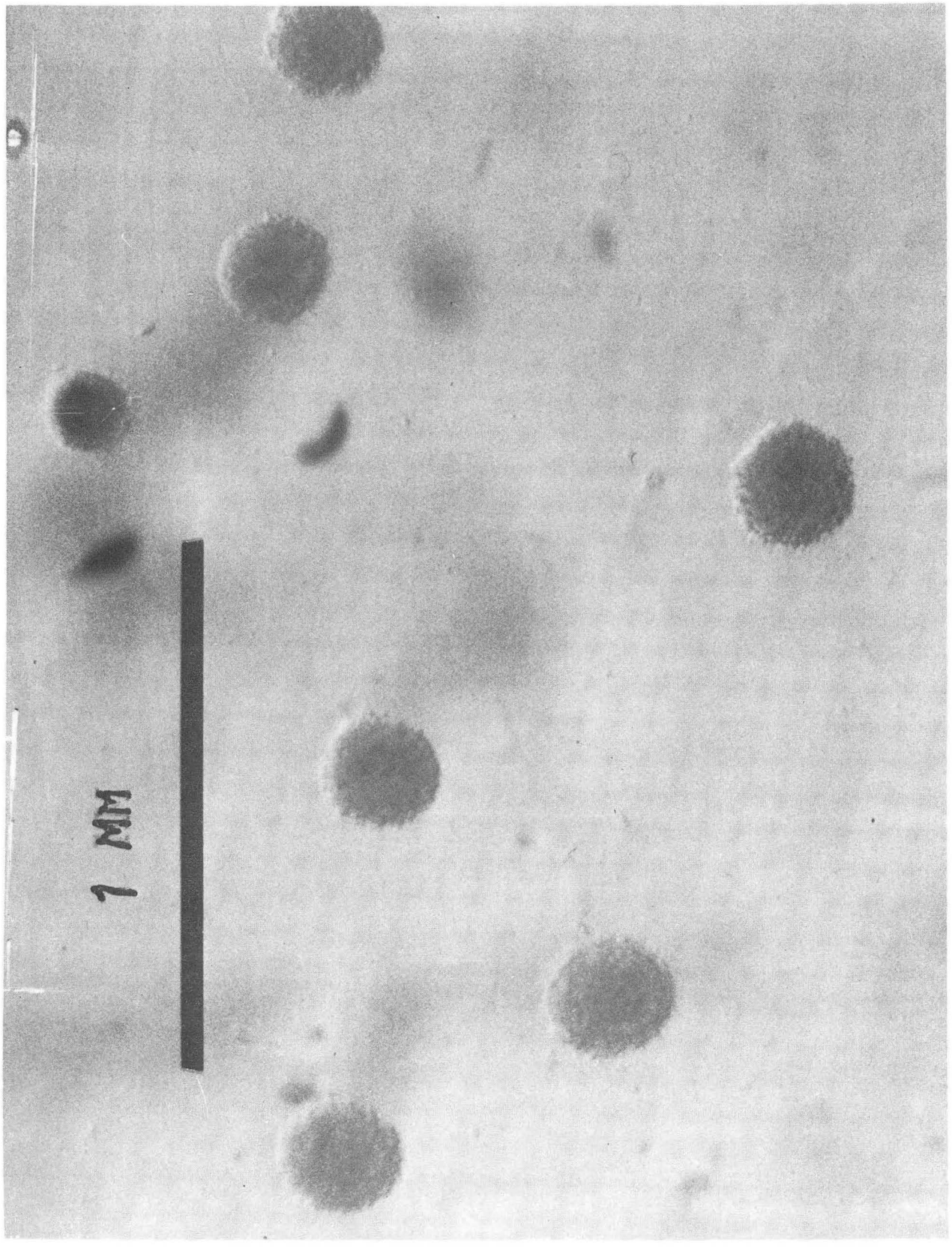

Fig. 5

0 0 0 0 3 7 0 0 3 7 1

LONG-TERM EFFECTS OF ACCELERATED IONS

0 0 0 0 3 7 0 0 0 7 2

AGING IN LABORATORY MICE AFTER WHOLE-SKIN IRRADIATION WITH ACCELERATED HELIUM IONS

J. Leith, G. Welch, W. Schilling, R. McGregor, and C. Tobias

ABSTRACT

The whole skin of male CD-1 mice was exposed, in whole-body irradiation, to single doses of monoenergetic helium ions accelerated at the Berkeley 88-inch cyclotron. The maximum penetration in tissue was set at various depths from 12 mg/cm^2 to 51 mg/cm^2 and the dose levels varied between 75 and 10 Krads. Median lifespan of each of the irradiated groups was reduced, to a first approximation, in proportion to dose. The lifespan reduction was 2.6×10^{-4} per rad for the group where the range of the helium ions in tissue was 51 mg/cm^2. If the same factor were to apply to humans, it would indicate a median life span reduction of 6.6 days per rad of helium ions received by the whole skin. Some of the time-dose survival relationships indicate a biphasic response. The possibility that this response was related to skin carcinogenesis is being analyzed.

INTRODUCTION

There are important reasons why the aging response of the organism that has sustained radiation damage to a single organ system should be examined. For example, it has been shown that grossly evident residual skin damage in the rat and mouse after beta-ray and alpha-particle irradiation is associated with development of skin tumors

and with reduction in the life span (1-4). Our study was undertaken to examine such responses in mouse skin after whole-body skin irradiation with accelerated helium ions.

In orbital and planetary space flight, man is exposed to a number of sources of heavy-ion irradiation. These include protons in the Van Allen radiation belt, protons and helium ions in small and large solar flares and heavy ions from cosmic sources and the sun. In most space flight situations, particularly during solar flares, the skin receives the greatest dose and also the greatest number of stopping particles.

We also know that effects of high-LET radiation are greater than those for low LET and that high-LET effects are nearly additive, whereas low-LET effects are modified by extensive repair. For some biological end points, e.g. the production of dominant lethal mutations, high relative-biological effectiveness has been reported for fast neutrons of energy greater than 30 MeV, and many diverse data indicate that high-LET particles are more carcinogenic than those of low LET. For these reasons, we have initiated a systematic investigation of the effects of stopping particles in mouse skin. First, an assessment of acute effects was made (5, 8). Now, in this paper we present a preliminary analysis of the effects of a single dose of helium ions on the longevity of mice, followed by a preliminary assessment of the rate of tumor induction.

Skin may be regarded as an essential and more-or-less uniform, single organ system covering the body. From experience with

thermal burns, it is well-known that skin is essential in the sense that life cannot be maintained where the skin has sustained major damage. Radiobiologically, irradiation of the skin represents a special case of "partial body" exposure. From the viewpoint of Strehler and Mildvan (6), this may be considered as injury to a specific subsystem of the organism, the entire subsystem complement constituting the overall system's (organism) vitality. The organism's vitality may therefore be considered as the "weighted average" of all subsystem vitalities. As the aging response is known for whole-body x- and gamma-ray irradiations which injure all subsystems of the organism, it may be possible to draw tentative inferences as to the importance of radiation damage of skin in the overall aging process. Such data for heavy particles is almost completely lacking, although Ordy et al (7) have made interesting observations on the role of radiation damage to the central nervous system only, and the subsequent aging response.

We have also examined the aging response after radiation damage to skin, as a function of the amount of this subsystem damaged. To do this, we have used four different maximum penetration depths in the skin of mice, 51, 31, 22, and 12 mg/cm^2. Responses after such exposures may provide some insight into the relative roles of skin substructures (e.g. blood vessels, hair follicles, and epidermal cells) in radiation responses.

MATERIALS AND METHODS

Animals. Male, CD-1 mice, raised as pathogen-free, and obtained from the Charles River Breeding Laboratories, Cambridge, Massachusetts were used. The mice were maintained on "White Diet" prepared by Feedstuffs Inc., San Francisco, California, and were individually housed in pint Mason jars which were changed twice weekly. Mice were 10 weeks of age at irradiation, and weighed 35-40 grams at this time. Food and water were available *ad libitum*.

Irradiation Procedures. Animals were irradiated at the Lawrence Berkeley Laboratory's 88-inch cyclotron which is a spiral-ridged variable-energy machine capable of accelerating protons up to 55 MeV and e/m = 1/2 fully-stripped particles to 32.5 MeV/nucleon. Deuterons and helium ions are available at the maximum energy but the numbers of fully-stripped carbon, mitrogen, and oxygen ions are insufficient for tuning. Nitrogen+5, however, has been accelerated to 250 MeV (17.9 MeV/nucleon). For the present study a 40-MeV initial energy, helium-ion beam was used. It was first focused to an area of about one cm^2 then deflected periodically both horizontally and vertically by a pair of sweeping magnets, to cover uniformly an area 2.5×7.5 cm.

Doses were monitored with a parallel-plate transmission ionization chamber with a 1.0 mg/cm^2 aluminum-Mylar collecting electrode and 1.2 mg/cm^2 aluminum high-voltage and shielding electrodes. The gap between electrodes was 1.7 mm and the potential was 500 volts. It was calibrated on each run day with a Faraday cup. Dose penetration data were calculated for each run from measured Bragg

ionization curves. These were obtained from two ion chambers separated by Mylar absorbers. The ratio (ionization after absorber/ionization before absorber) vs absorber thickness gives a curve rising to a maximum followed by a sharp cutoff as shown by the light lines in Fig. 1. Also shown in Fig. 1 is the depth-dose curve in the mouse skin resulting when the mouse was rotated in the beam. It was obtained by calculation from the conditions as shown in the geometric cross section, Fig. 2 for the 51 mg/cm^2 penetration. Each mouse was contained in a 2.5-cm-diameter tubular holder with a 17.0 mg/cm^2 wall thickness (5 layers of 1-mil Mylar), and the penetration of the beam varied from maximum penetration at normal incidence (i.e., 51, 31, 22, and 12 mg/cm^2) to zero at some lateral position where the diagonal thickness of the holder just equals the range of the beam. The mouse was rotated at 18 rpm, hence the dose to all parts of the skin is made up of a spectrum of energies which can be approximated by the superposition of the family of Bragg curves shown in Fig. 1. The separation of these curves is 5 deg of the angle θ in Fig. 2

The dose distribution in various layers of the skin was obtained by integration of Bragg ionization data for all angles and intensities. Also included in the dose calculations was the fact that at any given instant only a fraction of the mouse was being irradiated. In a polar coordinate system these angles were 142°, 128°, 116°, and 92° respectively for the 51, 31, 22, and 12 mg/cm^2 penetration depths. Dose rates varied from 4500 to about 8000 rads/min. The high dose rate probably had no effect upon the experimental results, since a

different experiment with helium ions has shown that a 10-fold difference in dose rate was not significant in changing acute mortality responses (8). The heavy line in Fig. 1 represents the averaged Bragg curve in mouse skin for the penetrations depths indicated by the abscissa scale of residual range.

Experimental Design.

The maximum penetration depths, the doses received at each penetration depth, and the number of animals at each dose point are shown in Table 1. Also shown are the corresponding integral doses. Including controls, a total of 1136 animals were used.

For the CD-1 mice used, the basal layer of dividing epithelial cells is located at an average depth of about 30 mg/cm^2. The two deepest penetrations (31 and 51 mg/cm^2) therefore included the basal layer as well as most of the dermis, with its capillary circulation, innervation and hair follicles. When radiation was administered to the 12 and 22 mg/cm^2 depths, we assumed that most of the dermis was spared from direct irradiation and would have been damaged primarily by indirect effects.

The penetration depths of 51, 31, 22, and 12 mg/cm^2 were to the mouse's ventral surface where hair has its minimum thickness of about 9 mg/cm^2. Since the hair on the dorsal surface was about 18 mg/cm^2, the penetration there is 9 mg/cm^2 less and the average of 13.5 mg/cm^2 was used in calculating gram-rad doses of Table 1. For these, it was assumed that the mouse was a right-circular cylinder of 2.5 cm diameter and 7.5 cm length. The maximum penetration depths

and the amount of skin irradiated are shown in Table 2.

Mathematical Analysis of the Data

In the analysis of life-span data we assumed that the mortality rate of the population follows the relationship proposed initially by Gompertz to account for human mortality data (9-11).

The mortality rate $r(t)$ is defined as:

$$r(t) = -1/N\, dN/dt = r_0\, e^{mt}, \qquad [1]$$

where $N(t)$ = the number of individuals surviving at time t, and r_0 and m are constants. The values of r_0 and m are assumed to depend on administered dose, as well as on other factors. It is well-known that Eq. [1] does not hold for very young individuals. Many data show, however, that there is an initial age t_0, and that if $t \geq t_0$, the relationship has experimental validity. We may regard r_0 as depending on t_0 in the following manner:

$$r_0 = A e^{-mt_0}, \quad \text{so that}$$

$$r(t) = -1/N\, dN/dt = Ae^{m(t-t_0)}. \qquad [1a]$$

By integration and solution of [1] for t, the number of individuals N who survive to time t, from an original population N_0 at $t = 0$, can be calculated as

$$t = 1/m \ln (1 - m/r_0 \ln N/N_0). \qquad [2]$$

The median survival time S, that is, the time when 1/2 of the original population has died, is obtained from [2] by setting $N/N_0 = 1/2$:

$$S = 1/m \ln (1 - m/r_0 \ln 1/2). \qquad [3]$$

If S_0 is assigned to the median life-span of the nonirradiated control animals, the fractional change in the median life-span for a given dose D of radiation may be given by:

$$R(D) = S_0 - S(D)/S_0, \qquad [4]$$

where S represents the median life-span of an irradiated population.

We shall show that for a certain situation the fractional decrease of median life-span is approximately proportional to the dose (at dose levels greater than 75 rads). However, the data are not sufficient to show that the relationship is actually linear, as:

$$R(D) = S_0 - S(D)/S_0 = - \theta D. \qquad [5]$$

We have determined the value θ, the fractional life-span reduction per rad of helium ions on mouse skin. It is of some importance for space radiobiology to be able to estimate the value of θ for man for all varieties of space radiations. We have not, in this paper, yet attempted to estimate A, t_0, or m as functions of radiation dose or penetration depth; however, this will be accomplished in the near future.

Examination of the data also indicates that the irradiated mouse population is probably not homogeneous and that two or more subpopulations with different Gompertz constants may exist.

Pathology. Each animal was inspected for skin tumors at monthly intervals. Mice were allowed to die naturally unless they were moribund or the size or degree of ulceration of a tumor made it necessary to kill the animal. For the mice irradiated to 51 mg/cm^2 depth in tissue, 102 tumors were examined grossly and microscopically.

Tumor diameters and volumes were obtained by direct measurement of the lesions. Sections were routinely stained with hematoxylin and eosin.

Skin was taken for histology at autopsy from many of the mice and included skin with maximum clinical changes for the various doses and depths used. Histologically, skin changes were not uniform over the entire mouse, with the areas of the abdomen, neck, and head being generally the greatest affected.

Skin tumors were classified into 2 categories:

1. Epidermal. These consisted of keratinized epidermoid lesions, including skin papillomas and squamous cell carcinomas.
2. Dermal. This category included fibromas and fibrosarcomas.

Also, tumors were classified on the basis of the predominant mode of growth, as exophytic, endophytic, and subepidermal lesions. Tumors were considered exophytic when more than 3/4 of their cross-sectional area was above the skin surface.

RESULTS

In Figs. 3-7 are presented the survival curves for mice irradiated at the four different penetration depths. In Table 3 we present the median life-spans as a percent of the control median life-span from [4].

In Fig. 8 is presented a linear regression analysis of the derived median life-span versus absorbed dose for the mice irradiated at a maximum penetration depth of 51 mg/cm^2. It was found that median life-

span was shortened 0.158 days per rad, or approximately 2.6% of the median life-span for control animals per 100 rads of helium ions. The correlation coefficient for the regression line was 0.94 which is significant at the 0.05 level of significance.

Similarly in Figs. 9-11 are presented the median life-span data for the 31, 22, and 12 mg/cm^2 penetration depths in skin. For the 31 mg/cm^2 depth, the median life-span reduction was 0.132 days per rad, or approximately 6% of the median life-span of control animals per 100 rads of helium ions. The correlation coefficient for the regression line was 0.06, which again is significant at the 0.05 level of significance. However, the degree of reduction in median life-span for the 22- and 12- mg/cm^2 penetration-depth irradiated animals appears to ve definitely nonlinear which precludes a simple linear analysis of the responses.

All of the median life-span data plotted as the integral or gram-rad response as determined from the data of Tables 1 and 2 are plotted in Fig. 12.

In a separate series of experiments, the survival of CD-1 mice after helium ion exposure was studied with the added variable of keeping groups of animals at room temperature and in a 2°C cold room. For control animals no difference was seen in the survival curves of either environment. Similarly, for animals irradiated with 800 rads of helium ions at a penetration depth of 51 mg/cm^2 in skin, there was no significant difference in the survival curves. However, for animals irradiated with 1400 rads of helium ions, a very significant difference was

seen under the two conditions. The animals housed in the cold environment died very much sooner than the animals kept in the room temperature situation. However, the aninals housed in the cold environment showed a much less frequent incidence of skin tumors than did the mice kept at room temperature.

A preliminary analysis of tumor response for mice irradiated to a depth of 51 mg/cm^2 in tissue showed a total of 102 skin tumors. Some of these were ulcerated and others reached a large size without ulcerating. Histologically, an ulcerated tumor was not necessarily malignant and conversely a non-ulcerated tumor was not necessarily benign. Of the 102 tumors, 37 were epidermal in nature. Of these 37, 15 were highly keratinized sessile papillomas. The remaining 22 were squamous cell carcinomas. There were 65 tumors of irradiated dermis and 50 of these were malignant fibrosarcomas. The remaining 15 were fibromas of the dermis. The tumor response of the other penetration depths has not yet been analyzed, although qualitatively it may be stated that the tumor incidence decreases with decreasing penetration depth in skin.

DISCUSSION

It is apparent from the survival data (Figs. 3-7) that irradiation of "whole skin" with helium ions is capable of reducing the life-span of mice. The reduction in life-span appears to the approximately linear with dose at the 51 and 31 mg/cm^2 maximum penetration depths. The animals irradiated at the 22 and 12 mg/cm^2 penetration depths show a nonlinear type of median life-span reduction with increasing dose.

With regard to biphasic aging response seen with shallower penetration depth, there are at least three possible explanations:

a). In view of the nonuniform thickness of skin in various regions of the body it is possible that a definite portion of the epidermal and dermal cells received less dose (or no dose) than other portions; it is possible also that there are individual variations in skin thickness. These considerations may explain that a portion of the population shows near normal survival distribution.

b). Can there be two populations of skin cells of which one is relatively radioresistent? As, at the shallower penetration depths, the skin vascular bed is not being damaged as badly as epidermal cells, possibly there is a role of the dermal vascular bed in the long-term aging and cell survival response of epidermal cells. Leith et al (12), have shown that the acute survival of epidermal cells is dependent on penetration depth, and that epidermal survival increases with decreasing penetration depth for equal surface irradiation doses.

Interestingly, the data of Ordy et al (7) for median life-span reduction in mice after partial brain irradiation show a response similar in shape to that seen with the two shallower skin irradiations. Possibly, this represents a general response of damage to only part of an organism subsystem and is not a linear response as is seen when the whole system is irradiated.

c). There may exist different subpopulations of animals that die with different syndromes. Skin tumor incidence is high in the irradiation groups, but not all animals die with tumors. We plan to analyze mortality responses that relate tumor pathology to the overall time-

survival data.

The integral dose response (Fig. 12) of median life-span for all of the irradiated animals appears to be approximately similar for all of the irradiation depths when expressed as the amount of tissue irradiated. This is somewhat surprising as it was expected that the deeper penetrations would have been more effective per gram-rad in producing life shortening. There is some scatter in the points and more detailed mathematical analysis may clarify the relationships further.

We have presented evidence that single doses of helium ions applied to the whole skin of animals producing a shortening of the median life-span, for the 51 mg/cm^2 penetration depth, which is approximately linear with dose above 75 rads. This fractional decrease of median life-span, (θ in equation 5) is about 2.6×10^{-4} per rad. If the same value of θ were true in human populations, at a median life-span of 70 years, this would mean about 6.6 days per rad. On a flight to the planet Mars, astronauts may receive 40 rads per year, some of it high-LET radiation. In this regard, further studies are warranted to enable us to understand more quantitatively the magnitude of long-term effects from heavy ions. Among the subjects to be investigated are:

a. Acute and long-term effects of heavier ions, e.g., neon and iron, on such end points as longevity and carcinogenesis.

b. Additive effects of protracted exposures, and the degree of repair, if any, after such exposure.

c. The nature of functional relationships between heavy-ion dose and carcinogenesis. What is the probability that a single heavy-ion track

in tissue could be the causative agent of a local skin tumors?

d. What is the response of an individual to other environmental stresses of spaceflight, who has heavy-ion radiation damage to skin? We have already shown in this paper that exposure of a mouse to a cold environment in a chronic situation potentiates the long-term effects of skin irradiation with helium ions. Other effects, e.g., the role of skin irradiation in the susceptibility to infections remains to be demonstrated.

The answers to some of the above problems will necessitate considerable research effort, and the availability of accelerated heavy ions.

ACKNOWLEDGMENTS

We are pleased to acknowledge the cooperation of the crew of the 88-inch cyclotron headed by J. Bowen.

0 0 0 0 3 7 0 5 8 7 7

REFERENCES

1. Albert, R. E., F. J. Burns, and R. D. Heimbach, The Association between Chronic Radiation Damage of the Hair Follicles and Tumor Formation in the Rat, Radiat. Res., 30:590-599 (1967).
2. Albert, R. E., F. J. Burns, and R. D. Heimbach, Skin Damage and Tumor Formation from Grid and Sieve Patterns of Electron and Beta Radiation in the Rat, Radiat. Res., 30:525-540 (1967).
3. Hulse, E. V., R. H. Mole, and D. G. Papworth, Radiosensitivities of Cells from which Radiation-induced Skin Tumors are derived, Int. J. Radiat. Biol., 14:437-444 (1968).
4. Hulse, E. V., Incidence and Pathogenesis of Skin tumors in Mice Irradiated with Single External Doses of Low Energy Beta Particles, Brit. J. Cancer, 21:531-547 (1967).
5. Leith, J., E. Blakely, G. Welch, C. Tobias, and H. Aceto, Jr., Acute Physiological Effects of Accelerated Helium Ions on the Skin of Mice. Submitted to Radiation Research, 1972.
6. Strehler, B. L., Fluctuating Energy Demands as Determinants of the Death Process. In: The Biology of Aging, B. L. Strehler, Ed., (AIBS, Washington, D. C., 1960) pp. 309-314.
7. Ordy, J. M., T. Samorajski, T. J. Hershberger, and H. J. Curtis, Life-Shortening by Deuteron Irradiation of the Brain in C57BL/10 Female Mice, J. Gerontology, 26: 194-200 (1971).
8. Leith, J. T., and H. Aceto, Jr., Acute and Prolonged Chronic Effects of Mouse Skin Irradiation with Accelerated Heavy Ions. In: Symposium on Neutrons in Radiobiology, CONF-691106, Oak Ridge, Tennessee, 1969, pp. 140-150.

9. Noonan, T., F. Van Shyke, and J. Hursh, Effect of Single Doses of X-rays on the Survival Time of Rats, UR-161.

10. Sacher, G., After Survival of Mice treated with Single Doses of X-rays. CH3782. Univ. Chicago Metallurgical Lab.

11. Berlin, N. I., Radiation Effects and Aging. In: The Biology of Aging. B. L. Strehler, Ed., (AIBS, Washington, D. C., 1960) pp. 309-314.

12. Leith, J. T., W. A. Schilling, and G. P. Welch, Survival of Mouse Skin Epithelial Cells after Heavy-Particle Irradiation, Int. J. Radiat. Biol., 19, 603-609 (1971).

Table 1

Penetration depth in skin (mg/cm^2)	Dose (rads)	Integral dose (gram-rads)	Number of animals used
51	75	103.5	48
	150	207.0	36
	375	517.5	34
	600	828.0	48
	800	1104.0	44
	1000	1380.0	46
	1200	1656.0	43
	1400	1932.0	39
	1600	2208.0	42
31	125	100.0	48
	250	200.0	37
	370	296.0	47
	510	408.0	43
	1810	1440.0	44
	2600	2080.0	44
22	185	100.0	47
	370	200.0	39
	925	500.0	39
	2200	1188.0	47
	4200	2268.0	41
12	525	100.0	46
	1045	198.6	39
	2600	494.0	47
	4200	798.0	24
	10450	1985.5	37
Controls	---	---	40

Table 2

Maximum penetration depth in skin (mg/cm^2)	Approximate amount of tissue irradiated (grams)
51	1.38
31	0.80
22	0.54
12	0.19

Table 3

Penetration depth in skin (mg/cm^2)	Dose (rads)	Median survival time (days)	Percent of control
Controls	---	599	---
51	75	572	95.5
	150	559	93.3
	375	527	88.0
	600	532	88.8
	800	467	77.9
	1000	498	83.1
	1200	371	62.0
	1400	394	65.7
	1600	305	51.0
31	125	619	103.3
	250	583	97.3
	370	544	90.9
	510	523	87.2
	1800	390	65.0
	2600	257	42.9
22	185	590	98.5
	370	541	90.2
	925	460	76.9
	2200	450	75.0
	4200	417	69.6
12	525	558	93.1
	1045	550	91.7
	2600	508	84.8
	4200	483	80.7
	10450	422	70.5

FIGURE LEGENDS

Fig. 1. Penetration of helium-ion beam in tissue. Heavy line indicates summation of individual Bragg curves.

Fig. 2. Geometric cross section of animal holder illustrating the nature of the depth dose irradiation seen by the skin of the rotating mouse.

Fig. 3. Survival curves for animals irradiated to a maximum penetration depth of 51 mg/cm^2 in skin. (75-600 rads).

Fig. 4. Survival curves for animals irradiated to a maximum penetration depth in skin of 51 mg/cm^2 (800-1600 rads).

Fig. 5. Survival curves for animals irradiated to a maximum penetration depth in skin of 31 mg/cm^2.

Fig. 6. Survival curves for animals irradiated to a maximum penetration depth in skin of 22 mg/cm^2

Fig. 7. Survival curves for animals irradiated to a maximum penetration depth in skin of 72 mg/cm^2.

Fig. 8. Linear least squares regression analysis of the median life-span of mice irradiated to a maximum penetration depth in skin of 51 mg/cm^2 versus helium in dose in rads.

Fig. 9. Linear least squares regression analysis of the median life-span of mice irradiated to a maximum penetration depth in skin of 31 mg/cm^2 versus helium ion dose in rads.

Fig. 10. Median life-span of mice irradiated to a maximum penetration depth in skin of 22 mg/cm^2 versus helium ion dose in rads.

Fig. 11. Median life-span of mice irradiated to 12 mg/cm^2 in skin versus helium ion dose in rads.

Fig. 12. Median life-spans of mice irradiated at all penetration depths in skin versus helium ion dose expressed as the integral or gram-rad dose.

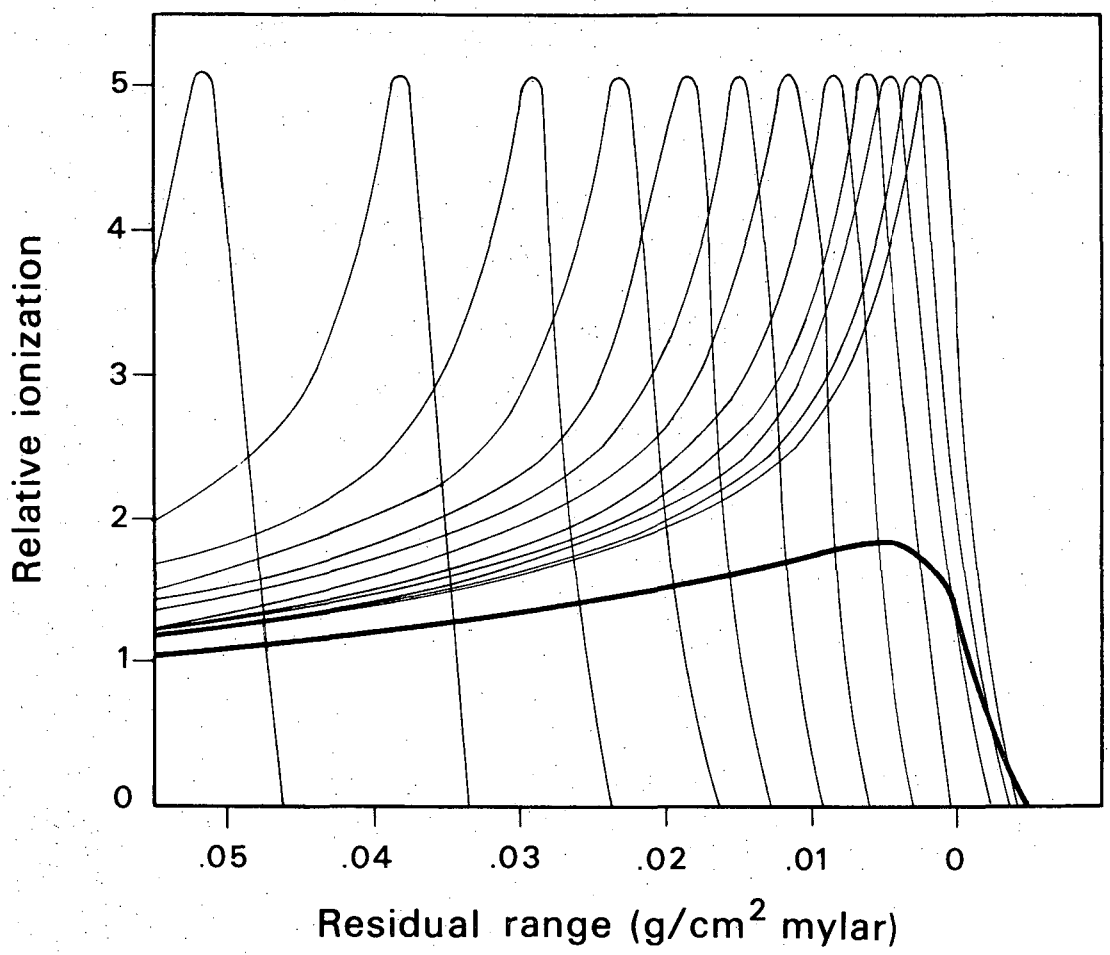

DBL 711-5615

Fig. 1

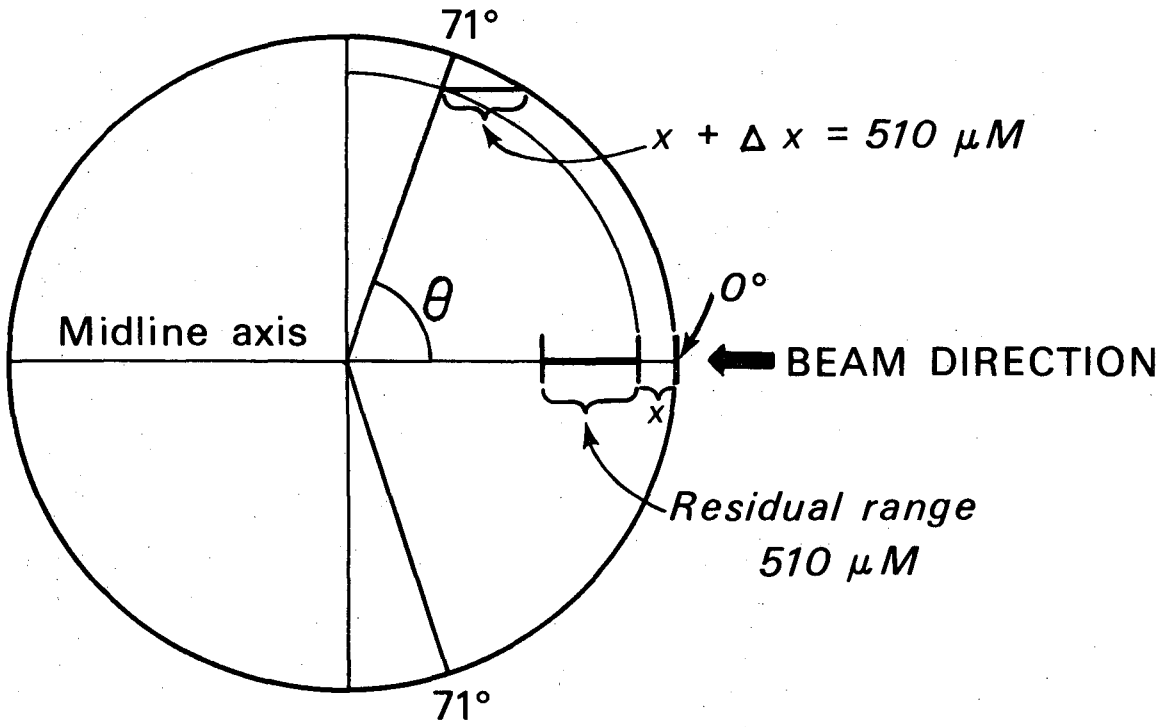

DBL 711-5605

Fig. 2

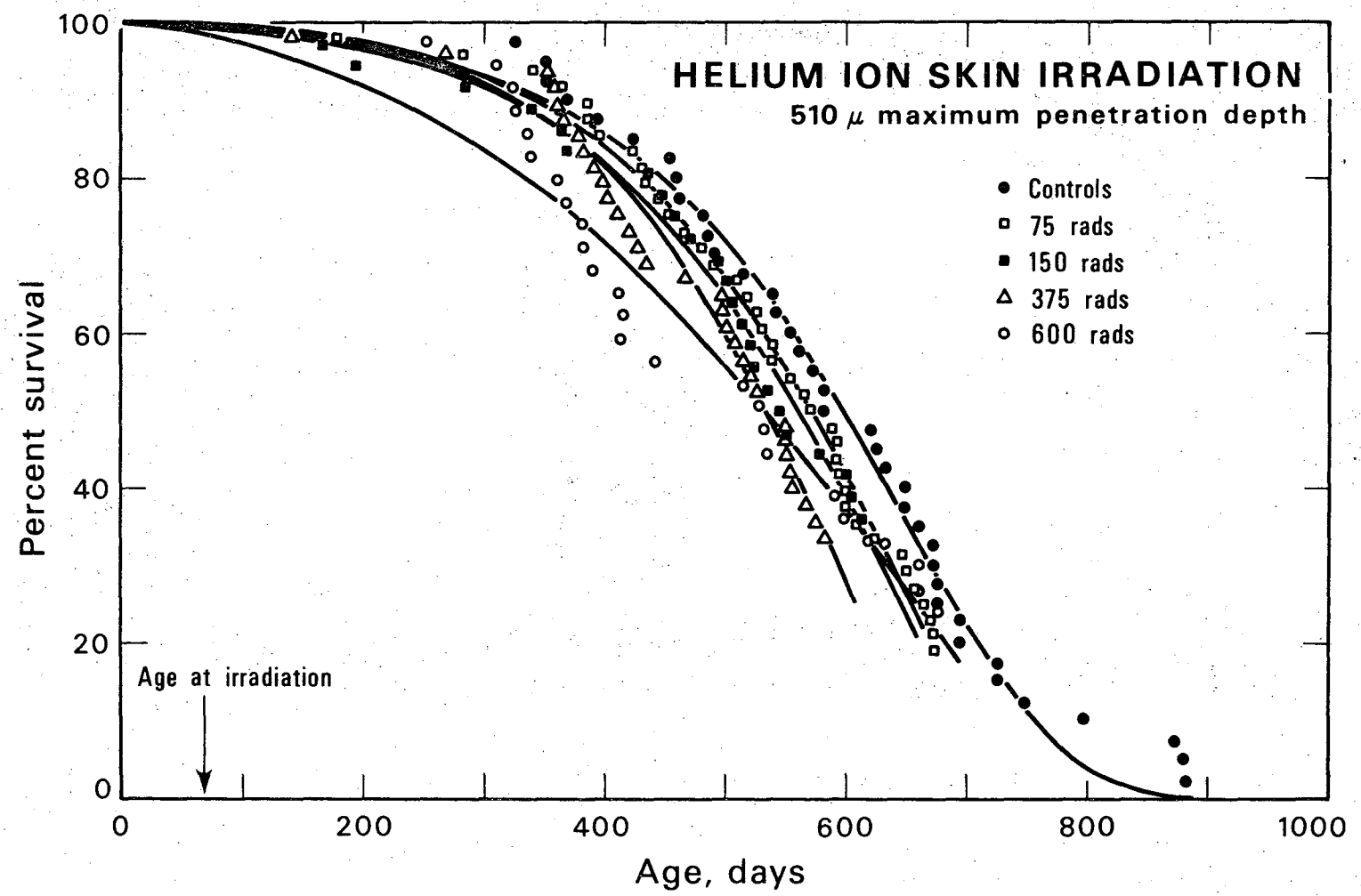

DBL 721 5117

Fig. 3

0 0 0 5 7 0 7 8 8 1

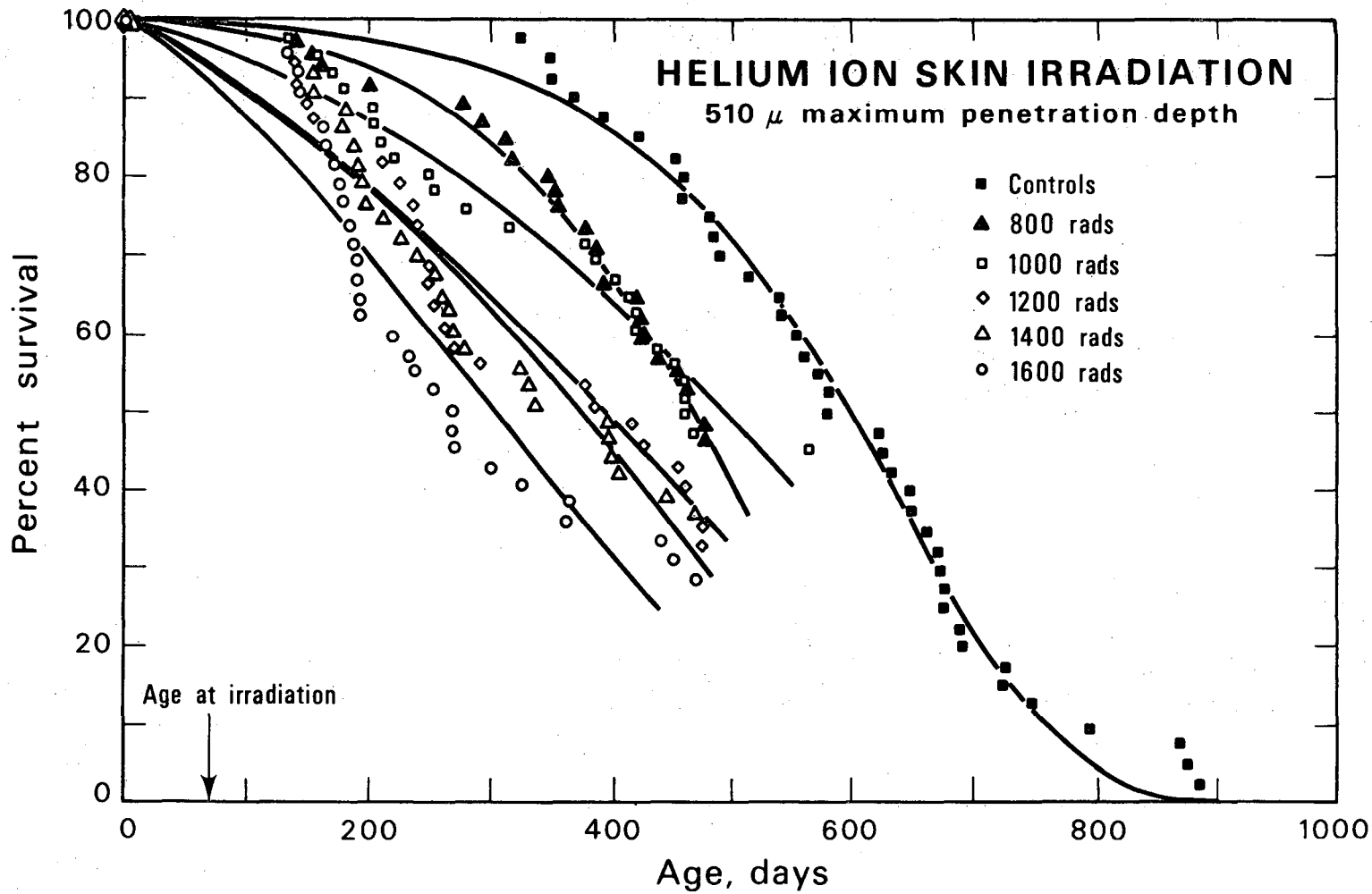

DBL 721 5116

Fig. 4

0 0 0 0 5 7 0 0 8 8 2

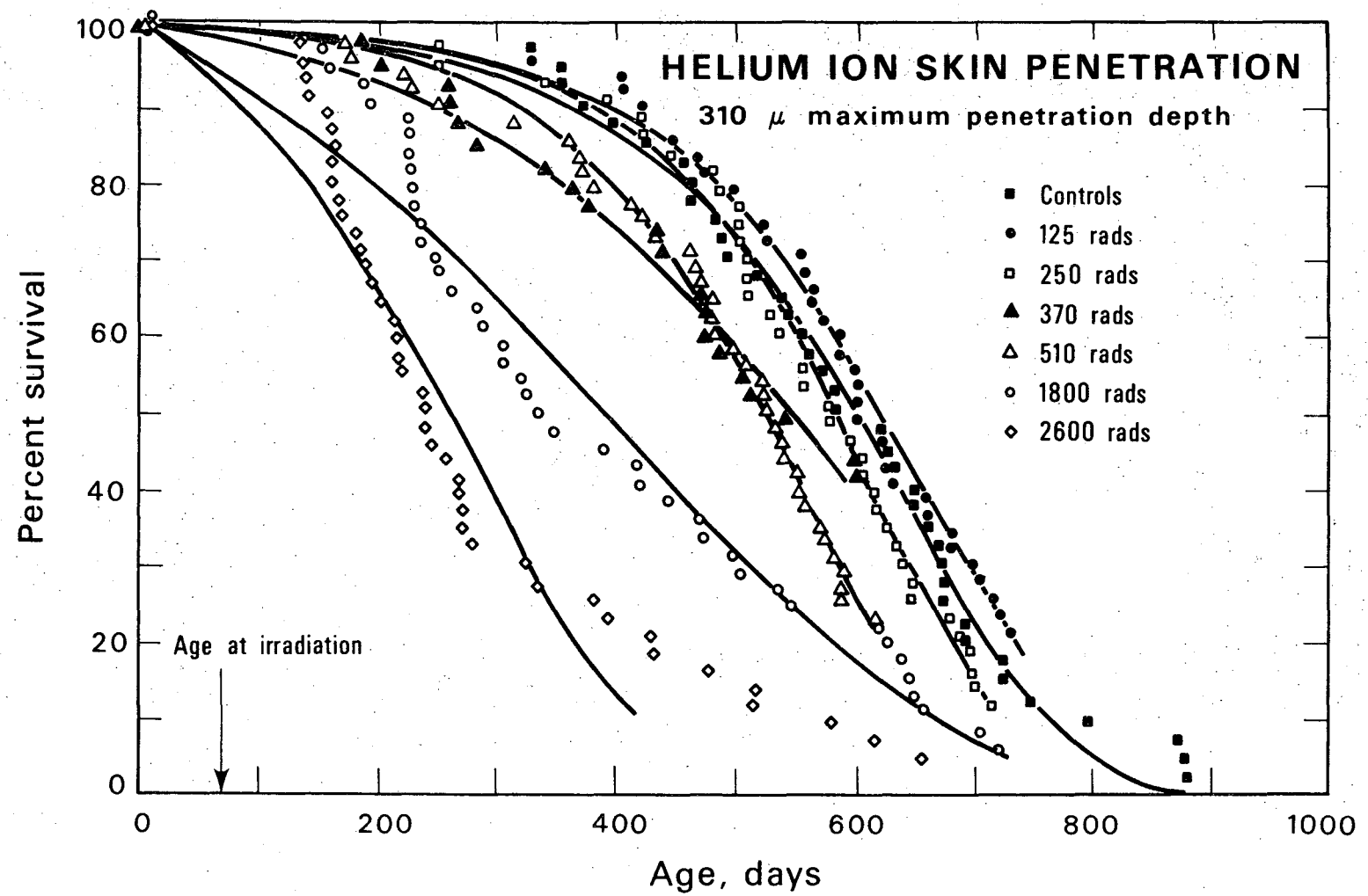

DBL 721 5115

Fig. 5

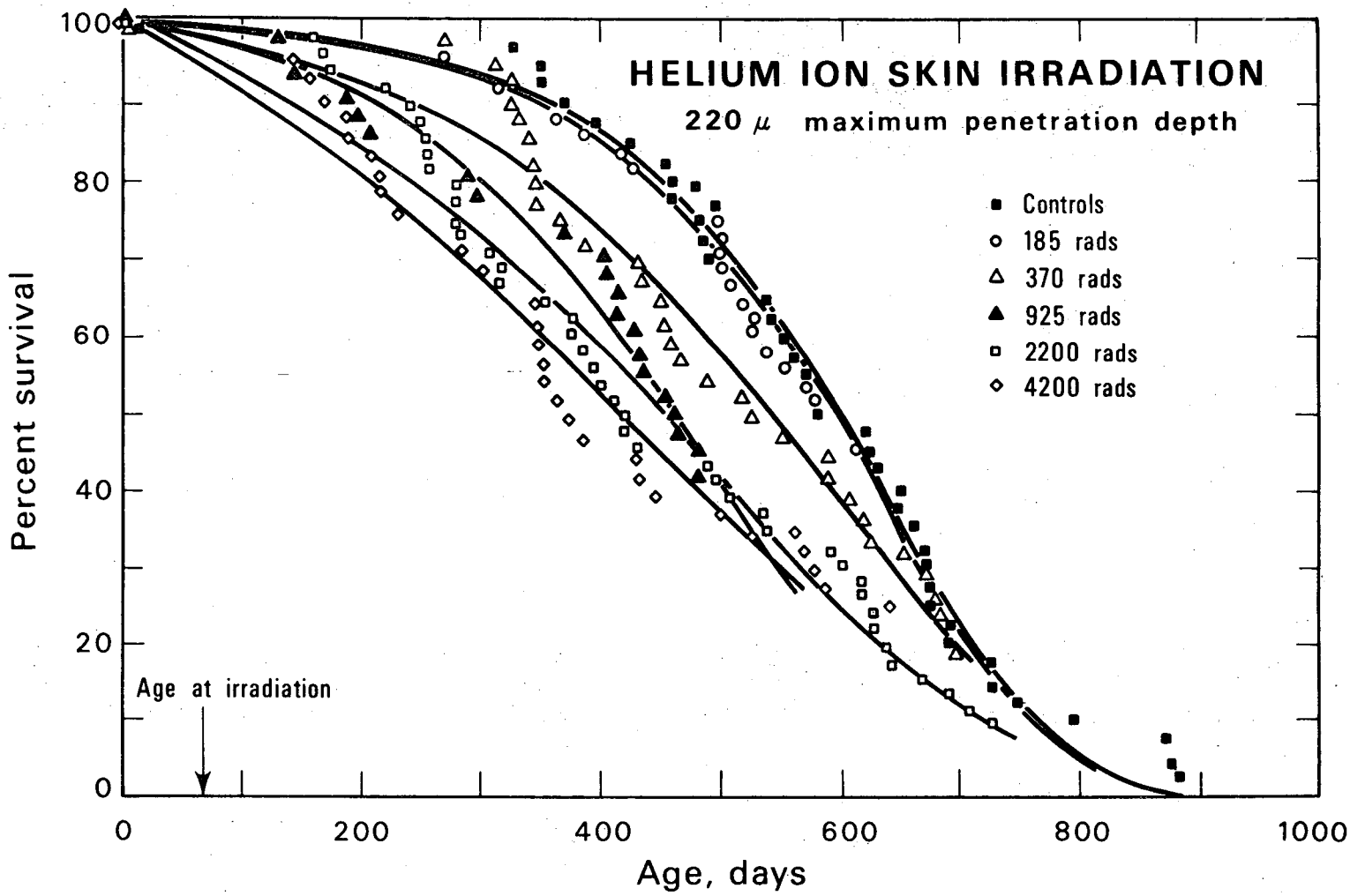

DBL 721 5114

Fig. 6

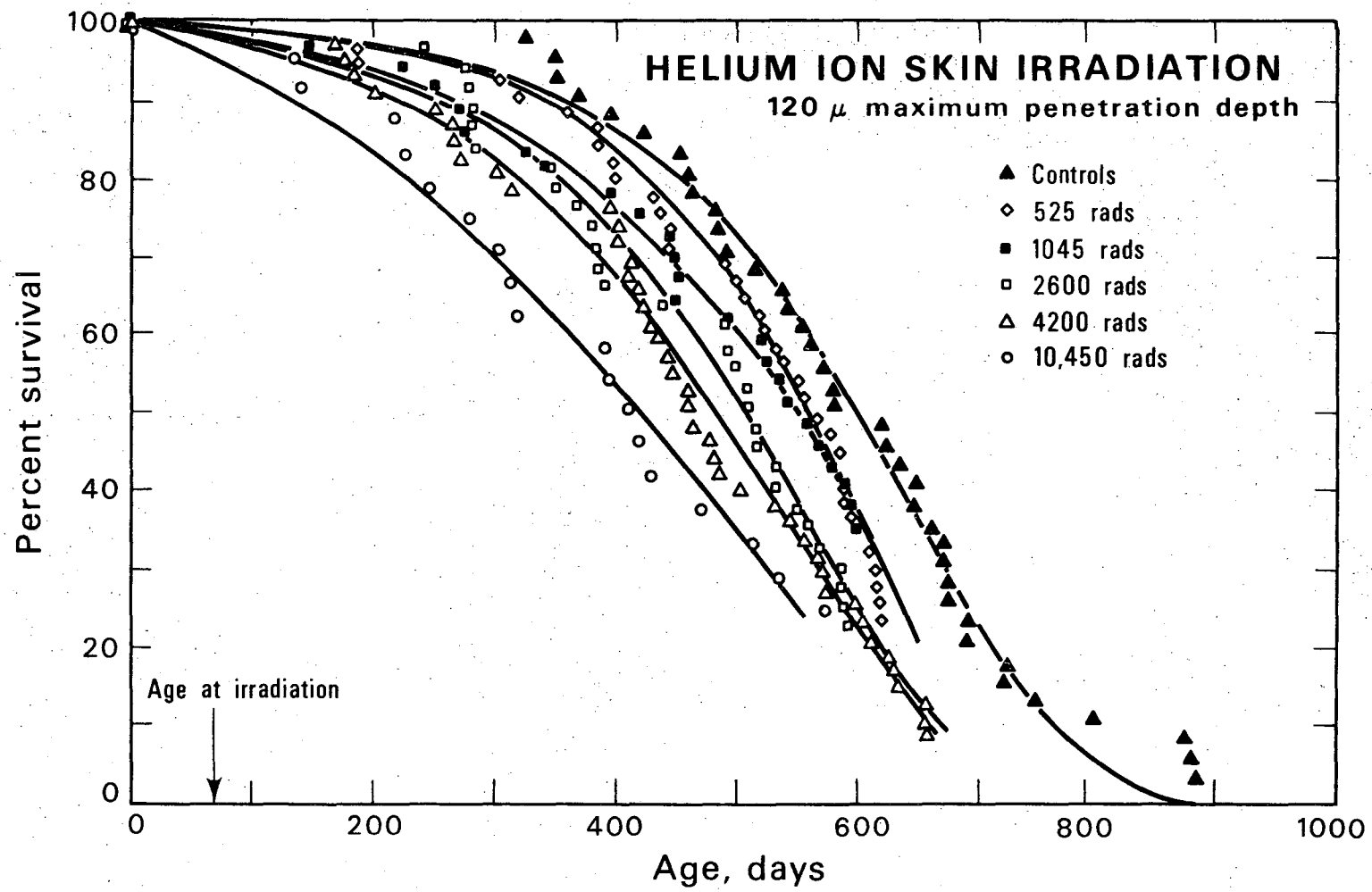

DBL 721 5113

Fig. 7

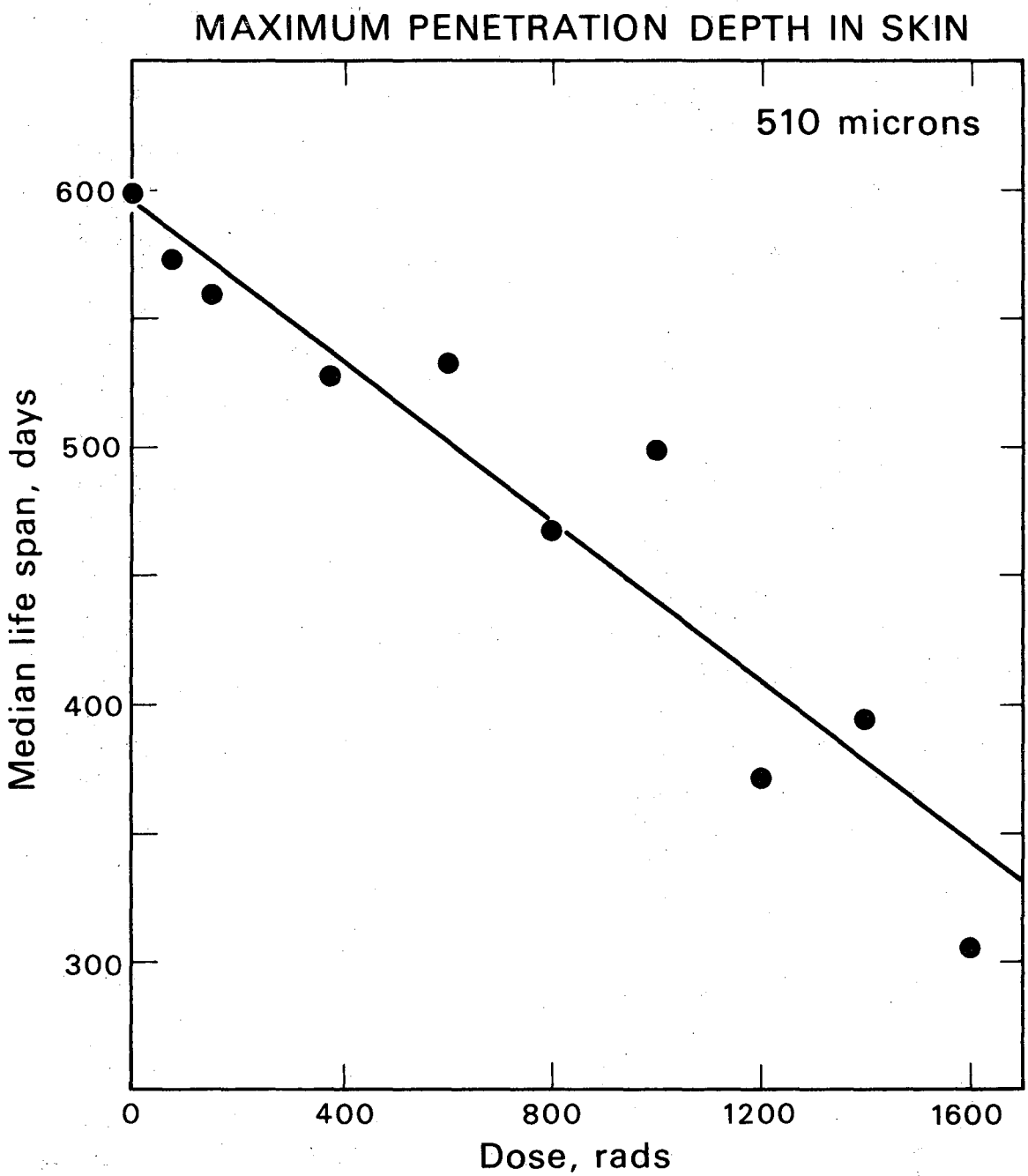

DBL 721-5127

Fig. 8

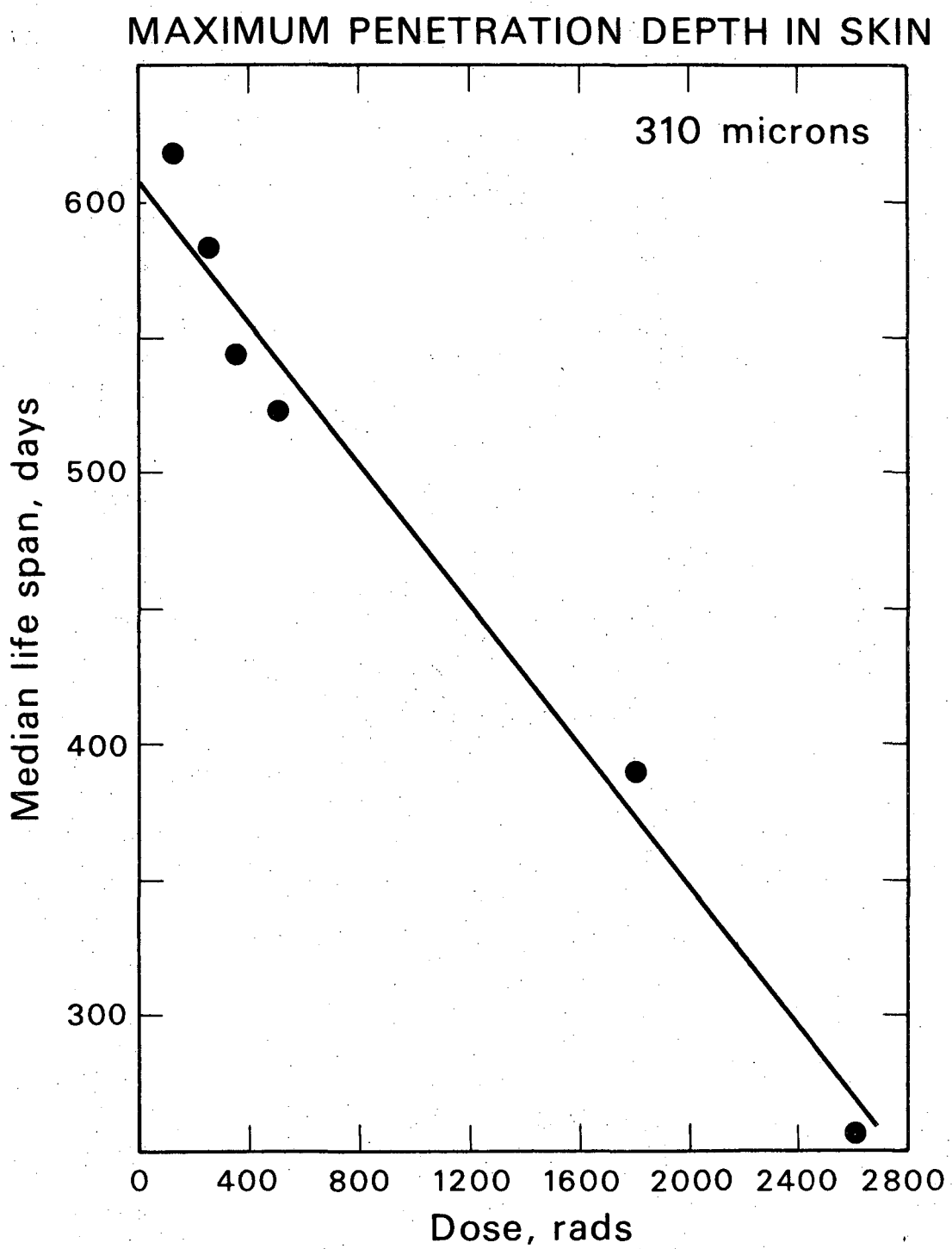

DBL 721-5128

Fig. 9

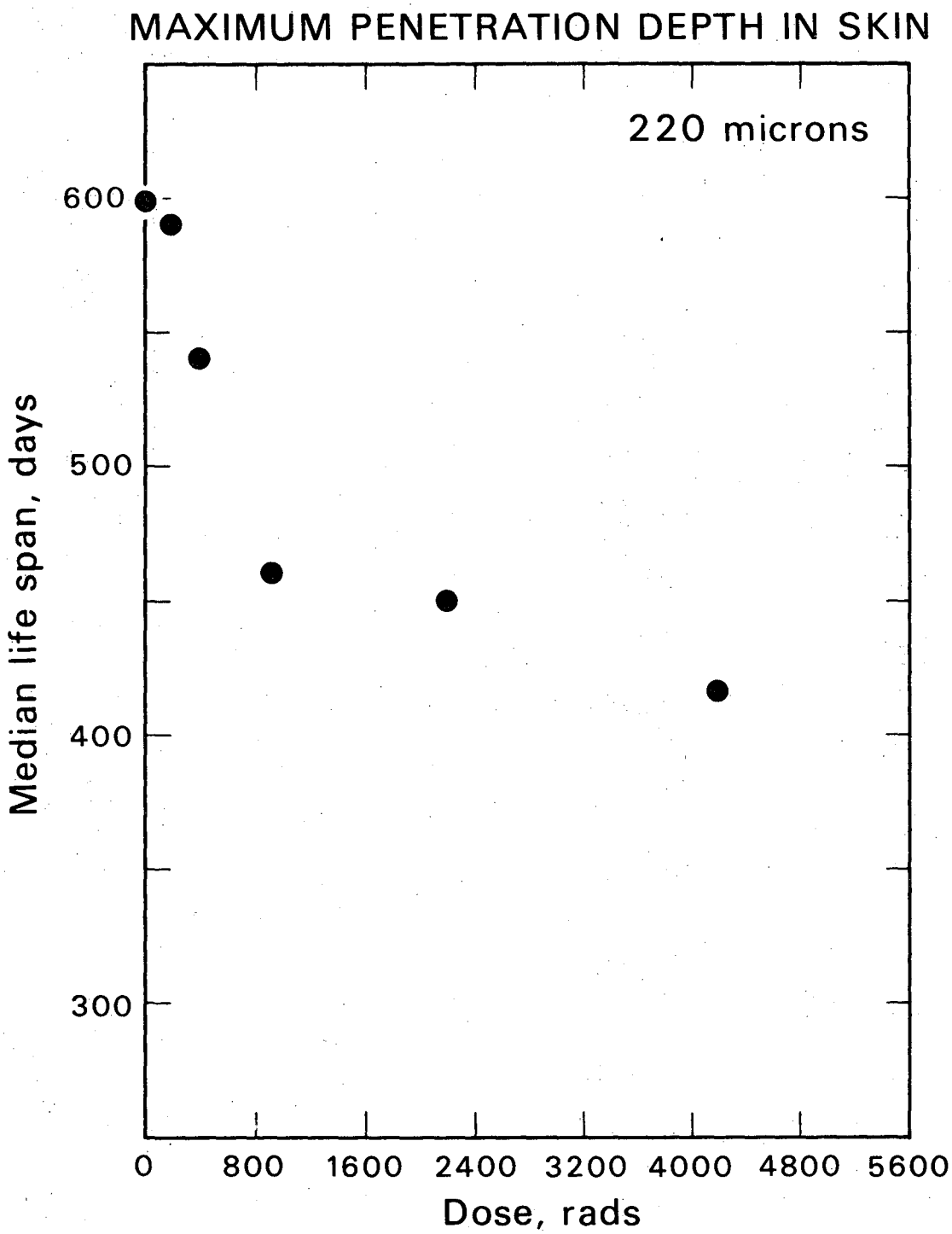

DBL 721-5129

Fig. 10

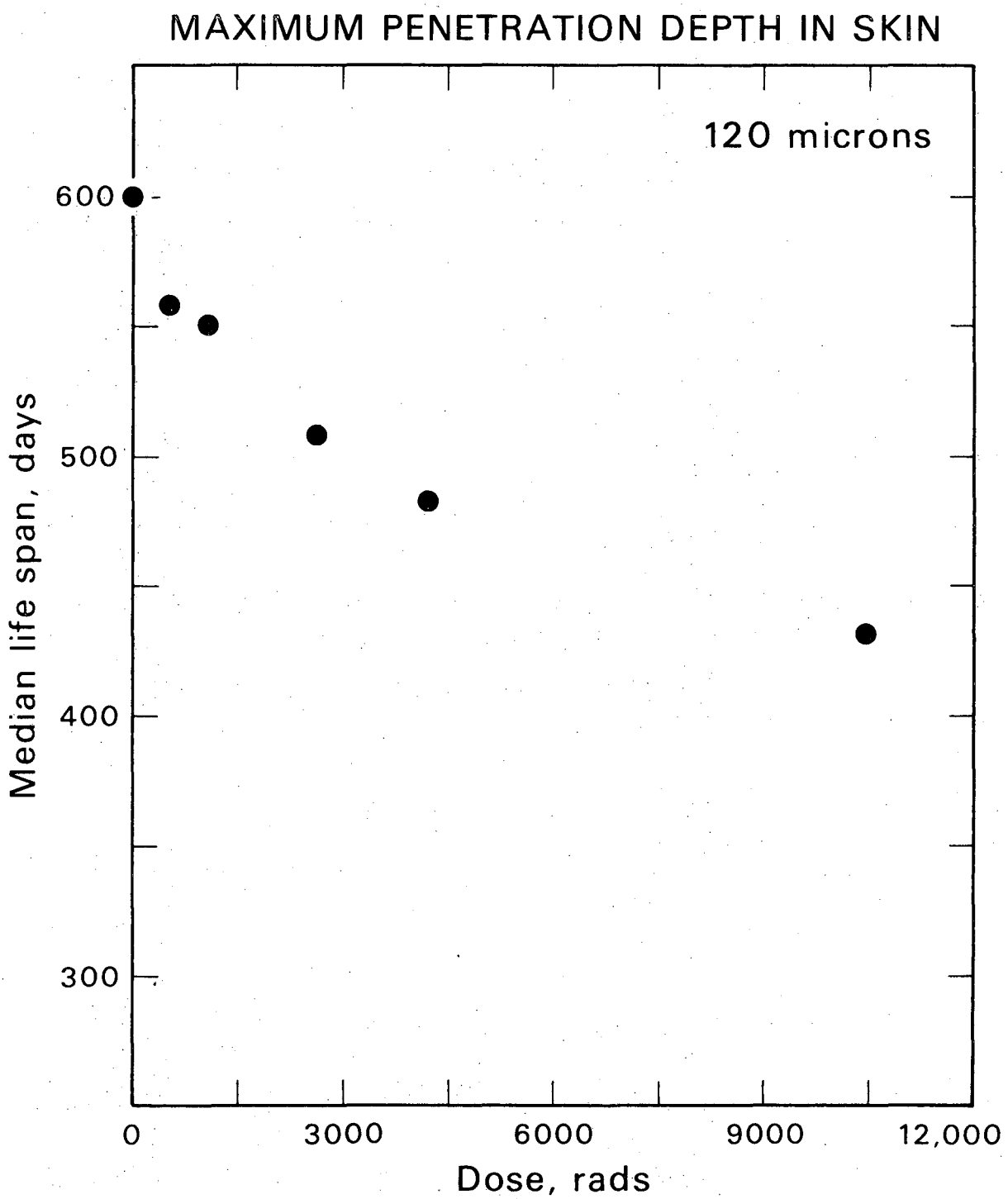

DBL 721-5130

Fig. 11

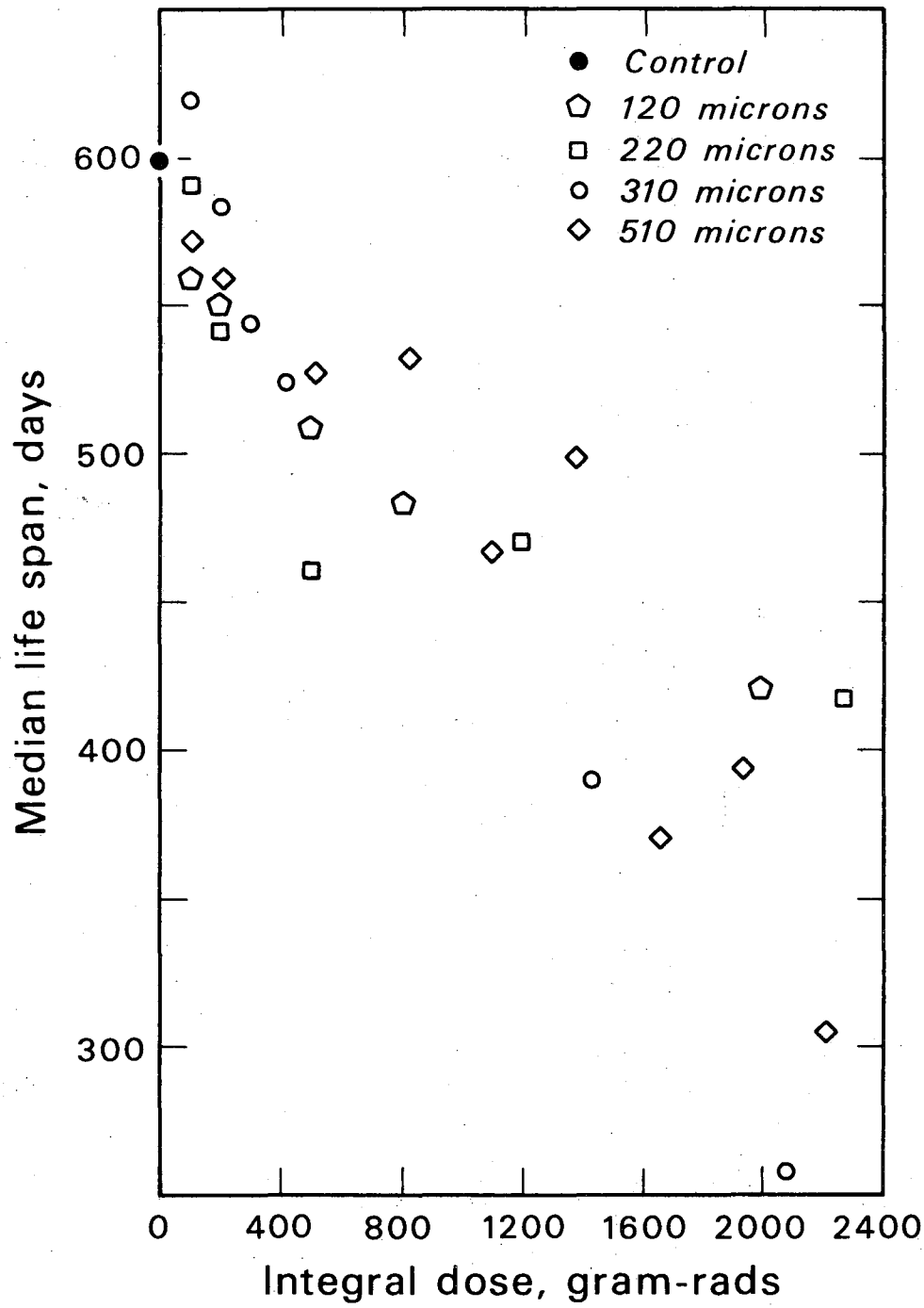

DBL 721-5131

Fig. 12

LEGAL NOTICE

This report was prepared as an account of work sponsored by the United States Government. Neither the United States nor the United States Atomic Energy Commission, nor any of their employees, nor any of their contractors, subcontractors, or their employees, makes any warranty, express or implied, or assumes any legal liability or responsibility for the accuracy, completeness or usefulness of any information, apparatus, product or process disclosed, or represents that its use would not infringe privately owned rights.

TECHNICAL INFORMATION DIVISION
LAWRENCE BERKELEY LABORATORY
UNIVERSITY OF CALIFORNIA
BERKELEY, CALIFORNIA 94720